2005

Synthesis of poly(DL-lactide-co-glycolide) nanoparticles with entrapped magnetite

Carlos Ernesto Astete R.
Louisiana State University and Agricultural and Mechanical College, castet1@lsu.edu

SYNTHESIS OF POLY(DL-LACTIDE-CO-GLYCOLIDE) NANOPARTICLES WITH ENTRAPPED MAGNETITE

A Thesis

Submitted to the Graduate Faculty of the
Louisiana State University and
Agricultural and Mechanical College
in partial fulfillment of the
requirements for the degree of
Master of Science in
Biological and Agricultural Engineering

in

The Department of Biological & Agricultural Engineering

by
Carlos Ernesto Astete R.
B.S., Catholic of Valparaiso University, Chile, 1993
M.B.A. Adolfo Ibanez University, Chile, 2000
December 2005

To whom I love, specially

Sara, Felipe, and Camila my lovely family

and

My Parents, Sara and Carlos

ACKNOWLEDGEMENTS

When I came to Louisiana State University, I was apprehensive about the interdepartmental relationships, the academic environment, and the support of the professors. It was really gratifying to find the stimulating, supporting, and friendly environment that gave me the option to develop my research in a high-quality way. I'm very grateful, and I would like to say thank you, to all people that were involved in my research, in a direct or indirect way, who enabled me obtain quality data needed for my thesis research.

A good work needs positive feedback from persons with constant preoccupation, compromise, and defined purposes. I am very thankful and grateful to my major professor Dr. Cristina Sabliov, in the Biological & Agricultural Department, at Louisiana State University. Her constant guidance, cooperation, and advice were a vital part for the completion of my research. Her constant feedback was a wonderful way to implement new ideas and to overcome the problems found in the path of my research. Along the same lines, all committee members were very helpful every time that I required their advice. In special, Dr. Challa Kumar helped with the magnetite formation and modification with oleic acid, and his constant advice was an invaluable source of inspiration. Dr. Todd Monroe was always a source of cooperation, and the access to his laboratory was vital for the success of my research. Thanks also go to Dr. Peter Rein for accepting to be part of my committee and for sharing experience and knowledge.

I am very thankful to Dr. Vladimir Kolesnichenko and Dr. Galina Goloverda, in the chemistry department, at Xavier University, for an invaluable source of cooperation and for giving me the opportunity to use their DLS instrument for size characterization.

The characterization was a crucial part of my research. The access to TGA equipment, whenever I needed it, was possible through Dr. Ioan Negulescu. His help in the data interpretation, his instruction, and advice were very significant.

Dr. Rafael Cueto, in the Chemistry Department, at Louisiana State University, was essential in understanding the size characterization by diffraction light scattering (DLS) technique. He was always open to help me in the DLS characterization.

I am delighted to thank Dr. Cindy Henke for her help and advice in using the transmission electron microscope. Her constant preoccupation to find a way to get better pictures of the nanoparticles was very helpful.

Dr. Paul Russo, Jose Villalobos, and Michelle O'Brien, thanks for your cooperation and help. The peaceful, stimulating, cooperating, and friendly atmosphere of Biological & Agricultural Department was important in the termination of my research and vital for a satisfying work.

Finally, I am very thankful and proud of my family, Sara, Felipe, and Camila, for their constant support and understanding of my research. The long hours required in the information search, nanoparticles formation and characterization, and writing were always easier with their encouragement and cooperation.

TABLE OF CONTENTS

ACKNOWLEDGEMENTS iii

LIST OF TABLES vii

LIST OF FIGURES viii

ABSTRACT x

CHAPTER 1. INTRODUCTION 1
1.1. Method Selection 2
1.2. Materials Selection 3
1.2.1. Polymer (PLGA) 3
1.2.2. Solvent (Ethyl Acetate) 4
1.2.3. Surfactant (SDS) 4
1.3. Processing Parameters 5
1.4. References 5

CHAPTER 2 SYNTHESIS AND CHARACTERIZATION OF PLGA NANOPARTICLES AND MAGNETIC POLYMERIC NANOPARTICLES: A REVIEW 8
2.1. Introduction 8
2.2. Synthesis of PLGA Nanoparticles 9
2.2.1. Emulsion Diffusion Method 9
2.2.2. Salting Out Method 16
2.2.3. Nanoprecipitation (Solvent Diffusion, or Solvent Displacement) Method 19
2.2.4. Emulsion Evaporation Method 25
2.2.4.1. Oil in Water Emulsion Method (Single Emulsion) 27
2.2.4.2. Double Emulsion (w/o/w) Method 32
2.2.5. Important Modifications of Traditional Methods 36
2.2.5.1. Membrane Emulsion Evaporation Method 37
2.2.5.2. Spray Dry Method for Water in Oil 37
2.2.5.3. Spryer Solvent Displacement with Dialysis and Freeze Dryer Stabilization 37
2.2.5.4. Double Emulsion with Emulsion Diffusion 38
2.2.5.5. Dialysis Method for Modified PLGA 39
2.3. Magnetic Polymeric Nanoparticles (MPNPs) 41
2.3.1. Polymerization Methods 41
2.3.2. Chemical and Physical Entrapment of Magnetite 48
2.3.2.1. Chemical Entrapment and Surface Modification of Magnetite: 48
2.3.2.2. Physical Entrapment 48
2.3.3. Surface Modification 49
2.4. Characterization 50
2.4.1. Morphology 50
2.4.2. Size and Size Distribution 51

2.4.3. Surface Properties 51
2.4.4. Active Component Entrapment 52
2.4.5. Other Techniques 52
2.5. Conclusions 53
2.6. References 54

CHAPTER 3. SYNTHESIS OF POLY(DL-LACTIDE-CO-GLYCOLIDE) NANOPARTICLES WITH ENTRAPPED MAGNETITE 68
3.1. Introduction 68
3.2. Objectives 69
3.3. Materials and Methods 69
3.3.1. Materials 69
3.3.2. Nanoparticles Preparation 70
3.3.2.1. Hydrophobic Magnetite 70
3.3.2.2. Single Emulsion Evaporation with Hydrophobic Magnetite 70
3.3.3. Nanoparticles Characterization 71
3.3.3.1. Morphology and Size 71
3.3.3.2. Size and Zeta Potential 71
3.3.3.3. Colorimetric Method for Iron Content 71
3.3.3.4. Thermogravimetric Analysis 72
3.3.3.5. Statistical Analysis 72
3.4. Results and Discussions 72
3.4.1. Single Emulsion Evaporation with Hydrophobic Magnetite 72
3.4.1.1. Morphology and Magnetite Distribution into the Polymeric Matrix 72
3.4.1.2. The Effect of Synthesis Parameters on Nanoparticle Physical Characteristics 76
3.4.1.3. Yield of Nanoparticles, Entrapment Efficiency of MOA, Remaining SDS, and Oleic Acid Amount over Magnetite 84
3.5. Conclusions 87
3.6. References 87

CHAPTER 4. CONCLUSIONS 90

CHAPTER 5. FUTURE WORK 91

APPENDIX
A.AUTHORIZATION FOR REPRODUCTIONS 93

B.STANDARD CURVE FOR IRON DETECTION 101

C.SIZE MEASUREMENTS WITH DLS (MALVERN ZETASIZER NANOSERIES) 102

D.STATISTICS ANALYSIS OF DATA 126

VITA 150

LIST OF TABLES

Table 2.1. Summary of important parameters for PLGA nanoparticles formation 42

Table 3.1 Size of PLGA nanospheres as a function of sonication wave amplitude 79

Table 3.2. Effect of sonication time of MOA on the PLGA nanosphere with magnetite entrapped in the polymeric matrix 80

Table 3.3. Mean size, polydispersity index, and zeta potential of nanoparticles for different molecular weights and magnetite concentration BEFORE dialysis..... 82

Table 3.4. Mean size, polydispersity index, and zeta potential of nanoparticles for different molecular weights and magnetite concentration AFTER dialysis 83

Table 3.5. Entrapment of magnetite oleic acid and SDS residue in nanoparticles 85

LIST OF FIGURES

Figure 2.1. Effect of PLGA concentration on the mean particle size of PLGA nanoparticles (PVA concentration of 2.5 % w/v). Reproduced from Ref. Kwon et al. [18] 10

Figure 2.2. a. The influence of surfactant on the mean size of PLGA nanoparticles. b. Surface tension of DMAB and PVA solution as a function of concentration (wt%). Reproduced from Ref. Kwon et al. [18]..... 12

Figure 2.3. Influence of the stirring rate on the main nanoparticle size (Aqueous phase: 10% (w/w) of Mowiol 4-88 and 60% (w/w) $MgCl_2$, organic phase: 17% (w/w) of polymer in THF (mean ± SD, n=3). Reproduced from ref. Konan et al. (2002) 19

Figure 2.4. TEM micrographs of blank and plasmid-loaded (A) PLGA: poloxamer (Pluronic F68) and (B) PLGA:poloxamine (Tetronic 908) blend nanoparticles. Reproduced from Ref. Csaba et al. [30]. 24

Figure 2.5. Efficiency of drug (U-86983) entrapment into PLGA nanoparticles by changing the pH of the aqueous phase from neutral to basic. Reproduced from Song et al. [60]. 31

Figure 2.6. Scanning electron microphotographs of 50:50 PLGA nanoparticles prepared from (a) DMAc or (b) acetone as a function of the initial solvent. Reproduced from ref. Jeong et al. [85]. 40

Figure 3.1. Surface modified magnetite with oleic acid (MOA). The MOA nanoparticle size was around 15 nm. The appearance of clustering was common by observed 73

Figure 3.2. PLGA (molecular weight (M.W.) 45 to 75 kDa) nanospheres with 4% MOA theoretical loading. The black circles are representing the MOA entrapped in the polymeric matrix. Clustering was present, and some PLGA nanoparticles are free of MOA. 73

Figure 3.3. PLGA (M.W. 45 to 75 kDa) nanospheres with 8% MOA theoretical loading. The black dots represent MOA entrapped in PLGA nanospheres. 74

Figure 3.4. Medium molecular weight (M.W. 45 to 75 kDa) PLGA nanospheres with 4% w/w of MOA theoretical loading. The big dark sphere (inside the dotted circle) manifests the presence of MOA. The appearance of clustering is observed in the surrounded PLGA nanospheres. 74

Figure 3.5. Low molecular weight PLGA nanospheres with 4% w/w of MOA theoretical loading. The black dots represent MOA entrapped in the PLGA nanoparticle. 75

Figure 3.6. Medium molecular weight PLGA (40 to 75 kDa) nanosphere with 4% w/w of MOA theoretical loading. The magnetite is clearly showed in the center of this nanosphere by darker spots. 75

Figure 3.7. Effect of SDS concentration on the size and polydispersity index of PLGA nanospheres (PLGA 5% w/v, molecular weight of 5 to 10 kDa, and copolymer molar ratio of 50:50), n = 2 77

Figure 3.8. Size distribution and undersize curve for PLGA nanospheres (PLGA 50:50, molecular weight 5 to 15 kDa). Three runs at 25 °C with detector at 70°. a. SDS concentration 0.4 mg/ml (replace) and b. SDS concentration of 4.8 mg/ml 78

Figure 3.9. Effect of PLGA and SDS concentration on the nanospheres size (PLGA molecular weight of 5 to 10 kDa, copolymer molar ratio of 50:50) 79

Figure 3.10. PLGA nanospheres size and polydispersity measured by DLS (at 70°, 25 °C). n = 3 82

Figure 3.11. a. SDS profiles acquired by TGA. Temperature was varied from 25 to 600 °C. A residue of 24.75% composed of sulfate and sodium group of the SDS molecule was found at 600 ºC. This residue present in all samples was used to calculate the amount of SDS remaining in the nanoparticles. b. A typical curve for the MPNPs formed with low molecular weight PLGA (CA64). The residue at 600 °C was due to the sodium and sulfate groups of SDS, and magnetite. 85

Figure 3.12. TGA data for magnetite and MOA (magnetite plus oleic acid). The initial decrease was due to the presence of water (approximately 2 wt% for magnetite and 1.15% for MOA). The 2.74 wt% and 3.64 wt% remaining could be explained by ammonium used in the magnetite formulation. 86

ABSTRACT

The goal of the research was to synthesize magnetic polymeric nanoparticles (MPNPs) under 100 nm in diameter, for future drug delivery applications. The thesis is divided into two main sections. In the first section, a quantitative, and comprehensive description of the top-down synthesis techniques available for poly(lactide-co-glycolide) (PLGA) and magnetic polymeric nanoparticles (MPNPs) formation is provided, as well as the techniques commonly used for nanoparticle characterization. In the second part, a novel way to form MPNPs is presented. The emulsion evaporation method was selected as the method of choice to form poly(lactide-co-glycolide) (PLGA) nanoparticles with entrapped magnetite (Fe_3O_4) in the polymeric matrix, in the presence of sodium dodecyl sulfate (SDS) as a surfactant. The magnetite, a water soluble compound, was surface functionalized with oleic acid to ensure its efficient entrapment in the PLGA matrix. The inclusion of magnetite with oleic acid (MOA) into the PLGA nanoparticles was accomplished in the organic phase. Synthesis was followed by dialysis, performed to eliminate the excess SDS, and lyophilization. The nanoparticles obtained ranged in size between 38.6 nm and 67.1 nm for naked PLGA nanoparticles, and from 78.8 to 115.1 nm for MOA entrapped PLGA nanoparticles. The entrapment efficiency ranged from 57.36% to 91.9%. The SDS remaining in the nanoparticles varied from 51.02% to 88.77%.

CHAPTER 1. INTRODUCTION

January 2005, FDA approves ABRAXANE® for breast cancer treatment, the first nanoparticle system for drug delivery [1, 2]. This system, based on nanoparticle Albumin-bound (nab®) Paclitaxel, showed better and faster rate of shrinking tumors in 460 patients with metastic breast cancer, almost double compared with solvent-based Taxol®. The application of nanotechnology to the health market is significant, considering the extensive research developed in this area during the last 20 years.

A basic requirement for the use of nanoparticles and other synthetic systems as drug delivery systems for human therapy is their biodegradability and biocompatibility. Another challenge for the use of nanoparticles as drug delivery systems is to minimize their side effects in the biological system in which dispersed. A controlled size distribution (monodisperse distribution of size), for accurate drug administration, is a central need for the use of nanoparticles in drug delivery systems. Moreover, the absence of toxic residues in the final nanosystem is required, and therefore stronger restrictions to the type of methods used for nanoparticles formation exist. Additionally, the stability of the nanoparticles should be addressed if parenteral administration of the nanoparticle is used. The aggregation process due to dispersion forces (i.e. electrostatic, hydrogen bonding, hydrophilic/hydrophobic, steric-Van der Waals) is the principal drawback of nanoparticle use in drug delivery. Therefore, the understanding of the complexity of the nanosystem, the biological system, and the interactions between the two is a basic requirement for successful implementation of new nano-systems designed for drug delivery.

The goal of the present research was to form nanoparticles from a preformed polymer (poly(lactide-co-glycolide)) with entrapped magnetite. The thesis is divided in two main sections. The first section contains a review of PLGA and magnetic polymeric nanoparticles (MPNPs) synthesis and characterization. A detailed description of the important parameters affecting the nanoparticle size is also provided. The second section of the thesis is focused on the entrapment of magnetite into the PLGA matrix. The formation process of MPNPs nanoparticles by emulsion evaporation method, the effect of surfactant, and the magnetite entrapment results are explained in detail. The selection of

the method, materials, and processing parameters to form MPNPs (Chapter 3) is based on the extensive literature cited in the first section of the thesis (Chapter 2), as follows.

1.1. Method Selection

Two main procedures can be followed to form polymeric nanoparticles, namely top-down and bottom-up techniques. The top-down methods use size reduction to obtain controlled-size nanoparticles. This size reduction is based on the application of strong shear stress by wave sound emission (sonication), high pressure (microfluidization), and high speed agitation (homogenization). The bottom-up methods start from individual molecules to form nanoparticles, by polymerization. The polymerization methods commonly used are emulsion polymerization (water in oil, oil in water, and polymerization in bicontinuous structures), dispersion polymerization, and interfacial polymerization [3]. Monomers, initiators, additives, and solvent are the basic chemical components used in the polymerization methods. The main drawbacks of the bottom-up methods are the presence of residual sub-products in the final nanoparticles that can impart toxicity to the nanoparticles, the difficulty in the prediction of polymer molecular weight, affecting the biodistribution and release behavior of the drug from the nanoparticle; and the possibility for drug inhibitions due to interactions, or cross reactions of the drug with activated monomers and H^+ ions present during polymerization [4]. To overcome these limitations, top-down methods were developed using naturals and synthetic polymers. The emulsion evaporation, salting out, nanoprecipitation, and emulsion diffusion are the main top-down methods used to form polymeric nanoparticles. During the last years, significant modifications of these methods have been developed (see Chapter 2 for details) in an attempt to avoid the use of toxic solvents and surfactants, to improve drug entrapment efficiency and nanoparticle stability, and to more efficiently use energy in droplet size reduction. All these methods involve two liquid phases, the organic phase which can dissolve the polymer and the other hydrophobic components, and the continuous aqueous phase.

Each synthesis method has advantages and disadvantages as described in detail in Chapter 2. Emulsion evaporation, was selected as the method of choice in the present research due to its advantages described as follows. The versatility and flexibility of the method allows for the use of different polymers and solvents. Emulsion evaporation

permits higher polymer concentration per batch production improving the nanoparticle yield by batch. It can be used for entrapment of hydrophobic and hydrophilic drugs. The hydrophobic drugs use oil in water (o/w) emulsion. The hydrophilic drugs require the use of double emulsion (w/o/w), and the first aqueous phase dissolves the hydrophilic drug. The fast evaporation rate of the solvent permits a reduction in the processing time [4, 5, 6, 7]; moreover the evaporation rate may be used to control the nanoparticle size as compared with other methods where evaporation follows the nanoparticle formation.

1.2. Materials Selection

1.2.1. Polymer (PLGA)

A wide spectrum of synthetic and natural polymers is available for nanoparticle formation, but their biocompatibility and biodegradability are the major limiting factors for their use in the drug delivery area. Natural polymers are more restricted due to variation in their purity. Also, some natural polymers require crosslinking, which can inactivate the entrapped drug [8]. Synthetic polymers, on the other hand, offer better reproducibility of the chemical characteristics of the synthesized nanoparticles as compared to the natural polymers. Synthetic polymers from the ester family, such as poly(lactic acid), poly(β-hydroxybutyrate), poly(caprolactone), poly(dioxanone), or other families such as poly(cyanoacrylates), poly(acrylic acid), poly(anhydrides), poly(amides), poly(ortho esters), poly(ethylene glycol), and poly(vinyl alcohol) are suitable for drug delivery due to their biodegradability, special release profiles and biocompatibility [9].

Poly(lactide-co-glycolide acid) (PLGA), from the ester family, has been widely used in the biomedical industry as a major components in biodegradable sutures, bone fixation nails and screws [10, 11]. It is a well-characterized polymer, its degradation sub-products are non toxic, it provides controlled drug release profiles by changing the PLGA copolymer ratio which affects the crystallinity (low crystallinity, more amorphous polymer means more fast degradation) of PLGA [9, 10, 11, 12, 13]. For these reasons, PLGA has been selected as the polymer of choice in the present research. PLGA of different molecular weights (from 10 kDa to over 100 kDa) and different copolymer molar ratios (50:50, 75:25, and 85:15) is available on the market. Molecular weight and copolymer molar ratio influence the degradation process and release profile of the drug

entrapped. In general, low molecular weight PLGA with higher amounts of glycolic acid offer faster degradations rates [13, 14].

1.2.2. Solvent (Ethyl Acetate)

The top-down method requires the dissolution of the polymer in the aqueous or organic phase. The solvent election is restricted to the method used; for example, nanoprecipitation and emulsion diffusion use water-soluble solvents (i.e. acetone, benzyl alcohol), and emulsion evaporation requires water immiscible solvents. The method selected to form the nanoparticles was emulsion evaporation, in which the polymer (PLGA) was dissolved in the organic phase (solvent). The chlorinate solvents have been extensively used with this method to dissolve the PLGA (i.e. methylene chloride, dichloromethane, chloroform), but their toxicity and inflammability are of concern [15, 16]. A solvent that could be used as an alternative to chlorinate solvents is ethyl acetate. The low toxicity, low boiling point (77 °C) and inflammability are the main advantages of using ethyl acetate to dissolve the polymer. Because ethyl acetate is partially water soluble however, it is required to saturate the solvent with water before emulsification [7, 17].

1.2.3. Surfactant (SDS)

The stability of the organic droplet (ethyl acetate and PLGA) in water, during the emulsification step, is insured by the addition of surfactants. A wide spectrum of surfactants are available for emulsion stabilization, ionic surfactants (cationic, anionic, zwitterionic) and nonionic surfactants. The nonionic surfactants are macromolecules formed by copolymers or tripolymers (amphiphilic) which can form stable micelles due to the hydrophobic hydrophilic interactions with the two phases. The anionic and cationic surfactants use electrostatic interactions to stabilize emulsions. The major nonionic surfactants used in the emulsion evaporation method are poly(vinyl alcohol) (PVA), poloxamer and poloxamines family, pluronic family (F68, F127, and others), sodium cholate, and tween 80. The formation of amphiphilic PLGA molecule has been studied to eliminate the surfactant addition during the emulsification step; this is accomplished by the attachment of a hydrophilic polymer (covalent link) to hydrophobic PLGA. Some of the common hydrophilic polymers used are poly(ethylene glycol) (PEG), chitosan, and poly(ethylene oxide) (PEO) [18, 19]. Anionic or cationic surfactants permit formation of

micelles under 100 nm [20, 21] because of the electrostatic interaction (and other properties like value of packing number, HLB value, surface tension, and morphology). Sodium dodecyl sulfate (SDS), an anionic surfactant, was selected because it has high HLB value (40) and forms micelles with sizes ranging between 20 to 150 nm in oil in water emulsion [7, 21, 22].

1.3. Processing Parameters

The method and material selection, as well as the synthesis parameters play an important role in forming nanoparticles of controlled physical and chemical properties. Process parameters like phase volume ratio, sonication time and amplitude, amount of surfactant, PLGA concentration, evaporation conditions, and purification play a key role in determining the final nanoparticle size. Synthesis parameters were selected as follows. The phase volume ratio used was 20%, value based on previous works [7, 23, 24]. In the sonication step (droplet size reduction), two main parameters were controlled, the amplitude and the sonication time. The amplitude, defined as the peak to peak displacement at the probe tip, and the sonication time were selected based on the work of Landfester, K. [25], which showed that amplitudes over 30% formed small nano-droplets for a sonication time of 500 seconds. The sonication time selected was 10 minutes with 39% amplitude, which were proven experimentally to form small size nanoparticles (See Chapter 3). The PLGA concentration used was 5 %w/v (mg PLGA/ml ethyl acetate) based on previous published studies [23, 24, 26]. Dialysis was selected as a purification method to reduce the excess of SDS as opposed to ultracentrifugation, because of the aggregation of the nanoparticles observed when centrifugation was used. The time of dialysis and number of washes was based on the published work of Jeong et al. [27, 28].

1.4. References

1. Abraxis Oncology. Home page, 2005. http://www.abraxane.com/PAT/About ABRAXANE.htm.

2. News-Medical.Net. Launch date announced for Abraxane to treat metastatic breast cancer, Pharmaceutical news, 25-Jan-2005. http://www.news-medical.net/?id=7489.

3. Nakache, E., Poulain, N., Candau, F., Orecchioni, A.M., and Irache, J.M., In the Handbook of nanostructured materials and nanotechnology. (E. Nalwa, H.S. ed.) Academic Press, **5**, 577-635 (2000).

4. De Jaeghere, F., Doelker, E., Gurny, R., In the Encyclopedia of control drug delivery. (E. Mathiowitz ed.) John Wiley & Sons, Inc. New York, v. 2: p. 641-664 (1999).

5. Chung, T.W., Huang, Y.Y., Liu Y.Z., Effects of the rate of solvent evaporation on the characteristics of drug loaded PLLA and PDLLA microspheres. International Journal of Pharmaceutics, **212**, 161-169 (2001).

6. Chung, T.W., Huang, Y.Y.; Tsai, Y.L., and Liu Y.Z., Effects of solvent evaporation rate on the properties of protein-loaded PLLA and PDLLA microspheres fabricated by emulsion-solvent evaporation process. Journal of Microencapsulation, **9**:463-471 (2002).

7. Desgouilles, S., Vauthier, C., Bazile, D., Vacus, J., Grossiord, JL., The design of nanoparticles obtained by solvent evaporation: a comprehensive study. Journal of American Chemical Society, **19**:9504-9510 (2003).

8. Hans, M.L., Lowman, A.M., Biodegradable nanoparticles for drug delivery and targeting. Current Opinion Solid State Matter Science, **6**, 319-327 (2002).

9. Ghosh, S., Recent research and development in synthetic polymer-based drug delivery systems. Journal of Chemical Reaserach, 241-246 (2004).

10. Moghimi, S.M., Hunter, A.C., and Murray, J.C., Long-circulating and target-specific nanoparticles: Theory to practice. Pharmacological Reviews, **53**, 283-318 (2001)

11. Gombotz, W., and Pettit, D., Biodegradable polymers for protein and peptide delivery, review. Bioconjugate Chemistry, **6**, 332-351 (1995).

12. Bala, I., Haribaran, S., and Kumar, R., PLGA nanoparticles in drug delivery: The state of the art. Critical Reviews in therapeutic Drug Carrier Systems, **21**, 387-422 (2004).

13. Anderson, J.M., Shive, M.S., Biodegradation and biocompatibility of PLA and PLGA microspheres. Advanced Drug Delivery Reviews, **28**, 5-24 (1997).

14. Alexis, F., Factors affecting the degradation and drug-release mechanism of poly(lactide acid and poly(lactic acid-co-glycolic acid). Polymer International, **54**, 36-46 (2005).

15. Quintanar-Guerrero, D., Allemann, E., Fessi, H., and Doelker, E., Preparation technique and mechanism of formation of biodegradable nanoparticles from preformed polymers. Drug Development and industrial Pharmacy, **24**(12): 1113-1128 (1998).

16. Allemann, E., Gurny, R., Doelker, E., Drug-release nanoparticles-preparation methods and drug targeting issues. European Journal of Pharmacy and biopharmacy, **39**(5): 173-191 (1993).

17. Blanco M.D., Alonso, M.J., Development and characterization of protein-loaded poly(lactide-co-glycolide) nanospheres. European Journal of Pharmaceutics and Biopharmaceutics, **43**, 287-294 (1997).

18. Gref, R., Luck, M., Quellec, P., Marchand, M., Dellacherie, E., Harnisch, S., Blunk, T., and Muller, R.H., Stealth corona-core nanoparticles surface modified by polyethylene glycol (PEG): influences of the corona (PEG chain length and surface density) and of the core composition on phagocytic uptake and plasma protein adsorption. Colloids and Surfaces B: Biointerfaces, **18**, 301-313 (2000).

19. Csaba, N., Caamano, P., Sanchez, A., Dominguez, F., Alonso, M.J., PLGA:poloxamer and PLGA:poloxamine blend nanoparticles: new carriers for gene therapy. Biomacromolecules, **6**, 271-278 (2005).

20. Landfester, K., On the stability of liquid nanodroplets in polymerizable miniemulsions. Journal of Dispersion Science and Technology, **1-3**, 167-173 (2002).

21. Landfester, K., Miniemulsions for nanoparticle synthesis. Topics in Current Chemistry, **227**, 75-124 (2003).

22. Tiarks, F., Willert, M., Landfester, K., Antonietti, M., The controlled generation of nanosized structures in miniemulsions. Progress in Colloid Polymer Science, **17**, 110-112 (2001).

23. Pietzonka, P., Rothen-Rutishauser, B., Langguth, P., Wunderli-Allenspach, H.; Walter, E., Merkle, H.P., Transfer of lipophilic markers from PLGA and polystyrene nanoparticles to caco-2 monolayers mimics particle uptake. Pharmaceutical Research, **19** (5), 595-601 (2002).

24. Panyam, J., Zhou, W.Z., Prabha, S., Sahoo, S.K., Labhasetwar, V., Rapid endo-lysosomal escape of poly(DL-lactide-co-glycolide) nanoparticles: implications for drug and gene delivery. *The FASEB Journal*, **16**, 1217-1226 (2002).

25. Landfester, K., Quantitative considerations for the formulation of miniemulsions. Progress in Colloid Polymer Science, **117**, 101-103 (2001).

26. Gutierro, I., Hernandez, R.M., Igartua, M., Gascon, A.R., Pedraz, J.L., Size dependent immune response after subcutaneous, oral and intranasal administration of BSA loaded nanospheres. Vaccine, **21**, 67-77 (2002).

27. Jeong, Y.I.; Cho, C.; Kim, S.; Ko, S.; Kim, S.; Shim, Y., and Nah, J., Preparation of poly(DL-lactide-co-glycolide) nanoparticles without surfactant. Journal of Applied Polymer Science, **80**, 2228-2236 (2001).

28. Jeong, Y.I., Shim, Y.H., Song, K.C., Park, Y.G., Ryu, H.W., Nah, J.W., Testosterone-encapsulated surfactant-free nanoparticles of poly(DL-lactide-co-glycolide): preparation and release behavior. Bulletin of Korean Chemical Society, **23**, 11, 1579-1584 (2002).

CHAPTER 2. SYNTHESIS AND CHARACTERIZATION OF PLGA NANOPARTICLES AND MAGNETIC POLYMERIC NANOPARTICLES: A REVIEW[1]

2.1. Introduction

Synthetic polymers and natural macromolecules have been extensively researched as colloidal materials for nanoparticle production designed for drug delivery. Synthetic polymers have the advantage of high purity and reproducibility over natural polymers. Among the synthetic polymers, the polyesters family (i.e. poly(lactic acid) (PLA), poly(e-caprolactone) (PCL), poly(glycolic acid) (PGA)) are of interest in the biomedical area because of their biocompatibility and biodegradability properties. In particular, poly(lactide-co-glycolide) (PLGA) has been FDA approved for human therapy [1].

The size and size distribution of the PLGA nanoparticles and magnetic polymeric nanoparticles (MPNPs) among other physical characteristics, are affected by the technique used for the nanoparticle production and the pertinent synthesis parameters, i.e. PLGA molecular weight, the addition of active components, surfactants, and other additives [2-8]. The current review is designed to present the reader with comprehensive information on PLGA nanoparticle synthesis, control of nanoparticle properties (i.e. size, size distribution, zeta potential, morphology, hydrophobicity/hydrophilicity, drug entrapment) by manipulation of the synthesis parameters, methods for NPMPs synthesis, and methods available for nanoparticle characterization. The words *nanoparticles* and *nanospheres* will be used interchangeably in this review based on the term preferably used by the cited authors; both terms denote particles smaller than 1 μm (1000 nm).

A number of reviews published in the literature focused on polymeric nanoparticle synthesis in general and PLGA nanoparticles in particular [7, 9-16]. The current review differs from the aforementioned reviews in several ways. First, it focuses specifically on PLGA nanoparticles, covering topics such as synthesis, size control and characterization. Second, it addresses in detail all top-down techniques available for PLGA nanoparticle formation. Third and last, in-depth discussions of available methods

[1] Reprinted with permission from "Brill Academic Publishers"

to control the size, size distribution, surface charge, and other nanoparticle properties are also presented.

2.2. Synthesis of PLGA Nanoparticles

Methods available for PLGA nanoparticle synthesis can be divided into two classes: bottom-up and top-down techniques. The bottom-up techniques such as emulsion or microemulsion polymerization, interfacial polymerization, and precipitation polymerization, employ a monomer as a starting point. Emulsion evaporation, emulsion diffusion, solvent displacement, and salting out are top-down techniques, in which the nanoparticles are synthesized from the pre-formed polymer. Table 1 summarizes the nanoparticles characteristics (size, nanoparticle yield) formed by different methods (emulsion diffusion, salting out, nanoprecipitation, emulsion evaporation, dialysis, solvent diffusion), as a function of important parameters (polymer concentration, copolymer ratio, polymer molecular weight, surfactant concentration, solvent used, phase volume ratio). The data is catalogued according to the method used for nanoparticle formation.

2.2.1. Emulsion Diffusion Method

In this synthetic scheme, the polymer (PLGA) is dissolved in an organic phase (e.g., benzyl alcohol, propylene carbonate, ethyl acetate), which must be partially miscible in water. The organic phase is emulsified with an aqueous solution of a suitable surfactant (i.e. anionic sodium dodecyl sulfate (SDS), non-ionic polyvinyl alcohol (PVA), or cationic didodecyl dimethyl ammonium bromide (DMAB), under stirring. The diffusion of the organic solvent and the counter diffusion of water into the emulsion droplets induce polymer nanoparticle formation [11].

Important parameters that affect the nanoparticle size synthesized by emulsion evaporation are: PLGA copolymer ratio, polymer concentration, solvent nature, surfactant polymer molecular weight, viscosity, phase ratios, stirring rate, solvent nature, temperature and flow of water added.

- Lactide/glycolide ratio

The common PLGA copolymer ratios (lactide/glycolide molar ratio) used are 50:50 and 75:25. The difference detected in nanoparticles size is minimal when different

copolymer ratios are used. Konan et al. [17] obtained nanoparticles with a mean size of 93 nm for 50:50 PLGA and 95 nm for 75:25 PLGA.

- PLGA concentration

The data obtained by Kwon et al. [18] showed the effect of PLGA concentration on the nanoparticle size. For an increased PLGA concentration from 1% to 4% w/v, an increase in the mean nanoparticle size from 205 nm to 290 nm was observed (Figure 2.1); PVA concentration was maintained at 2.5% w/v, and the solvent used was propylene carbonate (PC) in all experiments. The work of Lee et al. [19] showed similar results. At a fixed agitation (homogenizer speed 15000 RPM and agitator speed 400 RPM), the mean nanoparticle size obtained was 120 nm for 1% w/v PLGA, and 230 nm for 5% w/v PLGA. The solvent used was ethyl acetate, and the surfactant was 5% of Pluronic F-127 in aqueous suspension.

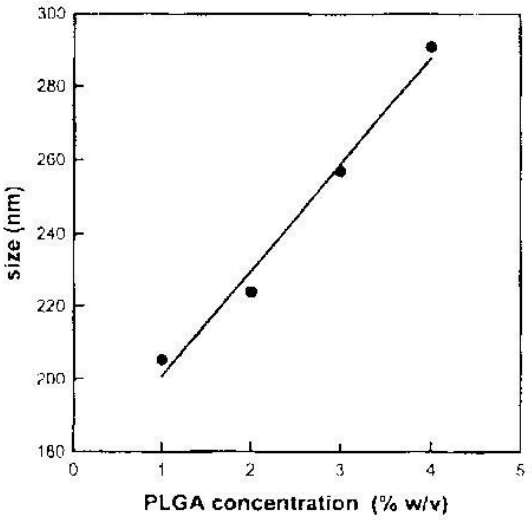

Figure 2.1. Effect of PLGA concentration on the mean particle size of PLGA nanoparticles (PVA concentration of 2.5 % w/v). Reproduced from Ref. Kwon et al. [18]

- Solvents (organic phase)

The nature of the organic phase affects the final nanoparticle size. This is clearly shown by Choi et al. [20]. Ethyl acetate, methyl ethyl ketone, propylene carbonate, and benzyl alcohol were used to dissolve the PLGA (75:25 with a molecular weight from 75 to 120 kDa), and the continuous phase contained the surfactant poloxamer 188. The smaller nanosphere size was 120 nm when ethyl acetate was used, and it was close to the

nanosphere size obtained with methyl ethyl ketone, 125 nm. The highest size nanoparticles of 260 nm were obtained with benzyl alcohol as the organic solvent. The experiments were carried out under a constant PLGA concentration of 2% w/v.

- Thermodynamic parameters

Choi et al. [20] studied the exchange solvent ratio, solubility, and polymer-solvent interaction in a quest for the right method to decrease nanoparticle size. The PLGA concentration used was 2 mg/ml, with four different solvents (ethyl acetate, methyl ethyl ketone, propylene carbonate, and benzyl alcohol). Ethyl acetate solvent formed the smallest nanospheres (approx. 120 nm in size). The authors suggest that solvents with low exchange ratio, ratio between diffusion from solvent to water and vice versa, and high polymer-solvent interaction parameter form small nanoparticles due to small supersaturation region produced.

- Surfactants (or stabilizer)

A wide variety of surfactants can be used for stabilization of the organic droplets, which contain the polymer. The effect of PEG, tween 80, gelatin, dextran, pluronic L-63, PVA, and DMAB as surfactants (for nanoparticle stabilization) was evaluated by Kwon et al. [18]. PVA and DMAB (a cationic surfactant) were the only surfactants that formed nanoparticles with the emulsion diffusion method. The smaller mean size of PLGA nanoparticles was obtained when DMBA was used (Figure 2.2.a). The mean size was 76 nm for a concentration of 2% w/v of DMAB. The mean PVA nanoparticle size was 210 nm for 5% w/v. When the DMAB concentration was increased from 2 to 4% w/v, a slight decrease in size of the nanosphere was noticed (from 80 nm to 75 nm). The smaller nanoparticle size formed with DMAB is attributed to the more pronounced surface tension reduction as compared with PVA, 22 dyne/cm at 10^{-2} % w/v for DMAB versus 37 dyne/cm at 10^{-1} % w/v for PVA (Figure 2.2.b).

Ravi Kumar et al. [21] studied the effect of PVA, and a mix of PVA and chitosan (needed to form positive charges over the surface of the nanospheres) in an attempt to improve the entrapment efficiency of DNA (DNA has negative charges allowing its migration to the external phase due to the repulsion with the negative charges of PLGA formed nanospheres in the presence of PVA).

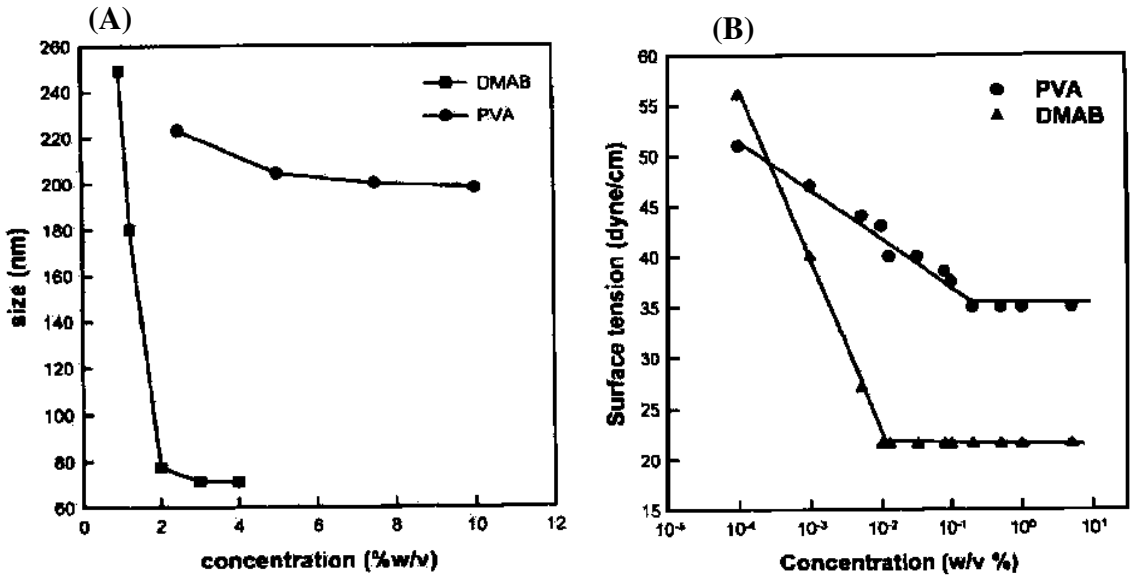

Figure 2.2. a. The influence of surfactant on the mean size of PLGA nanoparticles. b. Surface tension of DMAB and PVA solution as a function of concentration (wt%). Reproduced from Ref. Kwon et al. [18].

When PVA was used alone, the mean nanoparticle size was 111.7 ± 4.2 nm. The addition of chitosan alone did not allow formation of nanospheres, so the addition of a blend of PVA and chitosan was crucial for the formation of stable nanospheres with a positive surface charge. In a further work, Ravi Kumar et al. [22] prepared two surfactant blends and tested the DNA transfection in vivo. The first blend contained chitosan and PVA, and the second blend was a mix of chitosan, PVA, and PEG. The mean size was 180 ± 11 nm for both systems, with a zeta potential of 10 mV for the former, and 7 mV for the latter. They attributed the decrease of zeta potential to PEG chains present in the second blend, but there is no mention if there is a statistical difference between the data points.

- Viscosity of continuous and discontinuous phase

The viscosity of the continuous and discontinuous phase is an important parameter to take into account because it affects the diffusion process, a key step in forming smaller nanoparticles. Ahlin et al. [23] prepared dispersed phases with different viscosities by changing the PLGA molecular weight. A solution of 5% w/w PLGA in benzyl alcohol had viscosities of 0.03 Pa s, 0.036 Pa s, and 0.046 Pas for 50:50 PLGA (12000 Da), 75:25 PLGA (12000 Da), and 75:25 PLGA (63000 Da), respectively.

Nanoparticles with mean size of 175 nm, 220 nm, and 280 nm, were obtained by increasing viscosity of the organic solution from 0.03 to 0.046 Pa s. The viscosity of the continuous phase was determined to be 1.5 Pa s, 5 Pa s, and 13 Pa s for 10%, 15% and 20% w/w of aqueous PVA solution, respectively. The mean size of nanoparticles synthesized with 10% of PVA was 310 nm and 170 nm with 20% PVA. The conclusion reached was that the size of the nanoparticles increases with an increase in the viscosity of the dispersed phase, whereas a decrease in the nanoparticle size was observed for a more viscous continuous phase. Other polymers with the same viscosity should be studied for an accurate analysis of the viscosity effect on the nanoparticle size.

- Homogenizer speed and agitation speed

The homogenization of the oil-in-water emulsion is another important step in forming smaller nanospheres. Lee et al. [19] evaluated the effect of homogenizing speed (when the organic phase is added to the aqueous suspention). The speed range tested was from 5000 to 15000 RPM for a suspension with 5% w/v of PVA for a fixed time (7 min). A mean size of 200 nm was obtained for speeds up to 11500 RPM, and at higher revolutions (22000 RPM) the mean nanoparticle size decreased up to 120 nm with no further decrease in size at higher RPM.

Agitation is applied during the addition of excess of water to improve solvent diffusion and nanosphere precipitation. The nanoparticle size was reduced from 115 nm to 90 nm when the agitation speed was increased from 200 RPM to 600 RPM; increasing the agitation speed further to 1000 RPM did not affect the particle size [19]. In the work of Ravi Kumar et al. [21, 22], nanoparticles of 884 ± 17 nm mean size were synthesized when the emulsion was not homogenized and no additional water was added. When homogenization was included, the mean size decreased to 403 ± 8 nm. The mean size was further improved to 181 ± 3 nm by stirring at 1000 RPM and applying homogenization at 13500 RPM. In the studies mentioned above there is no description of the system hydrodynamics which could affect the nanosphere size, so the process scale up and reproducibility of the experiment should be complicated and reconsidered.

- Addition rate of water

The addition rate of water to allow the solvent diffusion was studied by Kwon et al. [18]. No significant size difference was detected for water added at 0.03 mL/s and 16

mL/s. When DMAB was used, the mean size was 76 nm and 78 nm at 0.03 mL/s and 16 mL/s, respectively. When PVA was used, the mean size was 220 nm and 204 nm, for 0.03 mL/s and 16 mL/s, respectively.

- Temperature of the water added for solvent diffusion

An important size reduction of the nanoparticles can be achieved by careful control of the water temperature added to improve the diffusion of the solvent. Kwon et al. [18] worked with PVA (5% w/v) and DMAB (2% w/v) with a constant water addition rate of 16 mL/s. For both surfactants, the mean size of nanoparticles was decreased with an increase in the temperature of the water added. For DMAB, the smaller size obtained was 65 nm (polydispersity of 0.056 ±0.019) at 60 °C, and the larger size was 78 nm (polydispersity of 0.023 ±0.012) at 25 °C. For PVA, the smaller size obtained was 170 nm (polydispersity of 0.063 ±0.034) at 60 °C, and the higher size was 204 nm (polydispersity of 0.064 ±0.028) at 25 °C. The main drawback of this approach is the effect of the water temperature on the polymer structure, because the T_g (glass transition temperature) of PLGA is lower than 60 °C. It is important to understand the effect of temperature on the polymer matrix when the working temperature is 60 °C and higher.

- Cryoprotectant

The most common way to stabilize a preparation of nanospheres is lyophilization. The sample is pre-frozen at low temperatures to form small crystals of water, important in that the water crystal disrupts the stabilizer shell around the particle, which results in clustering in the nanoparticle resuspension. Konan et al. [17] worked with trehalose as a lyoprotectant to preserve the nanoparticle size after lyophylization. The weight ratio used was of 2:1 trehalose to nanoparticles. The nanospheres size varied from 120 nm to 140 nm with the addition of trehalose for the 50:50 PLGA copolymer ratio, and from 125 nm to 200 nm for the 75:25 PLGA copolymer ratio. The re-suspension was carried in different mediums (distilled water, phosphate buffer saline (PBS), fetal bovine serum (FBS), human plasma, waymouth grouth) by 30 seconds of manual agitation. The only re-suspension media that showed increase in size was human plasma (from 125 nm to 155 nm for nanospheres prepared with 50:50 PLGA copolymer ratio). Ahlin et al. [24] worked with the same ratio of nanoparticles to trehalose (1:2 w/w for nanoparticles to trehalose) for entrapment of enalaprilat. The mean nanoparticle size before lyophilization

was 204 ± 6 nm. Nanoparticles undergoing lyophilization without trehalose measured 283 ± 65 nm. The nanoparticle mean size was 255 ± 30 nm and 210 ± 12 nm for nanoparticle to trehalose ratios of 1:1 and 1:2, respectively. The PI for the three resuspensions was higher (0.9 ± 0.09, 0.91 ± 0.15, and 0.59 ± 0.11 for 0, 1:1, and 1:2) compared to the sample before lyophilization (0.13 ± 0.1). This suggested that the aggregation is reduced with the increase of trehalose amount, but it is not eliminated.

- Drug entrapment

The drug entrapment affects the final nanosphere mean size and stability over time. This effect can be positive, reducing the mean size of nanospheres, or negative, increasing the mean nanospheres size. Ahlin et al. [24] entrapped enalaprilat, which was dissolved in the organic phase, benzyl alcohol. The free drug nanospheres had a mean size of 183 ± 5 nm. The nanospheres with entrapped drug had a mean size of 204 ± 6 nm. The effect of the drug on the nanoparticle stability, defined as the size variation as a function of time, was also studied. The mean size after 15 days for the free drug nanosphere was almost constant (181 ± 6 nm), and for the nanospheres with the entrapped drug was 730 ± 200 nm. This data suggests that the diffusion of enalaprilat drug from PLGA matrix induced formation of PLGA nanoparticle clusters, increasing the final mean nanoparticle size.

A positive effect of the drug entrapped on the nanoparticle size is shown in the work of Konan et al [17]. Benzyl alcohol was the organic phase used and meso-tetra(p-hydroxyphenyl)porphyrin (p-THPP) was the drug. The preparation with 50:50 copolymer ratio and free drug nanospheres had a size of 124 ± 2 nm. When the drug was incorporated, the size was reduced to 93 ± 0 nm for a theoretical loading of 15%. The samples with 75:25 copolymer ratio and free drug nanospheres had a mean size of 132 ± 12 nm. The addition of the drug decreased the size to 95 ± 6 nm for a theoretical loading of 15%. Both copolymer ratios showed a mean size increase with further increases in theoretical loading of drug. It should be highlighted that increases in the theoretical drug loading decreases the entrapment efficiency. The higher entrapment efficiency (76.3% ±1.4%) was for the 5% theoretical drug loading.

Advantages (A)/Disadvantages (D)

- (A) The use of non highly toxic solvents (i.e. benzyl alcohol)

- (A) Reduced energy consumption because it only requires mild stirring. The process does not require high stress shear (i.e. sonication or microfluidization)
- (D) The requirement of large amounts of water for nanoparticles formation
- (D) Large time of emulsion agitation
- (D) The size is highly sensitive to polymer concentration if the process does not use shear stress for size reduction (high speed agitation or sonication)
- (A/D) Suitable for hydrophobic active components. The hydrophilic components have a high migration tendency due to the diffusion of the polar solvent to the aqueous phase and therefore the drug entrapment efficiency is low

2.2.2. Salting Out Method

In this synthesis method, the polymer is dissolved in the organic phase, which should be water-miscible, like acetone or tetrahydrofuran (THF). The organic phase is emulsified in an aqueous phase, under strong mechanical shear stress. The aqueous phase contains the emulsifier and a high concentration of salts which are not soluble in the organic phase. Typically, the salts used are 60% w/w of magnesium chloride hexahydrate [25, 26] or magnesium acetate tetrahydrate in a ratio of 1:3 polymer to salt [27]. Contrary to the emulsion diffusion method, there is no diffusion of the solvent due to the presence of salts. The fast addition of pure water, to the o/w emulsion, under mild stirring, reduces the ionic strength and leads to the migration of the water-soluble organic solvent to the aqueous phase inducing nanosphere formation [5]. The final step is purification by cross flow filtration or centrifugation to remove the salting out agent. Common salting out agents are electrolytes (sodium chloride, magnesium acetate, or magnesium chloride) or non-electrolytes, such as sucrose [14].

Important parameters to be considered are: polymer concentration and molecular weight, stirring rate and time, nature and concentration of surfactant and solvent, and cryoprotectans.

- Polymer concentration

This method is more robust than emulsion-diffusion technique because the mean size is not highly sensitive to increments in polymer concentration. Konan et al. [25]

varied the PLGA concentration from 10% to 25% w/w. The mean size of 150 nm was constant up to a polymer concentration as high as 17% w/w. At concentrations higher than 20% w/w the size of the nanoparticles increased (to 300 nm for 25% w/w).

- Polymer molecular weight and copolymer molar ratio

The PLGA molecular weight impacts the final mean nanosphere size. In general, higher molecular weight forms higher mean size nanoparticles. The change in nanoparticle size was evaluated as the composition and molecular weight of PLGA was varied (12000 to 48000 for 50:50 PLGA; 12000 to 98000 Da for 75:25 PLGA). For the nanospheres with 50:50 PLGA, the mean size ranged from 102 ± 4 nm to 154 ± 17 nm for 12000 Da and 48000 Da, respectively. For the 75:25 PLGA, the nanoparticle mean size ranged from 132 ± 3 nm to 152 ± 25 nm for 12000 Da and 98000 Da, respectively. For the same molecular weight, the two copolymer ratio (50:50 and 75:25 with free carboxylic end groups) formed nanospheres with similar sizes (125 ± 9 nm compared with 132 ± 3 nm, respectively) [25].

- Solvent

The solvent plays an important role in the formation and mean size of the nanoparticles. Konan et al. [25] obtained different nanosphere sizes with acetone and THF. Smaller nanoparticles were obtained when THF was used. The samples using THF formed nanospheres in the range of 102 ± 4 nm to 166 ± 5 nm, and the mean size for the samples with acetone range from 120 ± 7 nm to 210 ± 66 nm. Acetone was used by Zweers et al. [26]. The mean nanoparticle size formed was 230 nm (polydispersity index (PI) of 0.09), and 139 nm (polydispersity index (PI) of 0.19) for PLGA and PEO-PLGA, respectively.

- Surfactant

The PVA family is widely used as surfactant for the preparation of PLGA nanoparticles. Konan et al. [25] tested two types of PVA: Mowiol® 4-88 (87.7% hydrolyzed with molecular weight of 26,000 Da), and Mowiol® 3-83 (82.6% hydrolyzed with molecular weight of 18,000 Da). PVA Mowiol® 3-83 was most efficient in lowering the size of the nanoparticles to 148 nm (±5 nm) in a concentration of 15% w/w. Zweers et al. [26] used PVA 80% hydrolyzed with molecular weight of 10 kDa, and the concentration in the aqueous suspension was 2 wt.%. The mean size obtained was 230

nm with PI of 0.09. The PVA or Mowiol® 4-88 were used by Eley et al. [27] to make nanoparticles with a normal size distribution between 400 to 1100 nm, as obtained by light scattering laser spectrophotometry.

- Stirring rate and time

The size can be controlled by stirring rate and time. This was shown by Konan et al. [25]. The stirring speed was varied from 2000 to 13500 RPM (figure 2.3), and the stirring time tested varied from 5 to 50 min. At 13500 RPM, nanospheres with a mean size of 155 nm were formed using THF as a solvent, with 17% w/w of polymer concentration, and 10% w/w of PVA. Nanoparticles sizes under 200 nm were obtained at 8000 RPM; no statistical analysis was provided to detect the significance of these differences. At an optimum stirring time of 15 minutes, nanospheres of 140 nm mean size were formed; no significant decrease in the mean size was notices after 25 minutes (the total size increment was 8 nm up to 45 minutes of stirring).

- Cryoprotectants in freeze-drying

The lyophilization step must be carried out in the presence of cryoprotectants to preserve the mean nanoparticle size obtained in the formation process. The sugar family is widely used as cryoprotectant. Konan et al. [25] tested trehalose, mannitol, glucose, and lactose. All lyoprotectants showed a good size preservation with just a slightly size increment for lyoprotectant to nanoparticles mass ratio over 0.5 (size was increased from 135 nm to 150 nm). The sample without cryoprotectant had a mean size of 480 nm after resuspension.

Advantages(A)/Disadvantages(D)

- (A) Reduced energy consumption because it only requires normal stirring. The process does not require high stress shear (i.e. sonication or microfluidization)
- (A) Low time consuming process
- (D) The main drawback is the requirement of purification step for salting out agent elimination, which is in higher amounts (at least three times more amount of salting out than polymer)

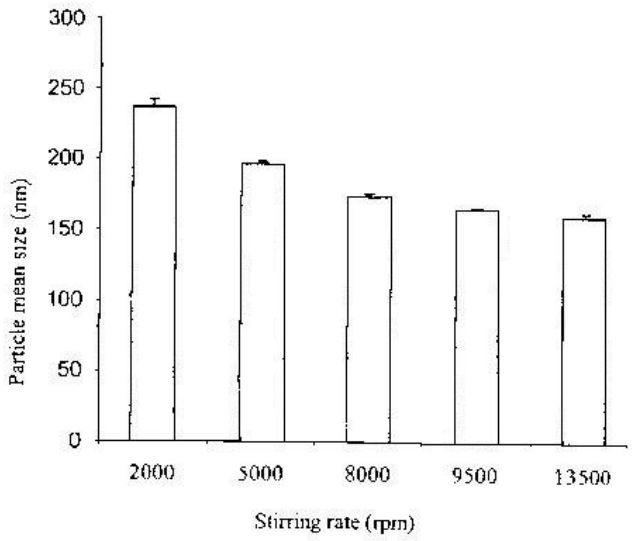

Figure 2.3. Influence of the stirring rate on the main nanoparticle size (Aqueous phase: 10% (w/w) of Mowiol 4-88 and 60% (w/w) $MgCl_2$, organic phase: 17% (w/w) of polymer in THF (mean ± SD, n=3). Reproduced from ref. Konan et al. (2002)

- (A/D) Suitable for hydrophobic components because the salting out agent is water soluble
- (A/D)The use of not highly toxic, but explosive, solvents (i.e. acetone, THF)

2.2.3. Nanoprecipitation (Solvent Diffusion, or Solvent Displacement) Method

Typically, this method is used for hydrophobic drug entrapment, but it has been adapted for hydrophilic drugs as well. Polymer and drug are dissolved in a polar, water-miscible solvent such as acetone, acetonitrile, ethanol, or methanol. The solution is then poured in a controlled manner (i.e. drop-wise addition) into an aqueous solution with surfactant. Nanoparticles are formed instantaneously by rapid solvent diffusion. Finally, the solvent is removed under reduced pressure.

Important parameters to be considered are: polymer/surfactant ratio, polymer concentration, surfactant nature and concentration, solvent nature, viscosity, additives, active component, and phase injection.

- Polymer concentration

The polymer concentration is maintained in the range of 1% w/v up to 10% w/v. Prakobvaitayakit and Nimmannit [28] tested three different concentrations of 50:50 PLGA for nanosphere formation. The nanoparticle mean size was 190 nm for 1 % w/v,

and the size increased to 238.9 nm for 10% w/v. Govender et al. [29] used a concentration of 1% w/v to synthesize nanospheres of 157.1 ± 1.9 nm in size. Csaba et al. [30] worked with a polymer concentration of 5 % w/v to form nanoparticles with a size range from 161 ± 7 nm to 269 ± 11 nm. This size range is correlated to the presence of different polymers in the polymer blend used (detailed in the surfactant section). Niwa et al. [31] worked with two different concentrations of 0.39% w/v and 0.44 % w/v, and the mean size was 195 ± 34 nm and 283 ± 37 nm, respectively. In another work, Niwa et al. [32] used 0.77% w/v PLGA forming nanospheres with a mean size of 224 ± 14 nm. Ameller et al. [33] worked with a concentration of 2% w/v and obtained nanospheres with a mean size of 260 ± 50 nm, approximately (0.1 %w/w of poloxamer 188 was in the aqueous phase); a significant size reduction (approximately, 80 ± 20 nm for the same concentration) was achieved when PLGA was grafted to PEG (5 kDa) (no poloxamer in the aqueous phase) suggesting that the hydrophilic lattices provided by PEG stabilized the nanoparticles; the PLGA aggregation was reduced during nanosphere formation reducing the nanosphere mean size. The trend was maintained for other two polymers used, poly(D,L-lactide) (PLA) and poly(ε-caprolactone) (PCL), which were covalently grafted with PEG (5 kDa).

- Polymer molecular weight and copolymer ratio

The polymer molecular weight affects the size more significantly than the copolymer ratio, as follows. Niwa et al. [31] worked with different molecular weights, and copolymer ratios. The PLGA 50:50 with a MW of 66475 Da formed nanospheres with a size of 338 ± 67 nm, which was similar to the nanospheres size of 85:15 PLGA with a MW of 66671 Da, measuring 385 ± 51 nm in size. The 85:15 PLGA with a MW of 127598 Da formed nanospheres with mean size of 637 ± 40 nm. These nanospheres were prepared with a mix of chloroform and acetone for the entrapment of indomethacin.

- Solvent nature

The selection of good solvents to form smaller nanoparticles and to improve the entrapment efficiency of the active component is a complex and an important process. There is no clear definition of the ‘best solvent’ for this method. Niwa et al. [31] used a mix of organic solvents (acetone, methanol, dichloromethane, or chloroform) to dissolve PLGA and drugs (indomethacin and 5-fluorouracil). The size of the 85:15 PLGA

nanoparticles of two molecular weights (12279 Da and 66671 Da) changed when the mix of solvents was altered from 0.5:5:5 ml to 0.5:25:5 ml (dichloromethane /acetone /methanol). The first mix of solvents formed nanospheres with a mean size of 283 ± 37 nm and 213 ± 13 nm for the two molecular weights tested, and the second one formed nanospheres of 195 ± 34 nm, and 207 ± 13 nm. The reduction in size with increased acetone concentration is attributed to the reduction in the surface tension of the dichloromethane solution in the presence of acetone. The formation process performed with dichloromethane or chloroform formed nanospheres 1 μm and bigger in size.

Acetone is commonly used alone for the preparation of nanospheres. Ameller et al. [33, 34] obtained a mean size nanoparticles of 258 ± 97 nm with zeta potential of -53.4 ± 0.5 mV. Prakobvaitayakit and Nimmannit [28] formed nanospheres with a mean size varying from 190 nm to 643.9 nm. Panagi et al. [35] formed nanospheres with mean size of 154 ± 23.5 nm, polydispersity of 0.489, and zeta potential of 45.1 ± 1.9 mV with the same solvent. Oster et al. [36] obtained a mean size of 152 ± 3 nm and zeta potential of 35 ± 3 mV.

Saxena et al. [37] added methanol to acetonitrile (in which PLGA was dissolved) for a good dissolution of the active component. The mean size was 357 ± 0.21 nm with zeta potential of -16.3 ± 1.5 mV. The higher zeta potential (less negative) is attributed to the presence of PVA over the nanosphere surface.

Csaba et al. [38] worked with ethanol (organic phase) for the polymer nanoprecipitation. The mean size of the nanospheres (PLGA 50:50) obtained was 191.5 ± 7.1 nm. Other works used acetonitrile as the organic solvent. For example, Govender et al. [29] prepared nanospheres with a size of 157.1 ± 1.9 nm with acetonitrile.

- Surfactant

A variety of surfactants are used for nanoparticle formation and stabilization. The surfactant can be anionic, cationic or nonionic. Surfactants in the poloxamer and poloxamines family, formed with polyoxiyethylene and polyoxypropylene, are commonly used in nanoparticle synthesis. Surfactants of different HLB values can be obtained by varying the amount of monomers; less ethylene oxide monomers and more propylene oxide monomers form surfactants with lower HLB values. Csaba et al. [38] used poloxamer and poloxamines blended with PLGA in the organic phase. The samples

formed with more hydrophobic surfactants (HLB of 1 and 2.5) had an increased final size of up to 333.7 ± 82.1 nm for a mass ratio PLGA:surfactant of 50:75 mg/mg. The lower size nanoparticle formed was 159.8 ± 6.5 nm for the blend PLGA:Pluronic® F68 (HLB value of 29) of 50:75 mg/mg. Pluronic® F68 has shorter ethylene oxide chains and larger propylene oxide chains compared with the other surfactants tested. Ameller et al. [34] used poloxamer 188 with a concentration of 0.1% w/w forming PLGA nanospheres of 262 ± 52 nm mean size. The zeta potential obtained was -11 mV.

Another important surfactant used is PVA. Niwa et al. [31] tested different concentrations of PVA. The range tested was from 0.5 % to 2 % of PVA in the aqueous suspension leading to nanoparticle formation with a mean size of 300 nm (not significant difference in the range tested). Saxena et al. [37] obtained mean nanoparticle size of 357 ± 0.21 nm using 88 - 89 % hydrolyzed PVA.

- Additives

Certain compounds can improve the stability and size of the nanoparticles (fatty acids, short chains of carbons). Additionally, they can affect the entrapment efficiency of the active component. Govender et al. [29] found that fatty acid incorporation affected the entrapment efficiency of the active component (procaine hydrochloride and procaine dihydrate, water soluble drugs) reducing the nanoparticles mean size. The authors added caprylic acid, (molar ratio of 1:1 and 1:3), lauric acid (molar ratio of 1:1 and 1:3), PLA oligomers (molar ratio of 1:1), and poly(methyl methacrylate-co-methacrylic acid) (PMMA-MA) (molar ratio of 5:1). Lauric acid in a molar ratio of 1:1 increased the drug content from 11% to 34.8%, and the nanoparticle size was reduced from 157.1 ± 1.9 nm to 118.8 ± 1.4 nm (p value <0.05). With the 3:1 molar ratio, the size was lower (55.8 ± 1.5 nm) but the morphology was altered (irregular shape). Zeta potential showed a slight increase from -49.2 ±0.7 mV to -44.1 ± 1.8 mV. The longer carbon chain of lauric acid (in comparison to that of caprylic acid) was associated with the improvement in the nanoparticle characteristics.

- Active component entrapment

Entrapment of active components has an important effect on the final nanospheres final size; as a general rule, entrapment of hydrophobic active components leads to formation of smaller nanospheres, as compared to the entrapment of hydrophilic

components. The interaction between solvent, polymer and active component must be taken into account to improve the drug loading and the drug entrapment efficiency.

The entrapment of procaine hydrochloride (with a pH of 5.8 for aqueous solution) was found to increase the nanoparticle size from 157.1 ± 1.9 nm to 209.5 ± 2.7 nm for a theoretical drug loading of 0% to 10%, respectively. The drug content increased from 0.2 to 4.6% w/w when the theoretical drug loading was increased from 1% to 10% w/w, but the entrapment efficiency decreased from 14.5% to 6.3% [29]. Although, they reduced the nanosphere mean size by change of the aqueous pH (buffer at pH 9.3), the size for PLGA alone was 123.6 ± 2.3 nm, and for nanospheres with 10% w/w theoretical drug loading, the size was 186.5 ± 2.3 nm. In both cases, the entrapment formed bigger nanospheres in the presence of the drug, as compared with the PLGA alone. The nanospheres size was reduced with the entrapment of procaine dehydrate. When the theoretical drug loading of procaine dyhidrate was increased up to 10% w/w, the mean size was reduced from 157 ± 1.9 nm to 56.2 ± 1.9 nm. The drug entrapment efficiency ranged from 36.2% up to 44.1% [29].

The entrapment of plasmids in PLGA nanoparticles increased the nanoparticle size, which can be observed in the work developed by Csaba et al. [30] as depicted in Figure 2.4. The organic solvent used to dissolve the polymer blends was methylene chloride, and the polymer blends were PLGA: poloxamer and PLGA:poloxamine in a ratio of 50:50 mg/mg. Plasmid DNA encoding green fluorescent protein with CMV promoter (pEGFP-C1) in an aqueous solution was added to the organic phase. The mean size of naked PLGA nanospheres was 191 ± 7 nm with a polydispersity index (PI) of 0.046 and zeta potential of -60.1 ± 7.4 mV. When plasmid was added to the preparation with PLGA alone, the final size was 234 ± 13 nm with PI of 0.187 and zeta potential of -72.7 mV. The addition of plasmid increases the size all samples tested, but the exception was for poloxamine Tetronic® 904 (HLB of 14.5 and molecular weight of 6700). This sample showed a reduction of size from 168 ± 9 nm to 161 ± 7 nm, without and with plasmid, respectively. The zeta potential decreased from -38.4 ± 3.3 mV to -54.1 ± 2 mV for the same preparation and the PI was reduced from 0.179 to 0.154.

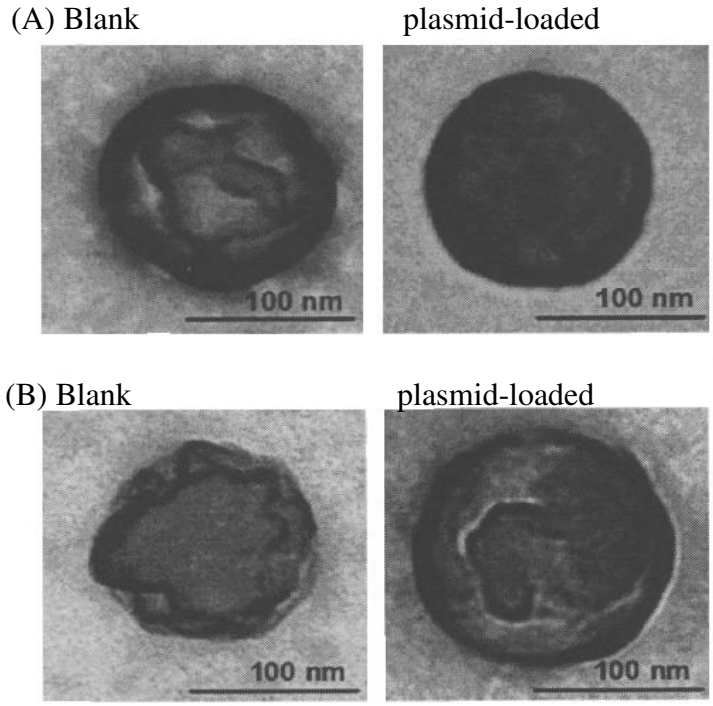

Figure 2.4. TEM micrographs of blank and plasmid-loaded (A) PLGA: poloxamer (Pluronic F68) and (B) PLGA:poloxamine (Tetronic 908) blend nanoparticles. Reproduced from Ref. Csaba et al. [30].

Saxena et al. [37] found that the retention of the ICG-NaI into the polymeric matrix was less than ICG because of the more hydrophilic nature of ICG-NaI. As a result of the lower retention of ICG-NaI, all further discussions will only consider ICG formulations. The mean nanoparticle size decreased with increasing concentration of ICG from 405 ± 0.05 nm with 1% w/w of drug to 307 ± 0.08 nm with 10% w/w of drug, and the nanoparticle recovery was improved from 48% to 65.3%, respectively. The drug entrapment was reduced from 9.92% to 1.14% and the drug content decreased from 0.21% to 0.17% with increasing amounts of ICG (1% w/w to 10% w/w). When the drug-polymer ratio was reduced drastically to 0.125% w/w, the drug entrapment increased to 74.47%. The drug content was 0.2%, and the nanoparticle recovery was slightly decreased to 45.7% for the lower drug concentration.

- Phase injection

The organic phase addition to the continuous aqueous phase should be controlled and constant, by mild stirring, to assure a uniform distribution and diffusion.

Prakobvaitayakit and Nimmannit [28] used a constant flow rate of 0.3 ml/min with mechanical stirring of 750 RPM. In the Govender et al. [29] work, they reported a drop wise organic phase addition. The stirring was done by a magnetic stirrer. The same procedure was followed by Saxena et al. [37]. Csaba et al. [30, 38] used vortex agitation for mixing both phases getting a fast organic phase dispersion and further moderate magnetic stirring. Other works using fast organic phase dispersion is that by Ameller et al. [33, 34].

Advantages (A)/Disadvantages (D)

- (A) The use of non highly toxic solvents (i.e. acetone).
- (A) Reduced energy consumption because it only requires regular stirring. The process does not require high stress shear (i.e. sonication or microfluidization).
- (A) Additives can be used for nanoparticle size reduction.
- (D) The solvent is removed by evaporation (time consuming).
- (D) The main drawback is the requirement of drugs that are highly soluble in polar solvents (i.e. acetone, ethyl acetate), but they should be slightly soluble in water to minimize losses during solvent diffusion. The drug can diffuse to the aqueous phase reducing the drug entrapped in the PLGA nanospheres [39].
- (D) The drug loading efficiency is lower for the hydrophilic drugs than hydrophobic ones because of their poor interaction (hydrophobic interaction) with the polymer leading to diffusion of the drug during the solvent displacement from the polymer in the organic phase to the external aqueous environment [15].
- (D) Nanoparticle size is very much affected by the polymer concentration; higher nanoparticle sizes are obtained at higher polymer concentrations.

2.2.4. Emulsion Evaporation Method

Emulsion evaporation is the oldest method used to form polymeric nanoparticles from preformed polymers. The method is based on the emulsification of an organic solution of the polymer in an aqueous phase followed by the evaporation of the organic solvent. The polymer is dissolved in a suitable solvent (e.g., ethyl acetate, chloroform,

methylene chloride). The organic phase or aqueous phase is poured into the continuous phase (aqueous or organic phase) in which a surfactant is dissolved to impart stability to the emulsion. Emulsification is carried out under high-shear stress to reduce the size of the emulsion droplet (directly related with the final size of the nanoparticles). The process of emulsification is followed by evaporation of the organic solvent under vacuum, which leads to polymer precipitation and nanoparticle formation.

Normal emulsions oil in water (o/w) or water in oil (w/o) and double emulsions (w/o/w) can be used to accommodate the entrapment of active components with different properties. The o/w emulsion is used for entrapment of hydrophobic compounds, whereas w/o/w double emulsion is used for the entrapment of hydrophilic compounds. The method is widely used for microencapsulation because it is easy to scale up, it doesn't require high shear stress, and it can be adjusted (by use of the double emulsion method) to encapsulate water soluble drugs [40-44].

The formation of the emulsion is a key aspect of this method [45], considering that the size of the emulsion droplet is directly related to the final nanoparticle size. Emulsions can be classified in microemulsions, miniemulsions (or nanoemulsions), and macroemulsions. The microemulsions are transparent and thermodynamically stable emulsions, with droplets mean sizes from 20 to 50 nm, obtained by conjugation of surfactant, solvent and co-surfactant. Microemulsions are thermodynamically stable due to the entropic effect of smaller droplets [46, 47]. The size of mini or nanoemulsions is in the order of 40 to 500 nm [48, 49]; high shear stress and enough surfactant amounts are needed to make stable nanoemulsions. Nanoemulsions are kinetically stable and the surfactant is used in the most efficient way [48]. The macroemulsion droplet size is in the micrometer range; macroemulsions are formed by mild stirring and surfactant addition for stability. Macroemulsions are unstable over time, so they tend to aggregate.

The procedure followed to form a miniemulsion involves the use of surfactants and the application of mechanical stirring with high RPM, high pressure or sonication, as well as the addition of hydrophobic components that act as a suppressant agent against Ostwald ripening (migration of small droplets to bigger ones) [50]. The effect of sonication on the droplet size was studied by Landfester et al. [51], and it showed that the amplitude of wavelength should be over 20% with 600 to 800 seconds of sonication to

form a stable miniemulsions with no more droplet size changes. The main draw-back of sonication is the lack of monodispersity of the emulsion formed [52].

Mason and Bibette [53, 54] showed that the application of laminar shear rate flow, as opposed to sonication, can result in a monodisperse droplet size. The formation of monodisperse viscous droplets in viscoelastic complex fluids by the application of shear stresses with laminar flows was experimentally studied. The emulsion was sheared in a thin gap of two glasses under a uniform shear flow to form a uniform droplet size distribution in the nanometer range by adjustment of the gap in where the sample is placed [53, 55, 56]. Some requirements must be met, such as the phases must be viscoelastic, and the initial emulsion droplets must be rather big in size (5 to 10 μm) for a monodisperse miniemulsion to result.

Advantages (A)/Disadvantages (D)

- (A) The use of non highly toxic solvents (i.e. ethyl acetate)
- (A) Additives can be used for nanoparticle size reduction
- (A) Suitable for hydrophilic (double emulsions) and hydrophobic active components.
- (D) High consumption of energy by the necessity of high stress shear (i.e. sonication or microfluidization)
- (A/D) The solvent is removed by evaporation (energy consumption), but the process time for solvent removal is reduced (special with fast evaporation with vacuum)
- (A/D) The addition of active component affects the final size of nanoparticles

2.2.4.1. Oil in Water Emulsion Method (Single Emulsion)

The method is based on the emulsification of an organic solution which contains the polymer and the active component in an aqueous phase, followed by the evaporation of the organic solvent. Different surfactants such as PVA, SDS, Pluronic F68 can be dissolved in the aqueous phase. The size reduction of the emulsion droplet is done by sonication or microfluidization for miniemulsion formation. The evaporation step is required to eliminate the organic solvent present in the organic phase. This leads to the precipitation of the polymer as nanoparticles with a diameter in the nanometers range.

Important parameters to be considered are: polymer molecular weight and concentration, copolymer ratio and end groups, surfactant nature, phase ratio, solvent nature, evaporation rate, drug entrapment, additives, shear stress, and sterilization.

- Polymer concentration

Polymer concentration is an important parameter to consider when forming nanoparticles. Julienne et al. [57] worked with 85:15 PLGA, MW of 87000 Da, and 88% hydrolyzed PVA in a fixed concentration of 0.5% w/v. Nanoparticles formed under these conditions at four PLGA concentrations, 0.79%, 2.5%, 5%, and 7.5% w/v had a mean size of 220, 178, 177, and 236 nm, respectively.

- Polymer molecular weight

Usually, the increase in molecular weight leads to formation of nanospheres of significantly bigger size, but the entrapment of active components reduces this effect. Panyam et al. [58] formed PLGA nanospheres (theoretical loading of dexamethasone was 20 % w/w) with a size of 260 nm (PI of 0.115) and 270 nm (PI of 0.228) for PLGA with molecular weight of 103,000 Da and 143,000 Da, respectively.

- Copolymer ratio and end groups

Different copolymer ratios have been tested with no significant difference in the mean nanospheres size. Panyam et al. [58] tested three different proportions of lactide molar ratios for the entrapment of dexamethasone. The 100% lactide polymer formed nanospheres with a mean size of 260 nm (PI of 0.255), which was the same for the sample with 75% of lactide, but the PI decreased to 0.115 with the decrease in the lactide. The sample with 50 % slightly increased the mean size to 270 nm with a PI of 0.228. Zeta potential varied from -23.9 ± 3.5 mV to -19.6 ± 1.5 mV, respectively. There is no mention of statistical analysis to detect significant differences in the parameters analyzed. Another important factor was the effect of end groups on the mean size. Samples prepared with ester end groups formed nanospheres with an average size of 740 nm (PI of 0.394); the mean size for acid PLGA end group was 240 nm (PI of 0.225). The PLGA used was 50:50 with a molecular weight of 12000 and 10000 Da, respectively.

- Surfactant

Many options of surfactant can be used for nanosphere formation by emulsion evaporation. Julienne et al. [57] tested PVA, methylcellulose (MC), gelatin, and lecithin.

For PVA, the concentrations tested were 0.1%, 0.2%, and 0.5% w/v. The size varied from 342 nm to 291 nm. When MC was used, the mean size obtained varied from 1880 nm to 1950 nm for the same concentrations. At a fixed surfactant concentration of 0.5% w/v, a PLGA concentration of 2% w/v and a phase ratio of 20% v/v (organic to aqueous phase), the mean sizes obtained were 288, 2013, 1400, and 298 nm for PVA, MC, gelatin, and lecithin, respectively.

The surfactant type is critical in forming small and stable nanospheres. Moreover, when the target applications of the nanoparticles are in the biomedical area, the presence of toxic surfactant residues over the surface of the nanospheres is of concern. To address this concern, researchers looked to find other surfactants, biodegradable and biocompatible to form nanoparticles. Mu and Feng (2003) use vitamin E TPGS (d-α-tocopheryl polyethylene glycol 1000 succinate), amphiphile molecule due to the presence of PEG chains) as a surfactant. Different surfactant concentrations were tested, from 15 mg/ml to 60 mg/ml. The smaller size nanoparticles were formed at a surfactant concentration of 60 mg/ml, measuring in size 567.4 ± 362.6 nm when 85:15 PLGA of a molecular weight of 90 to 120 kDa was used.

- Phase ratios

The phase ratio (organic to aqueous solvent) plays an important role in controlling the size of the nanospheres. In general, the lower ratio of organic-aqueous phase produces nanoparticle of smaller size. Juliene et al. [57] showed the effect with different ratios. At three organic:aqueous ratios, 10%, 25%, and 40% v/v nanoparticles of 106.8 nm (CV 43.1%), 111.2 nm (CV 29.4%), and 130.5 nm (CV 16.5) were formed. The samples were formed in the presence of 8 % w/v of PVA.

- Solvent

Several organic solvents can be selected based on two criteria, (1) the PLGA must be soluble in this solvent, and (2) the solvent must be completely immiscible with the aqueous phase. Solvents from the chlorinate family have been widely used in the emulsion evaporation method. Julienne et al [57] used methylene chloride to form PLGA nanospheres with a mean size of 177 nm (CV of 32%). The same solvent was used by Pietzonka et al. [59] with a mean size of 400 to 500 nm. Song et al. [60] used a mix of dichloromethane and acetone (8:2 v/v) and formed nanospheres with a mean size of 117

± 40 nm. Panyam et al. [58] used chloroform to dissolve the PLGA, and the drug (dexamethasone) was dissolved in methanol to form nanoparticles of a mean size of 240 nm (PI of 0.225).

- Evaporation rate

Fast evaporation of the organic solvent under vacuum is more efficient in forming smaller nanoparticles. Chung et al. [61, 62] compared vacuum solvent evaporation at 160 mmHg and normal evaporation at 760 mmHg as two methods to form microspheres of albumin-loaded poly L-lactide (LPLA) and poly D-lactide (DPLA). The fast rate of evaporation produced a mean particle size around 30% smaller than the mean particle size obtained under a normal rate of evaporation. The reduction in particle size coupled with the low glass transition (T_g) and melting temperature (T_m) of PLGA polymer (i.e. T_g of 25.7 °C for 50:50 PLGA with molecular weight of 5 to 15 kDa) makes the vacuum evaporation method indispensable in the formation of PLGA nanoparticles.

- Drug entrapment

In emulsion evaporation, as in other synthesis methods, entrapment of highly hydrophobic drugs tends to reduce the size of the nanospheres. This fact is clearly observed in the work of Mu and Feng [63]. Paclitaxel, an active drug used in breast cancer therapy is added at a 2.4% w/w concentration to form nanoparticles of an average size of 272.5 ± 169.5 nm in the presence of vitamin E TPGS as a surfactant. The samples without paclitaxel formed nanospheres with a mean size of 914.8 ± 380.1 nm and 699.3 ± 286.9 nm for 60 mg/ml and 15 mg/ml of vitamin E TPGS, respectively. Other paclitaxel concentrations (0.62% and 0.83% w/w) were tested, but the mean size was higher than that obtained with 2.4% w/w. The entrapment efficiency was 50.4% with a recovery yield of 41.7%.

The solubility of the drug in water is the main drawback in forming smaller size nanospheres and improving the drug entrapment efficiency. This effect was shown by the study of Song et al. [60] where the pH (aqueous phase) effect on the drug solubility was reflected on the drug loading and the size of the nanospheres (Figure 2.5). The higher drug (U-86983, anti-proliferative agent) entrapment efficiency was for basic pH (over 8) due less solubility at basic pHs. The drug load increased from 5.4% to 20.4%, and the entrapment efficiency increased from 28.2% to 84.3% by increasing the pH. Although,

there is high improvement in entrapment efficiency by increasing the pH (linear relation), the nanosphere mean size showed different pattern. The low pH (6.5) formed nanosphere with mean size of 142 ± 36 nm, and the mean size for higher pH (8.14) was 144 ± 37 nm. The smaller size was for pH 7.5 with an average of 88 ± 41 nm, and entrapment efficiency of 56.9%. The entrapment of the drug U61431F was done for pH 4 and 4.5. The sample with pH 4 formed nanospheres with mean size of 109 ± 41 nm, and entrapment efficiency of 86.1%. The pH 4.5 formed nanospheres with mean size of 115 ± 42 nm, and entrapment efficiency of 77.5%.

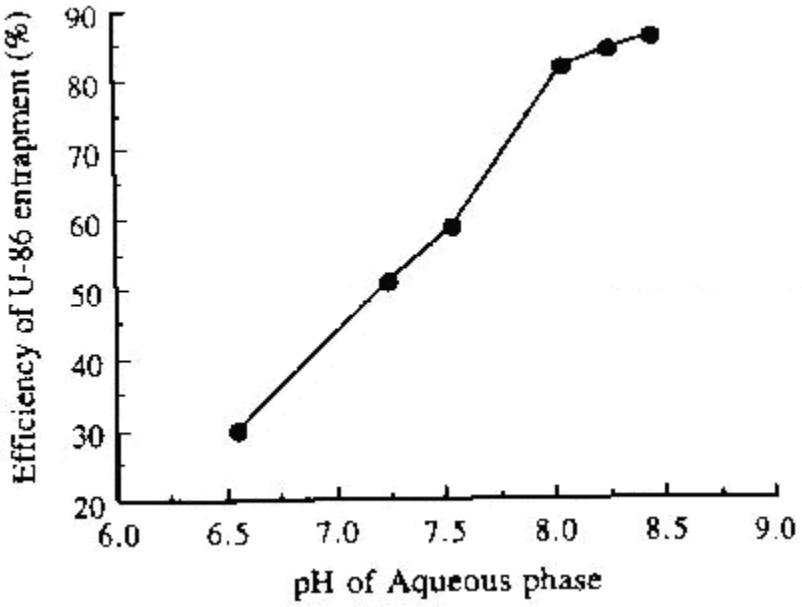

Figure 2.5. Efficiency of drug (U-86983) entrapment into PLGA nanoparticles by changing the pH of the aqueous phase from neutral to basic. Reproduced from Song et al. [60].

- Additives

Addition of hydrophobic additives can improve the nanosphere size, the drug entrapment efficiency, and release profile. Song et al. [60] tested wax (PLGA/wax of 80/20%) and palmitate (PLGA/palmitate of 80/20%) to improve the release profile (reduce the burst effect, fast initial drug release) of the drug U-86983 (an anti-proliferative agent). The mean size for the wax sample was 105 ± 38 nm, which was almost the same with the palmitate sample (107 ± 30 nm). The entrapment efficiency was

higher for the wax sample (85.3%) as compared with the palmitate sample (80%), but the burst effect was not reduced (around 40% of drug release in the first day).

- Shear stress

The emulsion formation requires a strong agitation to reduce the droplet size. This highly impacts the nanoparticles size. Julienne et al. [57] tested two methods of shear stress (mechanical stirring, high pressure homogenizer). They tested two homogenizer pressures of 100 and 200 bars (high pressure homogenizer). The mean size obtained was 178 nm (CV of 22%) and 188 nm (CV of 38%) for 100 and 200 bars, respectively. There is a favorable impact in the size reduction when the emulsion is homogenized with a high pressure homogenizer compared with just high stirring (10000 RPM). The nanosphere mean size with stirring was 288 nm (CV 37%), and the mean size for nanosphere using homogenization (high pressure of 300 bars) was 231 nm (CV of 21%). The samples used PVA at 5% w/v and phase ratio of 20%.

- Sterilization

The effect of sterilization on nanosphere size was evaluated by Song et al. [60]. The sterilization was done by γ- irradiation at 2.5 Mrad doses for nanospheres with 2 aminochromone drug family. The mean size slightly changed from 123 ± 38 nm before irradiation to 149 ± 43 nm after irradiation. The drug release was the same for both preparations, and the nanoparticles uptake was slightly increased from 13.4 μg/10 mg to 15.4 μg/10 mg artery, before and after irradiation.

2.2.4.2. Double Emulsion (w/o/w) Method

The first step of the double emulsion method is the formation of a water in oil (w/o) emulsion where the aqueous solution contains the hydrophilic active component and the organic phase contains PLGA and a suitable surfactant (Span 80, pluronic F 68, and others) with a low HLB. The miniemulsion is formed under strong shear stress (i.e. sonication, microfluidization, high speed homogenization). Next, the water in oil in water (w/o/w) emulsion formation is sonicated or homogenized for droplet size reduction. This second size reduction should be controlled to minimize the hydrophilic active component diffusion to the external aqueous phase. Evaporation, the final step, is used to remove the organic solvent. Evaporation is done under vacuum to avoid polymer and active component damage, and to promote final nanoparticle size reduction.

The main drawback of the double emulsion method is the large size of the nanoparticles formed and the leakage of the hydrophilic active component [64], responsible for low entrapment efficiencies. The coalescence and Ostwald ripening [65, 66] are the two important mechanisms that destabilize the double emulsion droplets, and the diffusion through the organic phase of the hydrophilic active component is the main mechanism responsible of low levels of entrapped active component [64]. One strategy followed by Song et al. [60] to reduce the nanoparticle size was to apply a second strong shear rate. The leakage effect can be reduced by using a high polymer concentration, and a high polymer molecular weight, accompanied by an increase in the viscosity of the inner water phase, and an increase in the surfactant molecular weight [60, 67].

Important parameters to be considered are: polymer/surfactants ratio, polymer concentration, surfactant nature, viscosity, solvent nature, shear stress, evaporation, additives, and first/second phase ratios.

- Polymer molecular weight and copolymer ratio

An interesting effect of nanosphere size reduction against molecular weight increase is shown by Prabha and Labhasetwar [68]. The molecular weights tested were 12, 53, and 143 kDa for 50/50 copolymer ratio, and the mean size achieved were 563 ± 6, 685 ± 40, and 375 ± 22 nm, respectively. The zeta potential was -17.8 ± 1.0 mV, -16.6 ± 1.4 mV, and -11.5 ± 3.4 mV, respectively. The PLGA copolymer ratio tested were 75:25 and 50:50 (molecular weight of 53 kDa) with mean size of 485 ± 11 nm and 685 ± 40 nm. The zeta potential was -16.6 ± 1.4 mV, and -18.2 ± 3.8 mV, respectively. The polymer concentration was maintained at 3 %w/v.

- Solvent

The chlorinate family is widely used for nanosphere preparation with double emulsion. Aukunuru et al. [69] used methylene chloride to dissolve PLGA, and entrapped a 19-mer antisense oligonucleotide (PS-ODN). The mean size obtained was 252 ± 3.4 nm with zeta potential of -12.98 ± 1.8 mV. Dillen et al. [70] used dichloromethane and formed nanospheres with a size of 209.5 ± 2.5 nm before freeze drying. The same solvent was used by Vandervoort et al. [71] with mean size of 204 ± 4 nm. Yan et al. [72] used ethyl acetate to dissolve PLGA, and insulin was added to the first aqueous solution. The smaller nanosphere size was 149.2 nm (PI of 0.09).

- Surfactant

Two surfactants are needed in double emulsion evaporation method, a hydrophobic surfactant for the first emulsion and a hydrophilic surfactant for the second emulsion. Vandervoort and Ludwig [73] evaluated a series of stabilizers against PVA. The stabilizers used were methylcellulose (MC), hydroxy-ethylcellulose (HEC), hydroxy-propylcelluloose (HPC) hydroxyl-propylmethylcellulose (HPMC), gelatin type A and B, carbomer (Carbopol® 980) and poloxamer (Lutrol® F68). The stabilizers used alone formed nanoparticles up to 3.2 μm with an exception for Carbopol® 980- and Lutrol® F68, which formed nanospheres with a size of 400 nm. In the presence of PVA, nanospheres under 1 μm were formed. The lower mean size was obtained by using a mix of the stabilizer (the concentration used was equivalent to the same viscosity of 1% PVA) and PVA. The mix of PVA with Carbopol and poloxamer were exceptions because the blend of carbopol and PVA showed a slightly increase in mean size (420 nm), and the blend of poloxamer and PVA showed no variation on the mean size. Zeta potential varied from +14 mV to -50 mV for all preparations. Almost all formulation showed negative values with the exception of gelatin type A, showing a zeta potential of +13 mV.

Another work dealing with PVA use as a surfactant in the second emulsion is that by Yan et al. [72]. PVA concentration was varied to study the entrapment of insulin in PLGA nanoparticles (molecular weight of 11000 Da). The PVA concentrations tested were 0.4%, 0.7%, and 1% w/v. The mean size was reduced from 266.7 nm (PI of 0.15 nm) to 149.2 nm (PI of 0.09), and the entrapment efficiency was improved from 19.3% (±4.2%) to 42.8% (±1.5%) by increasing the PVA concentration from 0.4 to 1% w/v. The insulin concentration for the higher entrapment efficiency was 3.048 mg/mL, the surfactant concentration was 1% w/v, and polymer concentration was 50 mg/mL.

Prabha and Labhasetwar [68] tested different PVA concentrations, varying from 0.5% to 2%. The 2% PVA samples formed smaller nanospheres size, 270 ± 1 nm with a PI of 0.2 (±0.01). They also quantified the amount of PVA bounded to the nanosphere surface and found that this amount was directly correlated to the amount of surfactant used in the preparation. The lower PVA concentration formed nanospheres with 2.2% ± 0.2% w/w PVA bounded, and the 5% PVA sample formed nanospheres with 5.3% ± 0.7% w/w PVA over the surface.

Aukunuru et al. [69] used a PVA concentration of 5% in the continuous phase. It was found that zeta potential increased to less negative values when the PVA concentration increased. Prabha and Labhasetwar [68] showed an increase in zeta potential from -31.3 ± 1.6 mV to -6.5 ±1.7 mV for PVA concentrations from 0.5% to 2%. Aukunuru et al. [69] obtained zeta potential value of -12.98 ± 1.8 mV. Sahoo et al. [74] showed a similar effect of PVA. The PVA concentration was varied from 0.5% w/v to 5% w/v. The mean size varied from 522 nm to 380 nm, and the zeta potential varied from -15.4 ± 0.8 mV to -8 ± 2.3 mV, respectively.

Yan et al. [72] studied the entrapment of insulin in PLGA nanoparticles (molecular weight of 11000 Da). The effect of surfactant concentration (poloxamer 188) on the nanoparticle size was tested. The lowest mean size obtained for 1% w/v of poloxamer 188 was 149.2 nm with a polydispersity index of 0.09, and the entrapment efficiency was 42.8% ± 1.5%. The large size obtained of 266.7 nm (PI of 0.15 and entrapment efficiency of 19.3% ± 4.2%) was for 0.4% w/v of poloxamer 188.

- Drug entrapment

Dillen et al. [75] showed a slight increase in the nanosphere size from 234.7 nm to 238.1 nm, when the drug ciprofloxacin was added. When boric acid was added to the first aqueous suspension to acidify and improve the drug entrapment, the size increased slightly from 234.7 nm to 239 nm and the entrapment efficiency was improved from 61.7% to 62.6%. The improvement was greater (79.9%) when the number of homogenization cycles was increased from one to three. The entrapment of hydrophilic drugs is improved by using high molecular weight of PLGA and high molecular weight of first surfactant, which results in a higher inner phase viscosity. Song et al. [60] tested two different molecular weights of PLGA (58 and 102 Da). The lower molecular weight resulted in an entrapment efficiency of 24.8% and 9.2% for a PLGA concentration of 3% and initial theoretical drug (bovine serum albumin, BSA) of 10%, and for a PLGA concentration of 6% with 14 % of BSA, respectively. The entrapment efficiencies were improved to 68% and 74.8% for high molecular weight, under the same conditions. The mean size obtained for these samples was 150 ± 38 nm.

- Shear stress

High shear stress for droplet size reduction is a basic requirement to make small nanoparticles by double emulsion. Homogenization by microfluidization has been used and found to affect the size of the nanoparticles as a function of the pressure and number of cycles. Dillen et al. [75] tested one and three cycles with a fixed pressure of 50 bars. The mean size obtained for one cycle was 234.7 nm, and the mean size was reduced to 188.7 nm with three cycles. Vandervoort et al. [71] tested the effect of pressure and homogenization cycles forming a wide spectrum of nanoparticle sizes and entrapment efficiencies. The size reduction was achieved by an increase in the homogenization pressure and cycles. The lowest PLGA nanoparticle size was for the PVA and PVA mixed with carbopol (204 ±4 nm, and 205 ±5 nm, respectively) with 500 bar and three cycles. The drug entrapment decreased with an increase in homogenization pressure and cycles; the PVA sample varied from 61.5% ±12.4% to 20% ±8.2%, and the PVA mixed with carbopol varied from 41.8% ±12.1% to 20.8% ±8.4% for the entrapment of pilocarpine HCl.

- Sterilization

Sterilization is an important step to obtain a suitable system to be used in vivo. Dillen et al. [75] observed that nanoparticle size increased from 255.8 nm to 295.1 nm following gamma irradiation for sterilization purposes. This effect of slight increment of size is similar to that showed by Song et al. [60] with single emulsion method.

2.2.5. Important Modifications of Traditional Methods

The methods detailed above are the main methods extensively employed in the synthesis of PLGA nanoparticles for different purposes. There is a continuous effort to improve the nanoparticle size (size reduction), to reduce the polydispersity index, to better entrap the active components (hydrophilics and hydrophobics), and to reduce the potential toxicity of the different components involved. These efforts stimulated research and discovery of new methods, based on slight modifications of standard methods, and the application of new synthesis steps in the PLGA nanoparticles formation. The use of microfluidizers, dialysis, spray drying, and mix of standard techniques are examples of new methods created to improve the PLGA nanoparticle physical characteristics.

2.2.5.1. Membrane Emulsion Evaporation Method

The aqueous and organic phases are separated by a membrane which has a defined pore diameter and distribution. The organic phase is forced through the pores to form an organic droplet which is detached from the membrane by a certain movement of the aqueous phase. The membrane has a hydrophobic or hydrophilic behavior as a function of the disperse phase (aqueous or organic solvent) [76]. This can lead to very uniform size distribution of nanoparticles, but the main drawback is the bigger size obtained compared to normal emulsion evaporation method [77]. The pore diameter affects the final size of the nanoparticles, and there is a relation pore to droplet diameter of 1:3 [78]. There are a number of criteria that have to be met in order to obtain nanoparticles in the nanometer range: the membrane must have a pore diameter between 100 and 200 nm, the applied pressure difference should be slightly greater than the critical pressure, the contact angle should be as small as possible, and the surfactant should be adsorbed fast at the oil water interface [76]. SPG (Shirasu Porous Glass) and PTFE (poly(tetrafluoroethylene)) are the main membranes used in this technique [79].

2.2.5.2. Spray Dry Method for Water in Oil

Pamujula et al. [80] developed a method to improve the entrapment efficiency of hydrophilic drugs. An emulsion was formed between the organic phase and water. The organic phase, consisted of a mix of dichloromethane and chloroform, containing the polymer, and lipophilic surfactant L-α-phosphatidylcholine. The aqueous phase contained the drug (amifostine). The final emulsion was injected in a standard 0.7 mm nozzle blowing into a chamber with hot air (55 °C). The mean size obtained was 257 nm (182-417 nm) and 240 nm (182-417 nm) for preparations with 40% w/w and 100% of theoretical drug loading, respectively. The main advantage of this method is the high entrapment efficiency for hydrophilic drugs, which were 90.9% ± 0.16% and 100.03% ± 2.01% for the same preparations.

2.2.5.3. Spryer Solvent Displacement with Dialysis and Freeze Dryer Stabilization

Kim et al. [81] modified the solvent displacement as follows. The organic phase was injected into an aqueous solution by a nozzle and the solvent removed by dialysis. The drug addition (paclitaxel) was done after dialysis, by adsorption onto the nanosphere surface. The system was stabilized by the addition of an aqueous solution of pluronic F-

68 and subsequently freeze dried. The solvent used in the organic phase (discontinuous) was tetraglycol. For the PLGA concentration tested, 0.5 wt% to 5 wt% the nanosphere mean size obtained were in the range of 150 nm to over 1.4 μm. The maximum entrapment efficiency was 28.5% ± 3.3% and loading amount of 9.4% ± 1.4 wt% for PLGA nanospheres formed with 0.05 wt% of paclitaxel-ethanol solution. A limitation of this procedure is the strong dependence of the nanosphere size with respect to the polymer concentration.

2.2.5.4. Double Emulsion with Emulsion Diffusion

Cegnar et al. [82] modified the normal emulsion solvent evaporation method. The evaporation step, required for the solvent elimination, was changed by the addition of large amounts of distilled water to promote the diffusion of the solvent from the polymer (organic phase) to the aqueous suspension to improve the energy consumption. PVA was used as surfactant in the emulsion, and it was added to the second aqueous phase, in low concentrations (0.3% w/v), to avoid aggregation. Ethyl acetate was used as the organic solvent. The excess of PVA was reduced by centrifugation and wash steps with distilled water. Four 50:50 PLGA polymers (free carboxyl end groups with 12 and 48 kDa, and esterified carboxyl end group with 12 and 48 kDa) were employed to entrap cystatin, a cysteine protease inhibitor. The free carboxyl end group with 42 kDa 50:50- PLGA led to mean sizes varying from 300 nm to 350 nm with a polydispersity index of 0.3, and zeta potential of -30 mV. The free carboxyl end groups PLGA incorporated higher amounts of cystatin than esterified carboxyl end groups (free carboxyl end groups: for the 12 kDa was 57 ± 8%, and for 42 kDa was 35 ± 8%; esterified carboxyl end groups: for the 12 kDa was 12 ± 4%, and for the 42 kDa was 14 ± 6%).

In a further work, Cegnar et al. [83] optimized different parameters to obtain smaller nanoparticles with maximum cystatin activity into the matrix. The parameters tested were stirring rate (from 5000 to 15000 RPM), solvent (ethyl acetate and a mix of dichloromethane with acetone, DCMA), stirring with sonication, and polymer type. The stirring with sonication formed the smaller particles with slight difference for both solvents tested. The mean nanosphere size were 254 ± 16 nm and 235 ± 19 nm for ethyl acetate and DCMA preparations, respectively. The reduction in the cystatin activity was more pronounced with the mix of acetone and DCM (30%) compared with ethyl acetate

(15%). Therefore, a mix of sonication and mild stirring in ethyl acetate was applied to preserve up to 85% of cystatin activity. The mean nanoparticle size was 180 ± 9 nm for free carboxylic end group PLGA with molecular weight of 12 kDa. Best drug loading and entrapment efficiencies were obtained for the PLGA polymer with free carboxylic end groups, 2.6% ± 0.2% and 57% ± 8%, respectively.

2.2.5.5. Dialysis Method for Modified PLGA

This is a simple method that can be used for the preparation of nanoparticles with block-copolymers, graft copolymers, and amphiphilic materials [84, 85]. Typically, this method consists of using a dialysis device in which the organic solution is placed. The organic solution, containing the polymer and the lipophylic active component is dialyzed for at least 12 hours against distilled water to remove the organic solvent and the free active component.

Jeon et al. [84] investigated the effect of different solvents on the size of PLGA nanoparticles formed and release of norfloxacin. PLGA copolymer ratios used were 85:15, 75:25, and 50:50 with molecular weight of 48.4, 47.5, and 40.1 kDa, respectively. The experiments were developed with low PLGA concentration (0.2% w/v) suggesting that the mean size of nanospheres obtained by this method is highly sensitive to polymer concentration. The solvents studied were acetone, dimethylsulfoxide (DMSO), dimethylacetamide (DMAc), and dimethylformamide (DMF). The lowest mean size obtained was for DMF with 50:50 PLGA with 183 ± 70.6 nm (number average), and the drug content was 9.74 wt % with a loading efficiency of 10.8 wt %. The highest drug content (12.97 wt%) and loading efficiency (14.9 wt%) was for the 50:50 PLGA in DMAc, but the nanoparticle size obtained was higher (over 300 nm).

The solvent effect was further studied by Jeong et al. [85], who looked at different solvents (acetone, tetrahydrofuran (THF), DMF, DMAc, and DMSO). The lowest size nanosphere obtained was 200.4 ± 133 nm in the presence of DMAc as organic solvent (Figure 2.6). The nanoparticle sizes (number average) varied from 421.2 nm to 276.9 nm for 85:15 and 75:25 copolymer ratios, respectively. It should be noted that the entrapment efficiency was 13.3 wt% and 11.7 wt% for 85:15 and 50:50 ratios, respectively.

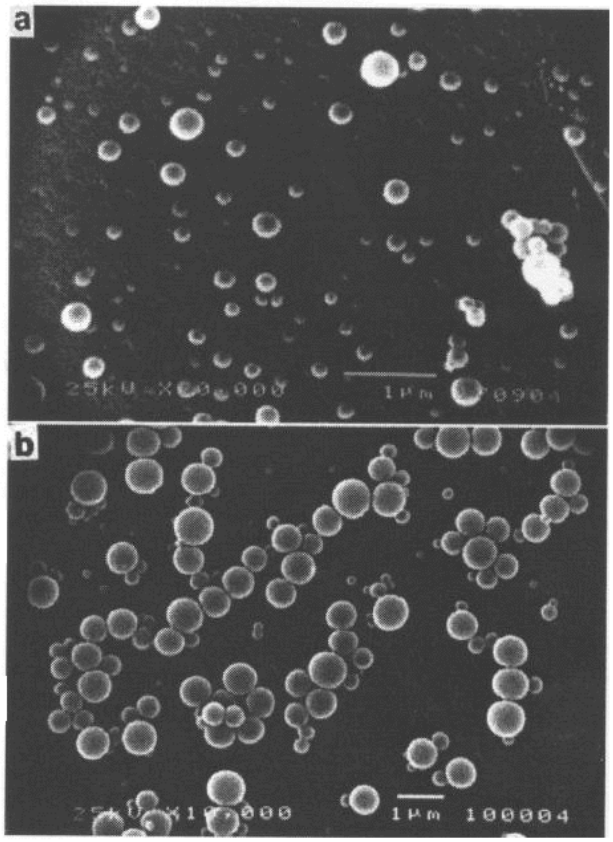

Figure 2.6. Scanning electron microphotographs of 50:50 PLGA nanoparticles prepared from (a) DMAc or (b) acetone as a function of the initial solvent. Reproduced from ref. Jeong et al. [85].

The study of testosterone-free surfactant PLGA nanoparticles was done by Jeong et al. [86]. They compared the dialysis method with solvent diffusion method in terms of PLGA nanoparticle size. The nanoparticles mean size obtained by dialysis method was 732.8 ± 190.7 nm with a drug loading of 8.5 wt% and an entrapment efficiency of 46.4 wt% using acetone. For DMF, the mean size was 164.1 ± 32.5 nm with a drug loading of 9.1 wt% and entrapment efficiency of 50.1 wt%. The solvent diffusion was done with acetone, and the mean size was 81.3 ± 10.4 nm with a drug loading of 11.2 wt% and entrapment efficiency of 63.1 wt%. The release profile for testosterone differed for each preparation suggesting that drug release is related more to the nanoparticle size than active component concentration and that it is regulated by diffusion pathways more than polymer degradation. Nanoparticle synthesized using the acetone-solvent displacement method was released faster than the nanoparticles prepared with the dialysis method (almost 100% after 3 days for the former, and almost 60% for the latter).

A further work of Jeong et al. [87] studied the addition of PLA-poly(ethylene glycol) diblock copolymer to the organic phase with dissolved PLGA. The organic solvent used was dimethylformamide. The organic solution was placed in a dialysis tube with a cutoff of 12,000 g/mol. The mean nanoparticle size (number average) was 295.3 ± 171.3 nm and 307.6 ± 27.2 nm for the PLGA and PLGA/(PLA-PEG) blend, respectively. The entrapment of adriamycin-HCl (ADR) increased the mean size to 307.6 ± 27.2 nm and 348.4 ± 176.6 nm for 1:1 and 1:2 PLGA/ADR weight ratio, respectively. Poly(L-lysine)-grafted-PLGA polymer was another modification done to PLGA by Jeong et al. [88, 89] to obtain an amphiphilic polymer suitable for micelle formation under dissolution in water. The polymer concentration used was 0.4% w/v. The mean size ranged from 149.6 ± 4.8 nm to 69.4 ± 2.8 nm for 3% or 8% of polymer grafting, respectively.

2.3. Magnetic Polymeric Nanoparticles (MPNPs)

There are numerous methods available to form magnetic polymeric nanoparticles (MPNPs), divided in two main classes, 1) polymerization techniques, starting with a monomer, and 2) chemical and physical entrapment of magnetite in a preformed polymer. Polymerization methods include emulsion or microemulsion polymerization, interfacial polymerization, precipitation polymerization, and suspension polymerization. When a preformed polymer is the starting material, the methods used are impregnation of magnetite in the polymer matrix, polymer immobilization onto inorganic magnetite, incorporation of magnetite by precipitation, and others.

2.3.1. Polymerization Methods

The materials resulting from the inclusion of magnetite (inorganic material) into a polymer matrix (organic material) are usually named polymer latexes [128, 129] or nanocomposites [130]. Both names, the first originating from colloidal chemistry and the last from nanotechnology, define a mixture of two materials forming a new material with improved properties.

Table 2.1. Summary of important parameters for PLGA nanoparticles formation

Year	Author	Method	Polymer conc. (mg/mL)	Ratio	M.W. kDa	Surfactant conc. (% w/w)	Solvent	Phase vol. (mL/mL)	Nanopart. yield (%)	Active component	Initial conc. (mg/mL)	Nanoparticle size (nm)	Entrapment efficiency (%)	Nanoparticle loading (% w/w)	Notes
2001	Ahlin [23]	ED	5% w/w	50/50 75/25	12 and 12, 63	PVA at 10, 15, 20% w/w	Benzyl alcohol	10/20	na.	na.	na.	310 190 165	na.	na.	Viscosity effect
2001	Kim [90]	ED	20	75/25	75 to 120	PVA Pluronic F68 and F127	Benzyl alcohol	10/20	na.	Estrogen	na.	Approx. 200 132 and 146	na.	na.	Surfactant effect
2002	Ahlin [24]	ED	5% w/w	50/50	12	PVA at 10, 15, 20% w/w	Benzyl alcohol	2.1g/4g	na.	Enalaprilat	2% w/v	183±5 204±6	46.4±1.7	13.2±0.5	Drug effect
2004	Ravi Kumar (a) [21]	ED	20	70/30	na.	100 mg PVA 30 mg chitosan	Ethyl acetate	10/10 + extra water	na.	DNA	10	181.5±3	na.	na.	DNA on surface
2005	Lee [19]	ED	20	75/25	75 to 120	Pluronic F68 and F127 (5%)	Ethyl acetate	10/20	na.	Magnetite (40%magn. content)	5 mg	95 to 210	na.	na.	Test stirring rates
2002	Konan [25]	SO	17% w/w	50/50	12, 48	PVA 82.6% hydrated (15w/w%)	THF and Acetone	5 g / 20 g	na.	na.	na.	102±4 154±17 137±6	na.	na.	Agitation effect
2004	Eley [27]	SO	20% w/w	na.	na.	PVA	Acetone	na.	65	Coumarin-6	1%	400 to 1100	50-55	na.	Vitro, vivo release
2004	Zweers [26]	SO	2%wt.	57/43	11.4	PVA at 2 wt.%	Acetone	5 g / 7.5 g	na.	na.	na.	230 (0.09)*	na.	na.	Degradation
1993	Niwa (b) [32]	NP	8	85/15	12, 66, 127	PVA at 2% w/v	Acetone, DCM, water	17 / 50	76.3-79.4-94.5	Nafarelin Acetate	17.6% w/v	311±20 224±14 233±31	4.96 11.8 8.22	0.15 0.37 0.22	Hydrophilic drug

Year	Author	Method	Polymer conc. (mg/mL)	Ratio	M.W. kDa	Surfactant conc. (% w/w)	Solvent	Phase vol. (mL/mL)	Nanopart. yield (%)	Active component	Initial conc. (mg/mL)	Nanoparticle size (nm)	Entrapment efficiency (%)	Nanoparticle loading (% w/w)	Notes
1993	Niwa (a) [31]	NP	4.4	85/15	66, 127	PVA at 2% w/v	Chloroform acetone	27.5 / 50	77.7-76.7	Indomethacin	10% w/w	385±51 637±40	50 - 33	5.85-3.91	Low- water soluble drug
1993	Niwa (a) [31]	NP	5	85/15	12, 66, 127	PVA at 2% w/v	DCM, acetone, methanol	27.5 / 50	96.6-83.9-93.7	5-fluorouracil	10% w/w	195±34 207±13 199±11	1.62 5.42 15.0	0.15 0.59 2.65	Water soluble drug
1994	Stolnik [92]	NP	20	75/25	63	Poloxamine and PLA:PEG (1% w/v)	Acetone and water	na.	na.	na.	na.	161±3.7 147±3.6 160±3.8	na.	na.	Surface modific.
1997	Hawley [91]	NP	0.1% w/v	75/25 65/35 55/45	50	PLA:PEG (1.5:0.75 1.5:2 2:5)	Acetone and water	10/20	na.	na.	na.	84.8±3.4 90.3±2.8 99.3±4.0	na.	na.	Surface modific.
1998	Kawashima [93]	NP	33.3	50/50	20	PVA at 1% w/v or span 80 (100 mg)	Acetone+MeOH in water or oil	2+1/25	92.6 77.7 66.9	Elcatonin	1% w/w	250(0.06) 700(0.2-0.3) 800(0.3-0.5)	19.5 44.5 2.05	0.208 0.567 0.0303	Highly water soluble drugs
2000	Muraka-mi [94]	NP	40	50/50	na.	PVA at 4% w/w	Acetone or AN	125/300	na.	na.	na.	258	na.	na.	Matrix material
2002	Ricci [95]	NP	7.74	85/15	105	PVA at 1% w/v	acetone + DCM/ water	7.75/25	na.	Leucinostatin-A	0.77	213±11	na.	20.8	Drug entrapment
2002	Casco-ne [96]	NP	2.5% w/v	50/50	40 to 75	PVA at 5%	Acetone and DCM	na.	na.	Dexamethasone	na.	100-300	na.	na.	PVA hydrogel
2003	Jiang [97]	NP	25	50/50 75/25	7.5 and 25	PVA 97% hyd (1%)	Acetone + ethanol	8/40	> 90	na.	na.	na.	na.	na.	effect of solvents
2003	Prakobvaitayakit [28]	NP	10 to 100	50/50	na.	Pluronic F68 (0.25%)	Acetone	10 / 25	na.	Itraconazole	0.2 to 1.8	190 to 644	na.	na.	

Year	Author	Method	Polymer conc. (mg/mL)	Ratio	M.W. kDa	Surfactant conc. (% w/w)	Solvent	Phase vol. (mL/mL)	Nanopart. yield (%)	Active component	Initial conc. (mg/mL)	Nanoparticle size (nm)	Entrapment efficiency (%)	Nanoparticle loading (% w/w)	Notes
2003	Ameller [34]	NP	20	na.	75	poloxamer 188 (1%)	Acetone	1 / 2	na.	Antistrogen RU 58668	$2x10^{-5}$ to 10^{-3} M	249 ±64	94.1	3.1	Surface modific.
2004	Saxena [37]	NP	4.2, 4.2, 33.3	50/50	na.	PVA	Methanol + acetonitrile	8+16/120	49.4 65.3 45.7	ICG and ICG-NaI	0.21, 0.42, 0.04	338±0.12 307±0.02 357±0.06	2.92±0.4 1.5±0.08 74.5±0.7	0.3±0.04 0.17±0.01 0.2±0.0	Drug effect
2000	Dawson [98]	EEV	1% w/v	50/50	na.	Tween 80	DCM	na.	na.	DiO	0.1	130 to 600	na.	na.	Surface modific.
2002	Pietzonka (b) [99]	EEV	50	na.	na.	PVA 0.2%	Met-chlor / water	10/50	na.	Nile red or coumarin-6	0.10%	400-500	70-80	0.1	Cellular uptake
2003	Mu and Feng [63]	EEV	1.25-2.5	75/25 50/50	90-120 40-75	Vitamin E TPGS 0.03 g/mL	DCM	na.	41.7 37.7	Paclitaxel	2.4 and 0.62% w/w	272.5±169 369.1±80.8	50.4 - 83.8	na.	Effect of surfactant
2002	Pietzon-ka (a) [59]	EEV	10	na.	na.	PVA 0.2%	methylene chloride and water	10/50	na.	Coumarin-6	0.05	400-500	70-80	0.1	Cellular uptake
2003	Diwan [100]	EEV and DEV	30% w/v	50/50	7	PVA 7.5%	water/chl-met in water	0.06/0.6 0.66/4 4.66/16	na.	TMR dextran and BLP25	1% w/v and 0.2% w/v	290-325	na.	na.	Antigen delivery
2004	Panyam [58]	EEV	24.2	50/50	143, 12, 10	PVA at 2.5% w/v	Methanol+ chloroform	1/6	na.	Dexametha sone	4.8	270 (0.23)* 740 (0.39) 240 (0.23)	na.	6±0.4 9.3±2.5 6.3±1.7	Solid state solubility
2004	Feng [101]	EEV	na.	50/50	90-126	TPGS 0.025 and 1:2 (PLGA)	DCM and water	na.	na.	Paclitaxel	na.	369.1±80.8 552±81.4	83.8 100	1 and 10	Surfactant effect
2004	Bivas-Benita [102]	EEV	10% w/v	53/47	na.	Tween80 1%, poloxamer 0.5% w/v	DCM + acetone/ water	10/20	na.	V1Jns DNA plasmid	0.025	209±16	99.8±0.1	na.	Cationic NS for DNA entrapment

Year	Author	Method	Polymer conc. (mg/mL)	Ratio	M.W. kDa	Surfactant conc. (% w/w)	Solvent	Phase vol. (mL/mL)	Nanopart. yield (%)	Active component	Initial conc. (mg/mL)	Nanoparticle size (nm)	Entrapment efficiency (%)	Nanoparticle loading (% w/w)	Notes
2005	Win [103]	EEV	na.	50/50	40-75	PVA 2% and TPGS 0.03% w/v	DCM	na.	na.	Coumarin-6	0.05% w/v	216.6±8.8 295.4±14.8	na.	na.	Surface effect on uptake
2005	Elaman-chili [104]	EEV	50%	50/50	7	PVA 9%	chl-met/water	0.4/2	na.	BPL25 and MPLA	1% w/v 0.2% w/v	357	na.	1%	Antigen to dendritic cells
1997	Blanco and Alonso [105]	DEV	200	50/50	na.	PVA 1% w/v	EAc	0.05/1 1.05/2 2.05/100	na.	BSA	40	320±2 457±2 398±5	38.9±1.4 15.4±0.6 56.8±0.7	na.	Different parameters
2001	Jiao [106]	DEV	40	50/50	40	PVA at 0.1%	Methylene chloride	1/10 11/200	na.	Heparin	5000 IU	259±6	14±4	2792±801 IU/g poly.	In vitro studies
2002	Gutierro [107]	DEV	5% w/v	50/50	na.	PVA 8%	methylene chloride and water	0.25/5 2.25/25	na.	BSA	na.	200 and 500	na.	na.	Vaccine mucosal immunization
2002	Panyam [108]	DEV	30	50/50	143	PVA at 2.5% w/v	water/ chloroform/water	1/6 7/50	na.	DNA pGL3	10	97±3 (TEM)	89.8	2.1	DNA entrapment
2003	Sanchez [109]	DEV	50	50/50	98	poloxamer 10%, Sodium cholate 1% w/v	Methylene chloride	0.1/1 1.1/2 3.1/100	na.	Interferon alpha	na.	280±12	85.1±3.1	na.	Nano and micro particles
2003	Eyles [110]	DEV	10	50/50	20	PVA 2.5% w/v and 1.5% w/v	DCM and water	10/3 13/20	na.	Tetanus toxoid	na.	180 (0.1)*	na.	3.6	Vaccine entrapment
2004	Vander-voort [71]	DEV	100	52/48	40	PVA Poloxamer Carbopol	Methylene chloride	2/10 and 12/50	na.	Pilocarpine HCl	2.5% w/v	204±4 304±5 309±6	20±8.2 16.8±5.6 32.1±6.4	na.	
2004	Scholl [111]	DEV	200	50/50	na.	Pluronic 10% and 1%	Ethyl acetate	na.	na.	Recombinant Bet v1	4	270 and 360 (50% value)	na.	16.45 µg/mg pol.	Allergen vehicle

Year	Author	Method	Polymer conc. (mg/mL)	Ratio	M.W. kDa	Surfactant conc. (% w/w)	Solvent	Phase vol. (mL/mL)	Nanopart. yield (%)	Active component	Initial conc. (mg/mL)	Nanoparticle size (nm)	Entrapment efficiency (%)	Nanoparticle loading (% w/w)	Notes
2004	Weissenboeck [112]	DEV	200	50/50	na.	Pluronic F68 (10% w/v)	Eac	0.2/1 1.2/3	na.	Covalent link	na.	300-460 (50% value)	na.	na.	Surface modific.
2004	Dillen [70, 75]	DEV	100	52/48	40	PVA at 1% w/v	DCM and water	8/20	na.	Ciprofloxacin	2.5% w/v	209.5±2.5	61	na.	Viscosity effect
2004	Prabha (b) [113]	DEV	30	50/50	na.	PVA 2% w/v	Chloroform / water	0.2/1 1.2/na.	na.	p53 plasmid DNA	5	280(0.143)*	60 to 63	1.99 to 2.1	DNA entrapment
2000	Jeon [84]	Dya	2	50/50 85/15	40.1 48.4	NO surfactant	DMF	10/1Lx3 24 hr	na.	Norfloxacin	2	183±70.6 287.5±147.6	10.8 and 13.9	9.74 and 12.17	Free surfactant
2002	Horisawa [114]	SDO	33.3	75/25	19.9 9.9 5.9	Span 80 (33.3 mg/mL)	Acetone + methanol	3 solvent / 60 oil	75.3 35.8 25.6	BSP	3.3	302±43 379±64 463±74	60.0 31.5 6.8	5.45 2.86 0.62	Modified method
2004	Cegnar (b) [83]	DESD	50	50/50	12 12 48	PVA at 5% w/v	Eac	0.2/1 1.2/4 5.2/100	na.	Cystatin	0.012	380±130 180±9 331±25	12±4 57±8 45±8	0.6±0.2 2.6±0.2 2.1±0.4	Max. activity for entrapment
2004	Kim [81]	SDya	0.5% w/v to 5% w/v	75/25	90	Tween 80 at 5% w/w	Tetraglycol and water	10/100	70	Paclitaxel	0.05wt% to 1.0wt.%	150 to 1500	3.1±2.4 28.5±3.3	19.3±2.2 9.4±1.4	Hydrophilized PLGA

Notes: The data presented in the table is classified in function of the method. The main parameters presented are: polymer concentration in mg PLGA/ml of solvent; PLGA copolymer molar ratio; PLGA molecular weight (M.W.); surfactant concentration; solvent in the organic phase; phase volume ratio; nanoparticle yield (% of final nanoparticle obtained as a function of the initial amounts of components); active component used in the formulation; initial concentration of drug in the discontinuous phase; nanoparticle size, drug entrapment efficiency (drug entrapped / initial amount added); nanoparticle loading (amount of drug related to the amount of PLGA nanoparticle). When the units are different, they are detailed in the cells.

Abbreviations used:

E.D.: emulsion diffusion
S.O.: Salting out
N.P.: nanoprecipitation or solvent diffusion
EEV: Emulsion evaporation (single emulsion)
DEV: Double emulsion evaporation
Dya: Dialysis method, free of surfactant
SDO: Solvent diffusion in oil
NS: nanosphere
DESD: Double emulsion with solvent diffusion
SDya: spray injection and dialysis

*: Polydispersity index (0 to 1)
DiO: 3'3-dioctadecyloxacarbocyanine perchlorate (fluorescent dye)
BSP: Betamethasone Sodium phosphate
ICG: Indocyanine green (free of sodium iodide)
ICG-NaI: Indocyanine green sodium iodide
chl-met: mix of chloroform and methanol
MPLA: monophosphoryl lipid A
TMR-dextran: Tetramethylrhodamine conjugated dextran
TPGS: vitamin E succinate with polyethyleneglycol 1000
Polymer concentration is based on the organic phase

BLP25: MUC1 lipopeptide
BSA: bovine serum albumin
DMF: dimethylformamide
THF: tetrahydrofuram
AN: acetonitrile
EAc: athyl acetate
DCM: dichloromethane
DXM: dexamethasone
Met-chlor: Methylene chloride

Examples of this are the addition of 1 wt% of multiwalled carbon nanotubes to polystyrene to improve the tensile strength of polystyrene by at least 25% [131], the application of cellulose whiskers (nanocrystals) as mechanical reinforcing agents for low thickness polymer electrolytes for lithium batteries [132], or the use of iron oxides and ferrites to form conducting polymers [129].

Several monomers have been used to form the shell surrounding a magnetic nanoparticle by polymerization techniques. Sauzedde et al. [128, 133] worked with polystyrene (PS), poly N-isopropylacrylamide (NIPAM) and poly S/N-isopropylacrylamide (PNIPAM) to form a stable nanoparticle by precipitation polymerization. The maximum magnetite adsorbed was 1.24 g/g for PNIPAM, and the hydrodynamic diameter of the nanoparticles formed was 450 nm at 20 °C. When the adsorption was carried out at 40 °C, the mean size decreased to 215 nm, but the magnetite adsorbed decreased as well to 0.95 g/g.

Dresco et al. [134] used a single inverse microemulsion by seed copolymerization of methacrylic acid, hydroxyethyl methacrylate and cross-linker to form magnetic nanoparticles. Nanoparticles in the range of 80 to 320 nm were obtained. Arias et al. [135] used anionic polymerization to synthesize a shell of poly(ethyl-2-cyanoacrylate) with a magnetite core. The core/shell nanoparticles obtained were spherical in shape and measured around 144 nm (± 15 nm) with a polymer shell of 30 nm (approx.), for an initial weight ratio of 4 to 3 between monomer to magnetite. Landfester and Ramirez [136] studied miniemulsion polymerization technique as a way to form magnetic polymeric nanoparticles. The nanospheres made from polystyrene matrix with entrapped magnetite measured in average 60 nm, and the entrapment efficiency of magnetite ranged from 19.4% to 34.7% as measured by thermogravimetric measurements. Zheng et al. [137] used the same method to improve the magnetite content and the nanoparticle size distribution. The final nanoparticle mean size was around 120 nm as measured by DLS. Different ratios of magnetite/styrene monomers were tested. The lowest particle diameter (102 nm) was observed for the 1/1 ratio, and the highest diameter (128 nm) was for the 1/3 ratio. The magnetic content was found to change proportionally to the amount of magnetite used for the preparation of the magnetic core polymeric shell system, ranging from 27 to 55 %.

The polymerization techniques have the advantage of forming well controlled magnetic core polymeric shell nanoparticles, by close monitoring the magnetite to polymer ratio, as compared to other methods. A limitation of the polymerization techniques is that the polymeric shell, in some cases, is not thick enough to transport a suitable amount of drug [130, 138]. Other drawbacks are the risk of residual additives and the possibility of interactions or cross-reactions between the drug and the polymer during the polymerization process, leading to drug inactivation [117].

2.3.2. Chemical and Physical Entrapment of Magnetite

2.3.2.1. Chemical Entrapment and Surface Modification of Magnetite

Another procedure used to form polymeric latexes or nanocomposites is the attachment of preformed polymers to magnetite by chemical reaction. The polymer is formed previously and added to the magnetite synthesis or formed magnetite.

Burke et al. [130] worked with polyethylene, polystyrene and polyisobutylen to form a suitable polymeric shell for magnetic nanoparticles (called nanocomposites). The previously formed polymers were added to iron pentacarbonyl and kerosene to form the core/shell nanoparticle. The average size varied from 8 nm to 50 nm with a core size range of 3 nm to 45 nm. The iron content varied from 21 to 61 % wt %. In general, a smaller size distribution of nanoparticles was observed for polyethylene and polyisobutylene as compared to polystyrene shell nanocomposites.

2.3.2.2. Physical Entrapment

In the physical entrapment techniques (top-down techniques), the starting materials are the polymer and magnetite. No chemical reactions are involved in the process; magnetite is entrapped into the polymeric matrix by hydrophobic-hydrophilic, electrostatic, or steric interaction.

Emulsion evaporation, emulsion diffusion, salting out, nanoprecipitation or solvent displacement, are some of the common methods used to form nanoparticles from preformed polymers. These methods can be adapted to entrap magnetite. Jeong et al. [139] entrapped magnetite into a preformed polymer (PLGA) by the emulsion diffusion method. The nanoparticles obtained had an average size of 120 nm. Lee et al. [19] entrapped magnetite in PLGA by nanoprecipitation. The magnetite was suspended in acetone after the PLGA dissolution (150 mg), and the initial magnetite concentration

(theoretical loading) was 3.33 % w/w (related to PLGA weight). The nanoparticle size obtained ranged from 120 nm to 230 nm for PLGA concentration varied from 1% to 5%, respectively.

Emulsion evaporation is one of the oldest methods used with preformed polymers, and it has been extensively used to entrapment numerous drugs [63, 72, 121]. Hydrophilic compounds (normal magnetite) can be modified by adding a layer of oleic acid to the surface to ensure its entrapment in the PLGA (hydrophobic polymer) matrix by emulsion evaporation method.

2.3.3. Surface Modification

Surface modification is pursued not only to ensure effective magnetite entrapment in PLGA, but also in an attempt to improve stability of the magnetic nanoparticles, to increase their circulation half life, and improve the nanoparticle cellular uptake. Zaitsev et al. [140] used methacrylic acid for magnetite coating. The size of the nanoparticles formed was 5.7 nm. Dextran coated magnetite nanoparticles have been researched by Lacava et al. [141], who focused on long term retention of the particles in the liver and spleen. Magnetite nanoparticles with an average size of 9.4 nm were obtained. The use of triblocks copolymer is yet another approach to improve the stability of magnetite. Harris et al. [138] synthesized a triblock copolymer which was adsorbed onto the magnetite surfaces. The mean size of the nanoparticles was 8.7 nm (SD 2.7 nm). The amount of entrapped magnetite ranged from 6.9 to 45.4 wt%.

The incorporation of poly(ethylene glycol) (PEG) on the magnetite surface is another approach to improve stability and increase the circulation half life. Kim et al. [142] obtained nanoparticles of 4.2 nm in size. Gupta and Curtis [143] studied the effect of PEG coated magnetite on human fibroblasts cells suggesting that the cellular uptake is improved compared with unmodified magnetite. The size of the magnetite coated nanoparticles was around 40 -50 nm in diameter. Goodarzi et al. [144] used citric acid for surface modification to obtain a suitable aqueous suspension of magnetite. The size range ranged from 5 to 13 nm. The amount of citric acid attached to the surface was around 30% in weight as determined by thermogravimetric analysis (TGA).

Surfactants were used to stabilize magnetite and to form hydrophilic or hydrophobic magnetic nanoparticles. The adsorption of surfactants on the magnetite

surface was studied by Korolev et al. [145]. Oleic, stearic, and linoleic acids were tested in CCl_4, and oleic acid in hexane. A higher amount of oleic acid was adsorbed for both solvents on the magnetite surface as compared to stearic and linoleic acids, suggesting a better performance for this fatty acid. The nanoparticle size obtained varied between 5.7 nm and 9.3 nm, depending on the temperature. Montagne et al. [146] worked with oleic acid for stabilization of water-oil emulsion of maghemite (Fe_3O_2) ferromagnetic fluid. Wooding et al. [147] studied the effect of different carboxylic acids (C6 to C18) on the stability of surface modified magnetite in aqueous suspension for one and two surfactant layers. The surface covered was between 21 to 38 $Å^2$. Along the same lines, the addition of fatty acids (oleic acid, dodecanoic acid, etc.) was found to improve the stability of magnetite in aqueous and organic suspension. Xu et al. [131] used N-oleoylsarcosine to form a double layer on the magnetite surface by changing the amount of surfactant added to the suspension. The nanoparticle size varied between 8.1 nm and 20.7 nm. Landfester and Ramirez [136] used oleic acid to form a hydrophobic magnetite which was suspended in octane. The nanoparticle size was around 20 nm. A different approach was followed by Jain et al. [148], who mixed two surfactants to entrap a suitable drug. The first one was oleic acid which was attached to the magnetite surface. The second surfactant was Pluronic F-127 which was added to the system magnetite-oleic and stirred over night. The optimum composition was 70.1 wt% magnetite, 15.4 wt% oleic acid, and 14.5 wt% Pluronic F-127 determined by TGA. The drug (doxorubicin) loaded into the system was 8.2 ± 0.5 wt% with an entrapment efficiency of 82%.

Another option for magnetite surface modification is the incorporation of ligands like folic acid [149], proteins like HIV-1 tat peptide [150], or poly ethylene glycol (PEG) [142, 149], which was found to improve the half-life by limiting the mononuclear phagocyte system (MPS) uptake.

2.4. Characterization

2.4.1. Morphology

The methods most broadly used to characterize nanoparticle morphology are transmission electron microscopy (TEM), scanning electron microscopy (SEM), cryogenic transmission electro microscopy (cryo-TEM) and atomic force microscopy (AFM). TEM is used for shape, aggregation, and internal details. It is common to use a

negative staining with phosphotungstic acid solution (3% w/v, adjusted to pH 4.7 with KOH) [115]. Panyam et al. [108, 116] used negative staining with uranyl acetate for TEM. SEM is used for surface characterization (shape, distribution, aggregation) with a layer of gold [117] or nanoparticles alone [59, 60, 80, 81, 99]. Cryo-TEM is used to observe the micellar formation of PLGA-g-PEG [118]. Dailey et al. [119] used AFM to visualize three different formulation (PVA grafted PLGA polymer with different amounts of carboxymethyl cellulose) on mica with and without nickel chloride pretreatment. Ravi Kumar et al. [22] and Saxena et al. [37] used AFM for size and morphology of nanoparticles. Moreover, a three D image of one nanoparticle was obtained by Feng et al. [101].

2.4.2. Size and Size Distribution

Dynamic light scattering is the most widely technique used to determine size and size distribution. One of the most common used techniques is photon correlation spectroscopy at room temperature with water as suspension medium [17, 87, 116, 120]. Typically, the suspension is previously sonicated to reduce aggregation if the sample is a re-suspension of nanoparticles. Panyam and Labhasetwar [121] used TEM to determine the mean size of the nanoparticles. The same equipment is used to determine mean size and size distribution. The turbidity measurements are used to evaluate droplet size changes and aggregation during emulsification and evaporation [117].

2.4.3. Surface Properties

Laser doppler anemometry is used to measure the zeta potential, an important parameter when considering the stability of the nanoparticles [30, 34, 103, 105, 119] in vitro. The more negative or positive values of zeta potential are related to more stable particles; more repulsion between particles reduce the particle aggregation. For chemical characterization, Fourier transform infrared spectroscopy (FT-IR) is used when there is surface modification by the attachment of special components [122]. Gref et al. [123] used two-dimensional electrophoresis to determine the plasma protein adsorbed onto the nanoparticles surface. The surface hydrophobicity was measured by the binding constant of Rose Bengal [74].

2.4.4. Active Component Entrapment

The entrapment into the nanoparticles is described by two important parameters: theoretical drug loading, which is the ratio between mass of drug used in synthesis and mass of polymer used in synthesis, and nanoparticle recovery, which is the ratio between mass of nanoparticles recovered and mass of polymer and drug used in synthesis. The drug content is calculated by the ratio of mass of drug in nanoparticles to mass of nanoparticles recovered, and the drug entrapment by the ratio of mass of drug in nanoparticles to mass of drug used in synthesis [17, 31, 120]. The quantitative determination of active component entrapped in nanoparticles is done by extraction of the drug. The polymer dissolution in a suitable solvent (acetonitrile, ethyl acetate, and others) is required, washing steps with distilled water, and purification. The drug concentration of the final suspension can be measured by ultraviolet spectroscopy at defined wavelength (related to the active component) or HPLC. When the target is the quantification of surfactant attached to the surface, the thermo-gravimetric analysis is used [50].

2.4.5. Other Techniques

Gel permeation chromatography is suitable to determine the molecular weight of the polymers used for nanoparticle formation and for studies of degradation [87, 124]. Dailey et al. [119] studied degradation by measuring the lactic and glycolic acid present in the supernatant at different time intervals with a UV spectrophotometer. When the nanoparticles are tested in vitro, flow cytometry is used to determine the cell association in 3'3-dioctadecyloxacarbocyanine perchlorate (DiO) [98]. H-NMR is commonly used when the target is the identification of a specific structure in the nanoparticle and polymer blends [38, 125], but Chognot et al. [126] used to determine the molecular weight (M_n and M_w) of MPEO. To determine the PVA residues on the nanoparticles, a colorimetric method is used [17, 116] with measurements at 644 nm. Desgouilles et al. [127] used a small angle neutron scattering to investigate the nanoparticle structure. The sample was diluted in deuterium oxide (D_2O), and the sample-to-detector distance was 1.62 or 4.62 m with incident wavelengths of 6 or 15 Å. For porosity measurements, the true density was calculated with helium pycnometer equipment by Murakami et al. [94], and the formula used was Porosity = (1-(apparent density/true density))*100. The crystallinity of polymer

and drugs are estimated by x-ray diffraction [17, 58, 70] or using differential scanning calorimetry [70]. A common method used to determine the crystallinity of the polymer and drug entrapped is done by x-ray diffraction [17, 101].

2.5. Conclusions

Many methods are available to synthesize PLGA nanoparticles, starting with a preformed polymer. Each has its advantages and disadvantages, but the principal selection criteria should be the chemical characteristics of the active component and its interactions with the organic solvents, polymer, and surfactant, as well as the final use of the nanoparticles. Polymerization methods are widely employed for magnetic polymeric nanoparticles (MPNPs) synthesis as compared with methods based on preformed polymers. The final application of MPNPs is the limiting factor in selecting the adequate synthesis method. For example, the potential toxicity of chemical compounds (initiators, residual monomers, and additives) needed in some polymerization techniques limits the use of these methods in formation of nanoparticles for drug delivery applications.

The methods based on diffusion of the organic solvent to form the PLGA nanoparticles are limited to low polymer concentration to maintain a nanoparticle mean size of 200 nm. Methods that involve solvent evaporation are more time consuming and expensive, but are less sensitive to changing the polymer concentration. Emulsion evaporation, in particular, can be used for entrapment of hydrophilic (w/o/w emulsion) or hydrophobic (w/o emulsion) drugs, which is an advantage. The salting-out method is suitable for formation of nanoparticles at higher polymer concentration, but the involved purification process is a limitation of the synthesis method. Surfactant concentration, polymer concentration, polymer molecular weight, solvents, surfactant concentrations, and phase ratios play an important role in controlling the size of the nanoparticles in all methods available for nanoparticles formation. There are important advances in understanding the mechanisms involved and possible manipulation of the nanoparticle characteristics and the improvement in the drug entrapment efficiency by carefully controlling these parameters.

The availability of different characterization techniques makes the detailed analysis of the nanoparticle system possible. The nanoparticles size is affected by many parameters and researchers are continually attempting to decrease the average

nanoparticle size. Synthesis of PLGA nanoparticles smaller in size than 100 nm is not common by the methods detailed above; however, the advantages of smaller sizes should be studied in depth (i.e. nanoparticles designed for intracellular use should be smaller than nanoparticles designed for extra cellular use).

The magnetic polymeric nanoparticles (MPNPs) are synthesized by polymerization methods. The size range is from 30 nm to over 100 nm. The common structure of the MPNPs is a magnetic core with a polymer shell. The amount of magnetite entrapped ranged from 10 %wt. to 35% wt. The use of preformed polymer to entrap magnetite is limited, and nanoprecipitation is the only top-down method employed in forming MPNPs.

Formation of nanoparticles that can interact with the human body and can modify their responses based on changes in the environment is the next research step in the field. Several questions will be addressed to reach this goal, such as the addition of new polymers to form grafted PLGA, surface modification by adding new polymers or ligands, as well as the creation of nanoparticles with new properties for modulated responses and a better performance.

2.6. References

1. J. Anderson, M. Shive, Biodegradation and biocompatibility of PLA and PLGA microspheres. Advanced Drug Delivery Reviews. **28**, 5-24 (1997).

2. K. Westesen, H. Bunjes, G. Hammer, and B. Siekmann**,** Novel colloidal drug delivery systems. PDA Journal of Pharmaceutical Science & Technology **55**(4), 240-247 (2001).

3. I. Brigger, C. Dubernet, and P. Couvreur, Nanoparticles in cancer therapy and diagnosis. Advanced Drug Delivery Reviews, **54,** 631-651 (2002).

4. M. Chorny, I. Fishbein, H. Danenberg, and G. Golomb, Lipophilic drug loaded nanospheres prepared by nanoprecipitation: effect of formulation variables on size, drug recovery and release kinetics. Journal of Controlled Release, 83, 389-400 (2002).

5. G. Barrat, G. Courraze, C. Couvreur, E. Fattal, R. Gref, D. Labarre, P. Legrand, G. Ponchel, and C. Vauthier, Polymeric Micro- and Nanoparticles as drug Carriers. In Polymeric Biomaterials, second ed. (S. Dumitriu, ed.). Marcel Dekker Inc., New York, 753-781 (2000).

6. E. Nakache, N. Poulain, F. Candau, A. Orecchioni, and J. Irache, In the Handbook of nanostructured materials and nanotechnology. (E. Nalwa, H.S. ed) Academic Press, 5, 577-635 (2000).

7. M. Hans, and A. Lowman, Biodegradable nanoparticles for drug delivery and targeting. Current Opinion Solid State Matter Science, 6, 319-327 (2002).

8. G. Sekhara Rao, M. Satish Kumar, N. Mathivanan, and M. Bhanoji Rao, Nanosuspensions as the most promising approach in nanoparticulate drug delivery systems. Pharmazie, 59, 5-9 (2003).

9. E. Allemann, R. Gurny, E. Doelker, Drug-release nanoparticles- preparation methods and drug targeting issues. European Journal of Pharmacy and Biopharmacy, 39(5), 173-191 (1993).

10. S. Rani, R. Hiremath, and A, Hota, Nanoparticles as drug delivery systems. Indian Journal of Pharmaceutical Sciences, 61(2), 69-75 (1998).

11. D. Quintanar-Guerrero, E. Allemann, H. Fessi, and E. Doelker, Preparation technique and mechanism of formation of biodegradable nanoparticles from preformed polymers. Drug Development and industrial Pharmacy, **24**(12), 1113-1128 (1998).

12. S. Moghimi, A. Hunter, and J. Murray, Long-circulating and target-specific nanoparticles: Theory to practice. Pharmacological Reviews, 53, 283-318 (2001).

13. J. Panyam, and V. Labhasetwar, Biodegradable nanoparticles for drug and gene delivery to cells and tissue. Advanced Drug Delivery Review, 55, 329-347 (2003a).

14. K. Avgoustakis, Pegylated poly(lactide) and poly(lactide-co-glycolide nanoparticles: preparation, properties and possible applications in drug delivery. Current Drug Delivery, 1, 321-333 (2004).

15. I. Bala, S. Haribaran, and R. Kumar, PLGA nanoparticles in drug delivery: The state of the art. Critical Reviews in therapeutic Drug Carrier Systems, 21, 387- 422 (2004).

16. F. Alexis, Factors affecting the degradation and drug-release mechanism of poly(lactide acid and poly(lactic acid-co-glycolic acid). Polymer International, 54, 36-46 (2005).

17. Y. Konan, R. Cerny, J. Favet, M. Berton, R. Gurny, and E. Allemann, Preparation and characterization of sterile sub-200 nm meso-tetra(4-hydroxylphenyl)porphyrin-loaded nanoparticles for photodynamic therapy. European Journal of Pharmaceutics and Biopharmaceutics, 55, 115-124 (2003).

18. S. Kwon, J. Lee, S. Choi, Y. Jang, and J. Kim, Preparation of PLGA nanoparticles containing estrogen by emulsification-diffusion method. Colloids and Surfaces, A: Physicochemical and Engineering Aspects, 182, 123-130 (2001).

19. S. Lee, J. Jeong, S. Shin, J. Kim, Y. Chang, K. Lee, and J. Kim, Magnetic enhancement of iron oxide nanoparticles encapsulated with poly(D,L-lactide-co-glycolide). Colloids and Surfaces A: Physicochemical Engineering Aspects, 255, 19-25 (2005).

20. S. Choi, H. Kwon, W. Kim, and J. Kim, Thermodynamic parameters on poly(D,L-lactide-co-glycolide) particle size in emulsification-diffusion process. Colloids and Surfaces A: Physicochemical and Engineering Aspects, 201, 283-289 (2001).

21. M. Ravi Kumar, U. Bakowsky, and C. Lehr, Preparation and characterization of cationic PLGA nanospheres as DNA carriers. Biomaterials, 25, 1771-1777 (2004).

22. M. Ravi Kumar, S. Mohapatra, X. Kong, P. Jena, U. Bakowsky, and Lehr, Cationic poly(lactide-co-glycolide) nanoparticles as efficient in vivo gene transfection agents. Journal of Nanoscience and Nanotechnology, 4(8), 990-993 (2004).

23. P. Ahlin, N. Jerenec, and J. Kristl, Influence of formulation variables on the size of PLGA and PLA nanoparticles prepared by an emulsification-diffusion technique. Scientia Pharmaceutica, 69(3), S167-S168 (2001).

24. P. Ahlin, J. Kristl, A. Kristl, and F. Vrecer, Investigation of polymeric nanoparticles as carriers of enalaprilat for oral administration. International Journal of Pharmaceutics, 239, 113-120 (2002).

25. Y. Konan, R. Gurny, and E. Allemann, Preparation and characterization of sterile and freeze-dried sub-200 nanoparticles. International Journal of Pharmaceutics, 233, 239-252 (2002).

26. M. Zweers, G. Engbers, D. Grijpma, and J. Feijen, In vitro degradation of nanoparticles prepared from polymers based on DL-lactide, glycolide and poly(ethylene oxide). Journal of Controlled Release, 100, 347-356 (2004).

27. J. Eley, V. Pujari, and J. McLane, Poly(lactide-co-glycolide) nanoparticles containing coumarin-6 for suppository delivery: in vitro release profile and in vivo tissue distribution. Drug Delivery, 11, 255-261 (2004).

28. M. Prakobvaitayakit, and U. Nimmannit, Optimization of polylactic-co-glycolic acid nanoparticles containing itraconazole using 23 factorial design. AAPS PharmSciTech, 4(4), 1-9 (2003).

29. T. Govender, S. Stolnik, M. Garnett, L. Illum, and S. Davis, PLGA nanoparticles prepared by nanoprecipitation: drug loading and release studies of a water soluble drug. Journal of Controlled Release, 57, 171-185 (1999).

30. N. Csaba, P. Caamano, A. Sanchez, F. Dominguez, and M. Alonso, PLGA:poloxamer and PLGA:poloxamine blend nanoparticles: new carriers for gene therapy. Biomacromolecules, 6, 271-278 (2005).

31. T. Niwa, H. Takeuchi, T. Hino, N. Kunou, and Y. Kawashima, Preparations of biodegradable nanospheres of water-soluble and insoluble drugs with D,L-lactide/glycolide copolymer by a novel spontaneous emulsification solvent diffusion method, and the drug release behavior. Journal of Controlled Release, 25, 89-98 (1993).

32. T. Niwa, H. Takeuchi, T. Hino, N. Kunou, and Y. Kawashima, In vitro drug release behavior of D,L-Lactide/glycolide copolymer (PLGA) nanospheres with naferelin acetate prepared by a novel spontaneous emulsification solvent diffusion method. Journal of Pharmaceutical Sciences, 83(5), 727-732 (1993).

33. T. Ameller, V. Marsaud, P. Legrand, R. Gref, and J. Renoir, Pure antiestrogen RU 58668-loaded nanospheres: morphology, cell activity and toxicity studies. European Journal of Pharmaceutical Sciences, 21, 361-370 (2004).

34. T. Ameller, V. Marsaud, P. Legrand, R. Gref, G. Barrat, and J. Renoir, Polyester-Poly(ethylene Glycol) nanoparticles loaded with the pure antiestrogen RU 58668: Physicochemical and opsonization properties. Pharmaceutical Research, 20(7), 1063-1070 (2003).

35. Z. Panagi, A. Beletsi, G. Evangelatos, E. Livaniou, D. Ithakissios, and K. Avgoustakis, Effect of dose on the biodistribution and pharmacokinetics of PLGA and PLGA-mPEG nanoparticles. International Journal of Pharmaceutics, 221, 143-152 (2001).

36. C. Oster, M. Wittmar, F. Unger, L. Barbu-Tudoran, A. Schaper, and T. Kissel, Design of amine-modified graft polyesters for effective gene delivery using DNA-loaded nanoparticles. Pharmaceutical Research, 21(6), 927-931 (2004).

37. V. Saxena, M. Sadoqi, and J. Shao, Indocyanine green-loaded biodegradable nanoparticles: preparation, physicochemical characterization and in vitro release. International Journal of Pharmaceutics, 278, 293-301 (2004).

38. N. Csaba, L. Gonzalez, A. Sanchez, and J. Alonso, Design and characterization of new nanoparticulate polymer blends for drug delivery. Journal of Biomaterials Science. Polymer Edition, 15, 9, 1137-1151 (2004).

39. F. De Jaeghere, E. Doelker, and R. Gurny, In the Encyclopedia of control drug delivery. (E. Mathiowitz ed.) John Wiley & Sons, Inc. New York, 2, 641-664 (1999).

40. R. Alex, and R. Bodmeier, Encapsulation of water-soluble drugs by a modified solvent evaporation method. I. Effect of process and formulation variables on drug entrapment. Journal of Microencapsulation, 7(3), 347-355 (1990).

41. W. Obeidat, and J. Price, Viscosity of polymer solution phase and other factors controlling the dissolution of theophylline microspheres prepared by emulsion solvent evaporation method. Journal of Microencapsulation, 20(1), 57-65 (2003).

42. F. Mohammed, and M. Hassan, Formulation and evaluation of ciprofloxacin hydrochloride and norfloxacin microspheres prepared by an enhanced emulsion-solvent evaporation process. S.T.P. Pharma Sciences, 13(9), 319-327 (2003).

43. S. Takada, Y. Yamagata, M. Misaki, K. Taira, and T. Kurokawa, Sustained release of human growth hormone from microcapcules prepared by a solvent evaporation technique. Journal of Controlled Release, 88, 229-242 (2003).

44. S. Park, and S. Kim, Preparation and characterization of biodegradable poly(l-lactide)/poly(ethylene glycol) microcapsules containing erythromycin by emulsion solvent evaporation technique. Journal of Colloid Interface Science, 271, 336-341 (2004).

45. K. Holmberg, B. Jonsson, B. Kronberg, and B. Lindman, Surfactants and polymers in aqueous solution. Second edition, John Wiley & Sons, Ltd. The Atrium, England, 451-471 (2003).

46. M. Lopez-Quintela, Synthesis of nanomaterials in microemulsions: formation mechanisms and growth control. Current Opinion in Colloid and Interface Science, 8, 137-144 (2003).

47. B. Paul, and S. Moulik, Uses and Applications of Microemulsions. Current Science, 80(8), 990-1001 (2001).

48. K. Landfester, Miniemulsions for nanoparticle synthesis. Topics in Current Chemistry, 227, 75-124 (2003a).

49. K. Bouchemal, S. Briancon, E. Perrier, and H. Fessi, Nano-emulsion formulation using spontaneous emulsification: solvent, oil and surfactant optimization. International Journal of Pharmaceutics, 280, 241-251 (2004).

50. K. Landfester, Preparation of polymer and hybrid colloids by miniemulsion for biomedical applications. Surfactant Science Series, 115, 225-243 (2003b).

51. K. Landfester, J. Eisenblatter, and R. Rothe, Preparation of polymerizable miniemulsions by ultrasonication. JCT Research, 1(1), 65-68 (2004).

52. J. Bibette, F. Leal-Calderon, V. Schmitt, P. Poulin, Emulsion Science, Springer-Verlag, Berlin, 79-93 (2002).

53. T. Mason, and J. Bibette, Emulsification in viscoelastic media. Physical Review Letters, 77,16, 3481-3484 (1996).

54. T. Mason, and Bibette, Shear rupturing of droplets in complex fluids. Langmuir, 13, 4600-4613 (1997).

55. V. Schmitt, F. Leal-Calderon, and J. Bibette, Preparation of monodisperse particles and emulsions by controlled shear. Topics in Current Chemistry, 227, 195-216 (2003).

56. X. Zhao, and J. Goveas, Size selection in viscoelastic emulsions under shear. Langmuir, 17, 3788-3791 (2001).

57. M. Julienne, M. Alonso, J. Gomez Amoza, and J. Benoit, Preparation of poly(D,L-Lactide/glycolide) nanoparticles of controlled particle size distribution: application of experimental design. Drug Development and Industrial Pharmacy, 18(10), 1063-1077 (1992).

58. J. Panyam, D. Williams, A. Dash, D. Leslie-Pelecky, and V. Labhasetwar, Solid-state solubility influences encapsulation and release of hydrophobic drugs from PLGA/PLA nanoparticles. Journal of pharmaceutical Sciences, 93(7), 1804-1814 (2004).

59. P. Pietzonka, E. Walter, S. Duda-Johner, P. Langguth, and H. Merkle, Compromised integrity of excised porcine intestinal epithelium obtained from the abattoir affects the outcome of in vitro particle uptake studies. European Journal of Pharmaceutical Sciences, 15, 39-47 (2002).

60. C. Song, V. Labhasetwar, H. Murphy, X. Qu, W. Humphrey, R. Shebuski, and R. Levy, Formulation and characterization of biodegradable nanoparticles for intravascular local drug delivery. Journal of Controlled Release, 43, 197-212 (1997).

61. T. Chung, Y. Huang, and Y. Liu, Effects of the rate of solvent evaporation on the characteristics of drug loaded PLLA and PDLLA microspheres. International Journal of Pharmaceutics, 212, 161-169 (2001).

62. T. Chung, Y. Huang, Y. Tsai, and Y. Liu, Effects of solvent evaporation rate on the properties of protein-loaded PLLA and PDLLA microspheres fabricated by emulsion-solvent evaporation process. Journal of Microencapsulation, 9, 463-471 (2002).

63. L. Mu, and S. Feng, A novel controlled release formulation for anticancer drug paclitaxel (Taxol®): PLGA nanoparticles containing vitamin E. TPGS. Journal of Controlled Release, 86, 33-48 (2003).

64. M. Ficheux, L. Bonakdar, F. Leal-Calderon, and J. Bibette, Some stability criteria for double emulsions. Langmuir, 14, 2702-2706 (1998).

65. K. Pays, J. Giermanska-Kahn, B. Pouligny, J. Bibette, and F. Leal-Calderon, Coalescence in surfactant-stabilized double emulsions. Langmuir, 17, 7758-7769 (2001).

66. K. Pays, J. Giermanska-Kahn, B. Pouligny, J. Bibette, and F. Leal-Calderon, Double emulsions: how does release occur? Journal of Controlled Release, 79, 193-205 (2002).

67. A. Domb, and L. Bergelson, In the Microencapsulation: Methods and industrial applications. (Simon Benita ed.) Marcel Dekker, Inc., New York, 15, 411-534 (1996).

68. S. Prabha, and V. Labhasetwar, Critical determinants in PLGA/PLA nanoparticles-mediated gene expression. Pharmaceutical Research, 21(2), 354-364 (2004).

69. J. Aukunuru, S. Ayalasomayajula, and U. Kompella, Nanoparticles formulation enhances the delivery and activity of vascular endothelial growth factor antisense oligonucleotide in human retinal pigment epithelial cells. Journal of Pharmacy and Pharmacology, 55, 1199-1206 (2003).

70. K. Dillen, W. Weyenberg, J. Vandervoort, and A. Ludwig, The influence of the use of viscosifying agents as dispersion media on the drug release properties from PLGA nanoparticles. European Journal of Pharmaceutics and Biopharmaceutics, 58, 539-549 (2004).

71. J. Vandervoort, K. Yoncheva, and A. Ludwing, Influence of homogenization procedure on the physicochemical properties of PLGA nanoparticles. Chemical and Pharmaceutical Bulletin, 52, 1273-1279 (2004).

72. P. Yan, Z. Huiying, X. Hui, W. Gang, H. Jinsong, and Z. Junming, Effect of experimental parameters on the encapsulation of insulin-loaded poly(lactide-co-glycolide) nanoparticles prepared by a double emulsion method. Journal of Chinese Pharmaceutical Science, 11(1), 38-40 (2002).

73. J. Vandervoort, and A. Ludwing, Biocompatible stabilizers in the preparation of PLGA nanoparticles: a factorial design study. International Journal of Pharmaceutics, 238, 77-92 (2002).

74. S. Sahoo, J. Panyam, S. Prabha, and V. Labhasetwar, Residual polyvinyl alcohol associated with poly (dl-lactide-co-glycolide) nanoparticles affects their physical properties and cellular uptake. Journal of Controlled Release, 82, 105-114 (2002).

75. K. Dillen, J. Vandervoort, G. Van der Mooter, L. Verheyden, and A. Ludwig, Factorial design, physicochemical characterization and activity of ciprofloxacin-PLGA nanoparticles. International Journal of Pharmaceutics, 275, 171-187 (2004).

76. T. Nakashima, M. Shimizu, and M. Kukizaki, Particle control of emulsion by membrane emulsification and its applications. Advanced Drug Delivery Reviews, 45, 47-56 (2000).

77. N. Christov, D. Ganchev, N. Vassilena, N. Denkov, K. Danov, and P. Kralchevsky,. Capillary mechanisms in membrane emulsification: oil-in-water emulsions stabilized by tween 20 and milk proteins. Colloids and Surfaces A: Physicochemical and Engineering Aspects, 209, 83-104 (2002).

78. S. Joscelyne, and G. Tragardh, Membrane emulsification- a literature review. Journal of Membrane Science, 169, 107-117 (2000).

79. N. Yamazaki, H. Yuyama, M. Nagai, G. Ma, and S. Omi, A comparison of membrane emulsification obtained using SPG (Shirasu porous glass) and PTFE (poly(tetrafluoroethylene)) membranes. Journal of Dispersion Science and Technology, 23, 279-292 (2002).

80. S. Pamujula, R. Graves, T. Freeman, V. Srinivasen, L. Bostanian, V. Kishore, and T. Mandal, Oral delivery of spray dried PLGA/amifostine nanoparticles. Journal of Pharmacy and Pharmacology, 56, 1119-1125 (2004).

81. B. Kim, D. Kim, S. Cho, and S. Yuk, Hydrophilized poly(lactide-co-glycolide) nanospheres with poly(ethylene oxide)-poly(propylene oxide)-poly(ethylene oxide) triblock copolymer. Journal of Microencapsulation, 21(7), 697-707 (2004).

82. M. Cegnar, A. Premzl, V. Zavasnik-Bergant, J. Kristl, and J. Kos, Poly(lactide-co-glycolide) nanoparticles as carrier system for delivering cysteine protease inhibitor cystatin into tumor cells. Experimental Cell Research, 301, 223-231 (2004).

83. M. Cegnar, J. Kos, and J. Kristl, Cystatin incorporated in poly(lactide-co-glycolide) nanoparticles: development and fundamental studies on preservation of its activity. European Journal of Pharmaceutical Sciences, 22, 357-364 (2004).

84. H. Jeon, Y. Jeong, M. Jang, Y. Park, and J. Nah, Effect of solvent on the preparation of surfactant-free poly(DL-lactide-co-glycolide) nanoparticles and norfloxacin release characteristics. International Journal of Pharmaceutics, 207, 99-108 (2000).

85. Y. Jeong, C. Cho, S. Kim, S. Ko, S. Kim, Y. Shim, and J. Nah, Preparation of poly(DL-lactide-co-glycolide) nanoparticles without surfactant. Journal of Applied Polymer Science, 80, 2228-2236 (2001).

86. Y. Jeong, Y. Shim, K. Song, Y. Park, H. Ryu, and J. Nah, Testosterone-encapsulated surfactant-free nanoparticles of poly(DL-lactide-co-glycolide): preparation and release behavior. Bulletin of Korean Chemical Society, 23, 11, 1579-1584 (2002).

87. Y. Jeong, Y. Shim, C. Choi, M. Jang, G. Shin, and J. Nah, Surfactant-free nanoparticles of Poly(DL-Lactide-co-glycolide) prepared with Poly(L-lactide)/Poly (ethylene glycol). Journal of Applied Polymer Science, 89, 1116-1123 (2003).

88. J. Jeong, and T. Park, Poly(L-lysine)-g-poly(D,L-lactic-co-glycolic acid) micelles for low cytotoxic biodegradable gene delivery carriers. Journal of Controlled Release, 82, 159-166 (2002).

89. J. Jeong, Y. Byun, and T. Park, Synthesis and characterization of poly(L-lysine)-g-poly(D,L-lactide-co-glycolic acid) biodegradable micelles. Journal of biomaterials Science. Polymer Edition, 14, 1, 1-11 (2003).

90. H. Kim, S. Choi, H. Park, and Y. Jang, Preparation of PLGA nanoparticles containing estrogen by modified emulsification-diffusion method. Polymeric materials: Science & Engineering, 84, 972-973 (2001).

91. A. Hawley, L. Illum, and S. Davis, Preparation of biodegradable, surface engineered PLGA nanospheres with enhanced lymphatic drainage and lymph node uptake. Pharmaceutical Research, 14(5), 657-661 (1997).

92. S. Stolnik, S. Dunn, M. Garnett, M. Davies, A. Coombes, D. Taylor, M. Irving, S. Purkiss, T. Tadros, S. Davis, and L. Illum, Surface modification of poly(lactide-co-glycolide) nanospheres by biodegradable poly(lactide)-poly(ethylene glycol) copolymers. Pharmaceutical Research, 11(12), 1800-1808 (1994).

93. Y. Kawashima, H. Yamamoto, H. Takeuchi, T. Hino, and T. Niwa, Properties of a peptide containing DL-lactide/glycolide copolymer nanospheres prepared by novel emulsion solvent diffusion methods. European Journal of Pharmaceutics and Biopharmaceutics, 45, 41-48 (1998).

94. H. Murakami, M. Kobayashi, H. Takeuchi, and Y. Kawashima, Evaluation of poly(DL-lactide-co-glycolide) nanoparticles as matrix material for direct compression. Advanced Powder Technology, 11(3), 311-322 (2000).

95. M. Ricci, G. Basta, R. Calafiore, G. Luca, C. Nastruzzi, S. Giovagnoli and C. Rossi, Acta Technologiae et Legis Medicamenti, 13 (1), 73-81 (2002).

96. M. Cascone, Z. Zhu, F. Borselli, and L. Lazzeri, Poly(vinyl alcohol) hydrogels as hydrophilic matrices for the release of lipophylic drugs loaded in PLGA nanoparticles. Journal of Materials Science: Materials in Medicine, 13, 29-32 (2002).

97. X. Jiang, C. Zhou, and K. Tang, Preparation of PLA and PLGA nanoparticles by binary organic solvent diffusion method. Journal Central South University of Technology, 10(3), 202-206 (2003).

98. G. Dawson, and G. Halbert, The in vitro cell association of invasion coated polylactide-co-glycolide nanoparticles. Pharmaceutical Research, 17, 1420-1425 (2000).

99. P. Pietzonka, B. Rothen-Rutishauser, P. Langguth, H. Wunderli-Allenspach, E. Walter, and H. Merkle, Transfer of lipophilic markers from PLGA and polystyrene nanoparticles to caco-2 monolayers mimics particle uptake. Pharmaceutical Research, 19(5), 595-601 (2002).

100. M. Diwan, P. Elamanchili, H. Lane, A. Gainer, and J. Samuel, Biodegradable nanoparticle mediated antigen delivery to human cord blood derived dendritic cells for induction of primary T cell responses. Journal of Drug Targeting, 11(8-10), 495-507 (2003).

101. S. Feng, L. Mu, K. Win, and G. Huang, Nanoparticles of biodegradable polymers for clinical administration of paclitaxel. Current Medical Chemistry, 11, 413-424 (2004).

102. M. Bivas-Benita, S. Romeijn, H. Junginger, and G. Borchard, PLGA-PEI nanoparticles for gene delivery to pulmonary epithelium. European Journal of Pharmaceutics and Biopharmaceutics, 58, 1-6 (2004).

103. K. Win, and S. Feng, Effect of particle size and surface coating on cellular uptake of polymeric nanoparticles for oral delivery of anticancer drugs. Biomaterials, 26, 2713-2722 (2005).

104. P. Elamanchili, M. Diwan, M. Cao, and J. Samuel, Characterization of poly(D,L-lactic-co-glycolic acid) based nanoparticulate system for enhanced delivery of antigens to dendritic cells. Vaccine, 22, 2406-2412 (2004).

105. M. Blanco, and M. Alonso, Development and characterization of protein-loaded poly(lactide-co-glycolide) nanospheres. European Journal of Pharmaceutics and Biopharmaceutics, 43, 287-294 (1997).

106. Y. Jiao, N. Ubrich, M. Marchand-Arvier, C. Vigneron, M. Hoffman, and P. Maincent, Preparation and in vitro evaluation of heparin-loaded polymeric nanoparticles. Drug Delivery, 8, 135-141 (2001).

107. I. Gutierro, R. Hernandez, M. Igartua, A. Gascon, and J. Pedraz, Size dependent immune response after subcutaneous, oral and intranasal administration of BSA loaded nanospheres. Vaccine, 21, 67-77 (2002).

108. J. Panyam, W. Zhou, S. Prabha, S. Sahoo, and V. Labhasetwar, Rapid endo-lysosomal escape of poly(DL-lactide-co-glycolide) nanoparticles: implications for drug and gene delivery. The FASEB Journal, 16, 1217-1226 (2002).

109. A. Sanchez, M. Tobio, L. Gonzalez, A. Fabra, and M. Alonso, Biodegradable micro- and nanoparticles as long-term delivery vehicles for interferon-alpha. European Journal of Pharmaceutical Sciences, 18, 221-229 (2003).

110. J. Eyles, V. Bramwell, J. Singh, E. Williamson, and H. Alpar, Stimulation of spleen cells in vitro by nanospheric particles containing antigen. Journal of Controlled Release, 86, 25-32 (2003).

111. I. Scholl, A. Weissenbock, E. Forster-Waldl, E. Untersmayr, F. Walter, M. Willheim, G. Boltz-Nitulescu, O. Scheiner, F. Gabor, and E. Jensen-Jarolim, Allergen-loaded biodegradable poly(D,L-lactide-co-glycolic) acid nanoparticles down-regulate an ongoing th2 response in the BALB/c mouse model. Clinical and Experimental Allergy, 34, 315-321 (2004).

112. A. Weissenboeck, E. Bogner, M. Wirth, and F. Gabor, Binding and uptake of wheat germ agglutinin-grafted PLGA-nanoparticles by caco-2 monolayers. Pharmaceutical Research, 21(10), 1917-1923 (2004).

113. S. Prabha, and V. Labhasetwar, Nanoparticle-mediated wild-type p53 gene delivery results in sustained antiproliferative activity in breast cancer cells. Molecular Pharmaceutics, 1(3), 211-219 (2004).

114. E. Horisawa, T. Hirota, S. Kawazoe, J. Yamada, H. Yamamoto, H. Takeuchi, and Y. Kawashima, Prolonged anti-inflammatory action of DL-lactide/glycolide copolymer nanospheres containing betamethasone sodium phosphate for intra-articular delivery system in antigen-induced arthritic rabbit. Pharmaceutical Research, 19(4), 403-410 (2002).

115. T. Riley, T. Govender, S. Stolnik, C. Xiong, M. Garnett, L. Illum, and S. Davis, Colloidal stability and drug incorporation aspects of micellar-like PLA-PEG nanoparticles. Colloids and Surfaces B: Biointerfaces, 16, 147-159 (1999).

116. J. Panyam, S. Sahoo, S. Prabha, T. Bargar, and V. Labhasetwar, Fluorescence and electron microscopy probes for cellular and tissue uptake of poly(D,L-lactide-co-glycolide) nanoparticles. International Journal of Pharmaceutics, 262, 1-11 (2003).

117. D. Quintanar-Guerrero, E. Allemann, E. Doelker, and H. Fessi, A mechanism study of the formation of polymer nanoparticles by the emulsification-diffusion technique. Colloid and Polymer Science, 275(7), 640-647 (1997).

118. B. Jeong, C. Windisch, M. Park, Y. Sohn, A. Gutowska, and K. Char, Phase transition of the PLGA-g-PEG copolymer aqueous solutions. Journal of Physical Chemistry B, 107, 10032-10039 (2003c).

119. L. Dailey, E. Kleemann, M. Wittmar, T. Gessler, T. Schmehl, C. Roberts, W. Seeger, and T. Kissel, Surfactant-free, biodegradable nanoparticles for aerosol therapy based on the branched polyesters, DEAPA-PVAL-g-PLGA. Pharmaceutical Research, 20(12), 2011-2020 (2003).

120. Y. Konan, M. Berton, R. Gurny, and E. Allemann, Enhanced photodynamic activity of meso-tetra(4-hydroxyphenyl)porphyrin by incorporation into sub-200 nm nanoparticles. European Journal of Pharmaceutical Sciences, 18, 241-249 (2003).

121. J. Panyam, and V. Labhasetwar, Dynamics of endocytosis and exocytosis of poly(D,L-lactide-co-glycolide) nanoparticles in vascular smooth muscle cells. Pharmaceutical Research, 20(2), 212-220 (2003).

122. Y. Nam, J. Park, S. Han, and I. Chang, Intracellular drug delivery using PLGA NP derivatized with a peptide from a transcriptional activator protein of HIV-1. Biotechnology letters, 24, 2093-2098 (2002).

123. R. Gref, M. Luck, P. Quellec, M. Marchand, E. Dellacherie, S. Harnisch, T. Blunk, and R. Muller, Stealth corona-core nanoparticles surface modified by polyethylene glycol (PEG): influences of the corona (PEG chain length and surface density) and of the core composition on phagocytic uptake and plasma protein adsorption. Colloids and Surfaces B: Biointerfaces, 18, 301-313 (2000).

124. D. Birnbaum, and L. Brannon-Peppas, Molecular weight distribution during degradation and release of PLGA nanoparticles containing epirubicin HCL. Journal of Biomaterials Science. Polymer edition, 14(1), 87-102 (2003).

125. Y. Nam, H. Kang, J. Park, T. Park, S. Han, and I. Chang, New micelle-like aggregates made from PEI-PLGA diblock copolymers: micellar characteristics and cellular uptake. Biomaterials, 24, 2053-2059 (2003).

126. D. Chognot, J. Six, M. Leonard, F. Bonneaux, C. Vigneron, and E. Dellacherie, Physicochemical evaluation of PLA nanoparticles stabilized by water-soluble MPEO-PLA block copolymers. Journal of Colloidal and Interfaces Science, 268, 441-447 (2003).

127. S. Desgouilles, C. Vauthier, D. Bazile, J. Vacus, and J. Grossiord, The design of nanoparticles obtained by solvent evaporation: a comprehensive study. Journal of American Chemical Society, 19, 9504-9510 (2003).

128. F. Sauzedde, A. Elaissari, C. Pichot, Hydrophilic magnetic polymer latexes. 1. Adsorption of magnetic iron oxide nanoparticles onto various cationic latexes. Colloidal Polymer Science, 277, 846-855 (1999).

129. A. Elaissari, F. Sauzedde, F. Montagne, and C. Pichot, Preparation of magnetic latices. Surfactant Series Science, 115, 285-318 (2003).

130. N. Burke, H. Stover, and F. Dawson, Magnetic nanocomposites: preparation and characterization of polymer-coated iron nanoparticles. Chemistry of Materials, 14, 4752-4761 (2002).

131. X.Q. Xu, H. Shen, J.R. XU, and X.J Li, Aqueous-based magnetite fluids stabilized by surface small micelles of oleoylsarcosine. Applied Surface Science, 221, 430-436 (2004).

132. M.A. Samir, F. Alloin, A. Dufresne, Review of recent research into cellulosic whiskers, their properties and their application in nanocomposite field. Biomacromolecules, 6, 212-626 (2005).

133. F. Sauzedde, A. Elaissari, C. Pichot, Hydrophilic magnetic polymer latexes. 2. Encapsulation of adsorbed iron oxide nanoparticles. Colloidal Polymer Science, 277, 1041-1050 (1999).

134. P.A. Dresco, V.S. Zaitsev, R.J Gambino, and B. Chu, Preparation and properties of magnetite and polymer magnetite nanoparticles. Langmuir, 15, 1945-1951 (1999).

135. J.L Aries, V. Gallardo, S.A. Gomez-Lopera, R.C. Plaza, A.V. Delgado, Synthesis and characterization of poly(ethyl-2-cyanoacrilates) nanoparticles with a magnetic core, Journal of Controlled Release, 77, 309-321 (2001).

136. K. Landfester, and L. Ramirez, Encapsulated magnetite particles for biomedical application. Journal of Physics: Condensed Matter, 15, S1345-S1361 (2003).

137. W. Zheng, F. Gao, H. Gu, Magnetic polymers Nanospheres with high and uniform magnetite content. Journal of Magnetism and Magnetic Materials, 288, 403-410 (2005).

138. L. Harris, J. Goff, A. Carmichael, J. Riffle, J. Harburn, T. St. Pierre, and M. Saunders, Magnetite Nanoparticle Dispersions Stabilized with Triblock Copolymers. Chemistry of Materials, 15, 1367-1377 (2003).

139. J.R. Jeong, S.J. Lee, J.D. Kim, and S.C. Shin, Magnetic properties of Fe3O4 nanoparticles encapsulated with poly(D,L Lactide-co-Glycolide). IEEE Transaction on Magnetics, 40 (4), 3015-3017 (2004).

140. V.S. Zaitsev, D.S. Filimonov, I.A. Presnyakov, R.J. Gambino, and B. Chu, Physical and chemical properties of magnetite and magnetite-polymer nanoparticles and their colloidal dispersions. Journal of Colloid and Interface Science, 212, 49-57 (1999).

141. L.M. Lacava, V.A.P. Garcia, S. Kuckelhaus, R.B. Azevedo, N. Sadeghiani, N. Buske, P.C. Morais, Z.G.M. Lacava, Long-term retention of dextran-coated magnetite nanoparticles in the liver and spleen. Journal of Magnetism and Magnetic Materials, 272-276, 2434-2435 (2004).

142. D. Kim, M. Toprak, M. Mikhailova, Y. Zhang, B. Bjelke, J. Kehr and M. Mohammed, Surface modificarion of superparamagnetic nanosprticles for in vivo bio-medical applications. Materials Research Society. 704, 369-374 (2002).

143. A.K. Gupta, and A.S. Curtis, Surface modified superparamagnetic nanoparticles for drug delivery: interaction studies with human fibroblasts in culture. Journal of Materials Science: Materials in Medicine, 15,493-496 (2004).

144. A. Goodarzi, Y. Sahoo, M.T. Swihart, and P.N. Prasad, Aqueous ferrofluid of citric acid coated magnetite particles. Materials Research Society. 789, N6.6.1-N6.6.6 (2004).

145. V. Korolev, A. Ramazanova, and A. Blinov, Adsorption of surfactants on the superfine magnetite. Russian Chemical Bulletin, International Edition. 51 (11), 2044-2049 (2002).

146. F. Montagne, O. Mondain-Monval, C. Pichot, H. Mozzanega, A. Elaissari, Preparation and characterization of narrow sized (o/w) magnetic emulsion. Journal of Magnetism and Magnetic Materials, 250, 302-312 (2002).

147. A. Wooding, M. Kilner, and D.B. Lambrick, Studies of the double surfactant layer stabilization of water-based magnetic fluids. Journal of Colloid and Interface Science, 144, 236-242 (1990).

148. T.K. Jain, M.A. Morales, S.K. Sahoo, D.L. Leslie-Pelecky, V. Labhasetwar, Iron oxide nanoparticles for sustained delivery of anticancer agents. Molecular Pharmaceutics, 2 (3), 194-205 (2005).

149. Y. Zhang, N. Kohler, and M. Zhang, Surface modification of superparamagnetic magnetite nanoparticles and their intracellular uptake. Biomaterials, 23, 1553-1561 (2002).

150. C.B. Berry, and A.S.G. Curtis, Functionalization of magnetic nanoparticles for applications in biomedicine. Journal of Physics D: Applied Physics, 36, R198-R206 (2003).

CHAPTER 3. SYNTHESIS OF POLY(DL-LACTIDE-CO-GLYCOLIDE) NANOPARTICLES WITH ENTRAPPED MAGNETITE

3.1. Introduction

Biosensor development [1], imaging [2, 3], bio-separation [4], hyperthermia [5, 6], drug delivery [1, 7], targeted diagnostics and therapy [8] are some of the many biomedical areas where magnetic nanoparticles could be of relevant use. Magnetic-polymeric nanoparticles (MPNPs), made from organic and inorganic components, have unique characteristics due to the specific properties of the blend. The constituents of a MPNP play different roles: the polymeric matrix acts as a shell, reservoir, and vehicle for the active component, whereas magnetite is the component which makes targeting possible by external magnetic field manipulation. MPNPs can be used for delivery of active components such as drugs [7, 9, 10, 11], vaccines [12], proteins [13], DNA [14, 15, 16], antisense oligonucleotides [17], enzymes [18], and others.

In biomedical applications, synthetic polymers and natural macromolecules have been extensively researched as colloidal materials for the MPNPs production. Synthetic polymers have the advantage of high purity and reproducibility over the natural polymers. Among those, the polymers in the polyesters family are of interest because of their biocompatibility and biodegradability to nontoxic metabolites. Poly(lactide-co-glycolide) (PLGA) is a polyester that has been FDA approved for human therapy [19, 20].

The mainly technique used to form a magnetic core with a polymer shell is polymerization which is known as bottom up technique. Another interesting approach is the top down techniques due to the advantages discussed in chapter 1. In the top-down techniques, the starting materials are the polymer and magnetite. No chemical reactions are involved in the process; magnetite is entrapped into the polymeric matrix by hydrophobic-hydrophilic, electrostatic, or steric interaction.

The common top-down methods using preformed polymers are emulsion evaporation, emulsion diffusion, salting out, nanoprecipitation or solvent displacement. These methods can be adapted to entrap magnetite. Jeong et al. [21] entrapped magnetite

into a preformed polymer (PLGA) by the emulsion diffusion method. The nanoparticles obtained had an average size of 120 nm. Lee et al. [22] entrapped magnetite in PLGA by nanoprecipitation. The magnetite was suspended in acetone after the PLGA dissolution (150 mg), and the initial magnetite concentration (theoretical loading) was 3.33 % w/w (related to PLGA weight). The nanoparticle size obtained ranged from 120 nm to 230 nm for PLGA concentration varied from 1% to 5%, respectively. The emulsion evaporation is one of the oldest methods used with preformed polymers, and it has been extensively used to entrapment numerous drugs [23, 24, 25, 26]. The versatility of emulsion evaporation method permits to entrap magnetite by double emulsion due to the hydrophilic behavior of magnetite, although hydrophilic compounds (normal magnetite) can be tailored to hydrophobic compounds by addition of a surfactant layer (oleic acid) to the particle surface. This magnetite surface modification ensures its entrapment in the PLGA (hydrophobic polymer) matrix by emulsion evaporation method.

3.2. Objectives

The aim of this research was to synthesize PLGA nanoparticles with entrapped magnetite in the polymeric matrix, by emulsion evaporation method. Single emulsion evaporation was the technique used for the entrapment of surface modified magnetite with oleic acid (MOA). The nanoparticles were characterized in terms of size and size distribution with dynamic light scattering (DLS). The magnetite entrapment efficiency was measured by colorimetric method for free iron (Fe^{3+}) detection. The sodium dodecyl sulfate remaining in the nanospheres after dialysis was calculated by thermogravimetric analysis (TGA), and the morphology of the particles was visualized with Transmission Electron Microscopy (TEM).

3.3. Materials and Methods

3.3.1. Materials

Poly(DL-lactide-co-glycolide) (PLGA) 50:50, with a molecular weight of 5,000 – 15,000, PLGA 50:50, with a molecular weight of 45,000-75,000, and PLGA 85:15 with a molecular weight of 90,000 -120,000 were purchased from Sigma Aldrich (Sigma Chemical Co, St Louis, MO). Sodium dodecyl sulfate of 99% purity (20% w/v) was obtained from Amresco (Amresco inc., Solon, OH). Ethyl acetate at 99% of purity was acquired from EMD chemicals (EMD chemicals Inc., Gibbstown, NJ), and hydrochloric

acid 32 -38% was purchased from Fisher Chemical (Fisher Scientific International, Fairlawn, NJ). Oleic acid, trehalose, iron oxide, and potassium ferrocyanide were purchased from Sigma Aldrich (Sigma Chemical Co, St Louis, MO). Magnetite (Fe_3O_4) was obtained from the Center for Advanced Microstructures and Devices (CAMD).

3.3.2. Nanoparticles Preparation

3.3.2.1. Hydrophobic Magnetite

Magnetite was prepared by coprecipitation of ferrous salts (Fe(II) and Fe(III)) by addition of excess of ammonium hydroxide. The attachment of oleic acid to the surface was done after the formation of magnetite by addition of 15 ml of 20 %wt aqueous solution of oleic acid and 10% ammonium hydroxide. The solution was stirred with a magnetic bar for 30 minutes at 80 °C in an oil bath. Following stirring, the solution was placed on a magnet and washed three times, twice with distilled water and once with ethanol. The solution was dried with nitrogen for two hours and stored for further use.

3.3.2.2. Single Emulsion Evaporation with Hydrophobic Magnetite

PLGA nanoparticles were prepared using emulsion evaporation method. Typically, 125 mg of PLGA was dissolved in 2.5 ml of ethyl acetate. The magnetite-oleic acid (MOA) was suspended in ethyl acetate and sonicated for 10 min in an ice bath and it was added to the organic phase at two concentrations, 4% and 8% w/w (relative to PLGA). The organic phase was poured into to 2 mg/ml of aqueous SDS solution (distilled water saturated with ethyl acetate), and the emulsion was stirred with a homogenizer Ultra Turrax T18 (IKA Works Inc., Wilmington, NC) for 3 minutes at 12000 RPM. The emulsion was sheared with sonication in an ice bath at 4 to 6 °C using a probe-type sonicator VC505 (Vibracell, Sonic & Materials Inc., Denbury, CT) for 10 minutes in pulse mode (38% of amplitude). The organic solvent was evaporated with a rotoevaporator (Buchi R-124, Buchi Analytical Inc, New Castle, DE) for 7 min under vacuum (40 mmHg). After nanospheres formation, the purification (extraction of excess of SDS) was done by dialysis with a Spectra/Por® (Spectrum Laboratories Inc., Rancho Dominguez, Ca) membrane of a 100 kDa molecular weight cut off. The dialysis process was done with distilled water with three washes. Washes for the low molecular weight PLGA were performed at 20 °C (t_g is 25.7 °C). The first one was for two hours, the second one was for 8 hr, and the last one was over night. The amount of distilled water

was 1.5 l each time. Finally, the nanoparticles were pre-frozen at – 80 °C for three hours followed by lyophilization for 48 hours at -41 °C under 110 mmHg of vacuum (freezone 4.5, Labconco Corporation, Kansas City, Missouri) in the presence of trehalose. The final samples were injected with nitrogen (to avoid degradation due to humidity, hydrolysis) and stored at 4 °C.

3.3.3. Nanoparticles Characterization

3.3.3.1. Morphology and Size

Transmission electron microscope (TEM) JEOL 100-CX (JEOL USA Inc, Peabody, MA) was used for morphology studies. The aqueous dispersion (one drop) was placed over a copper grid of 400 mesh with carbon film. The droplet was reduced after 5 min with a filter paper to eliminate the excess of nanoparticles. Finally, the sample was air dried prior to placing it in the TEM.

3.3.3.2. Size and Zeta Potential

Diffraction light scattering was used for size and polydespesity index measurements (Zetasizer nano ZS, Malvern instruments Inc, Southborough, MA). Typically, a sample of 1.5 ml was placed in a cuvette at a concentration of 0.3 mg/ml. The measurements were done at 25°C. The viscosity and refraction index of the continuous phase were set equal to those specific to water. Zeta potential measurements were done with a disposable capillary cell with a volume of 1 ml. The mean value was determined using a mono-modal distribution.

3.3.3.3. Colorimetric Method for Iron Content

The magnetite with oleic acid entrapped into the polymeric matrix was measured by detection of free iron (Fe^{3+}) with a UV/vis spectrophotometer Genesys 6 (Thermo Spectronic Corp., Rochester, NY), colorimetric method, that uses the prussian blue reaction. The calibration curve was done with iron oxide at 99.999% of purity and potassium ferrocyanide solution at 4% w/v. Typically, a certain amount of PLGA nanospheres with entrapped MOA (10 mg) was digested with hydrochloric acid at 6 N (1 ml) for two hours or until the residue was white. A dilution step was added (10 ml) to insure that the concentration was in the calibration plot range. The solution formed a white-yellow color. Next, 0.3 ml of sample was reacted with equal amount of potassium ferrocyanide for 15 min. The absorbance was measured at 700 nm. To determine the

magnetite content, a final correction was applied to the iron content of magnetite (molar ratio of 72.4%).

3.3.3.4. Thermogravimetric Analysis

The sample was placed in the furnace of TGA 2950 thermogravimetric analyzer (TA instruments, New Castle, DE) over an aluminum pan under a nitrogen atmosphere to avoid oxidation. The temperature was varied from 25 to 600 °C with increments of 5 °C per minute.

3.3.3.5. Statistical Analysis

Data collected were analyzed by SAS software. The test performed was analysis of variance (ANOVA) with Tukey-kramer adjustment. $P<0.05$ was considered significant. The proc mixed procedure was used to analyze the interaction between the process parameters (molecular weight, MOA addition, and sonication amplitude) and their effect in the nanoparticle size.

3.4. Results and Discussions

3.4.1. Single Emulsion Evaporation with Hydrophobic Magnetite

3.4.1.1. Morphology and Magnetite Distribution into the Polymeric Matrix

The magnetite with oleic acid (MOA) nanoparticles analyzed by TEM showed a spherical shape with a narrow size distribution (Figure 3.1). The aggregation present in MOA was due to the solvent elimination prior to TEM analysis and to natural clustering of MOA.

The TEM pictures of the MPNPs formed with 4% MOA theoretical loading showed a good distribution and a small size of the nanoparticles. The presence of MOA into the polymeric matrix is identified by the black dots over the grey background representing the PLGA (Figure 3.2). A clear visual difference between 4% and 8% MOA theoretical loading was not possible by TEM. Figures 3.3 and 3.4 show MOA nanoparticle surrounded by PLGA. MOA aggregation affects the size and PI of PLGA nanoparticle with entrapped MOA. The distribution and density of MPNPs can be observed in Figure 3.5. MOA distribution into PLGA nanoparticles can be appreciated in Figure 3.6, where MOA is depicted by the black dots.

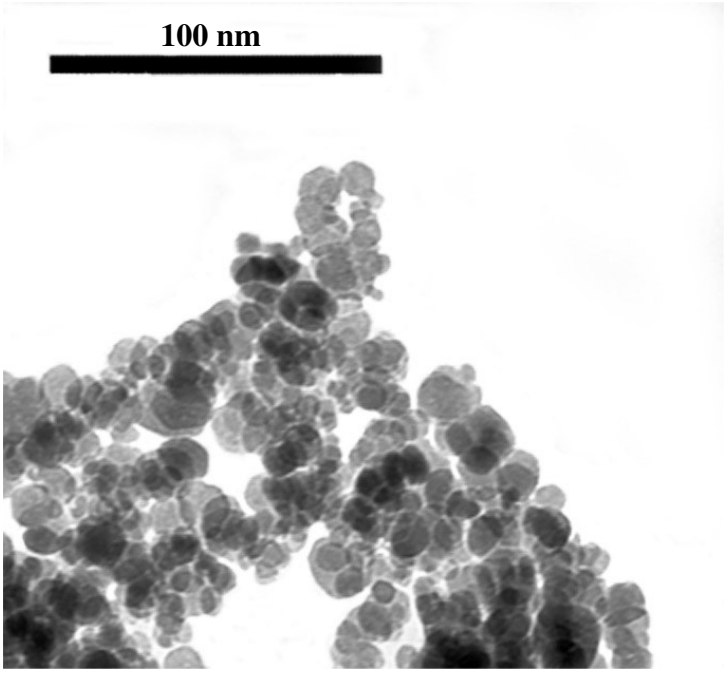

Figure 3.1. Surface modified magnetite with oleic acid (MOA). The MOA nanoparticle size was around 15 nm. The appearance of clustering was common by observed .

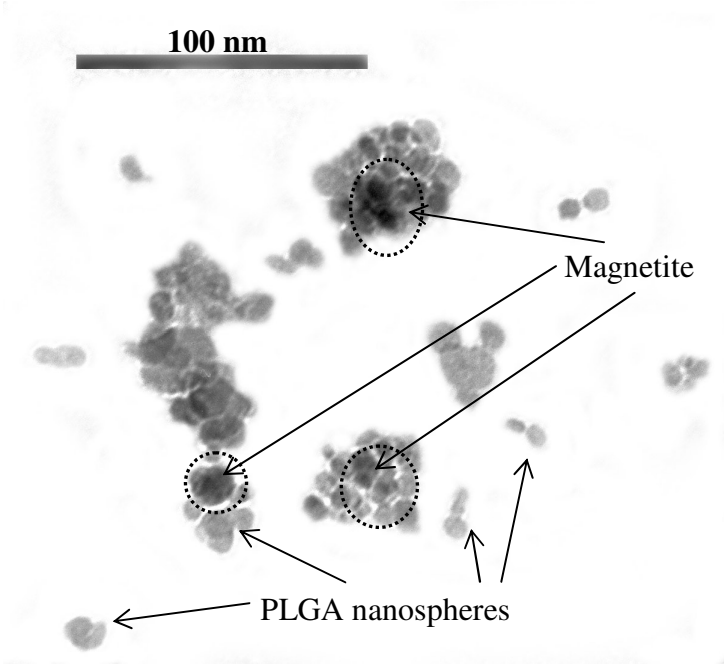

Figure 3.2. PLGA (molecular weight (M.W.) 45 to 75 kDa) nanospheres with 4% MOA theoretical loading. The black circles are showing the MOA entrapped in the polymeric matrix. Clustering was observed, and some PLGA nanoparticles are without MOA (empty PLGA nanoparticles).

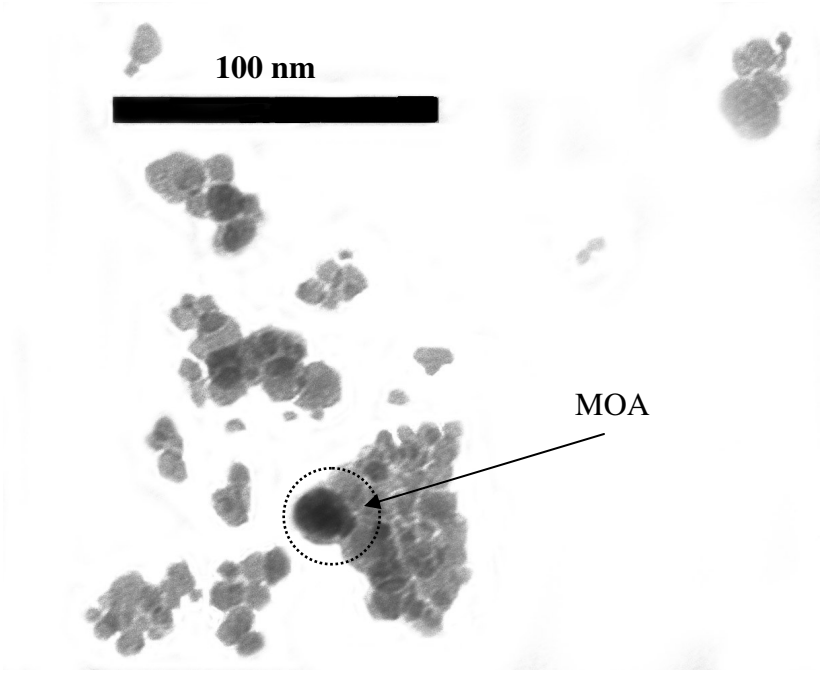

Figure 3.3. PLGA (M.W. 45 to 75 kDa) nanospheres with 8% MOA theoretical loading. The black dots represent MOA entrapped in PLGA nanospheres.

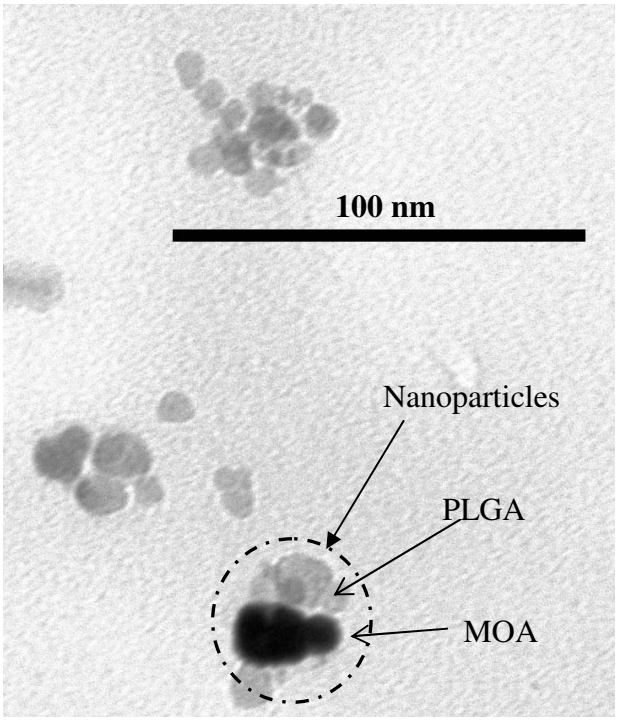

Figure 3.4. Nanoparticles formed with PLGA M.W. of 45 to 75 kDa with 4% w/w of MOA theoretical loading. The big dark sphere (inside the dotted circle) manifests the presence of MOA. The appearance of clustering is observed in the surrounded PLGA nanoparticles.

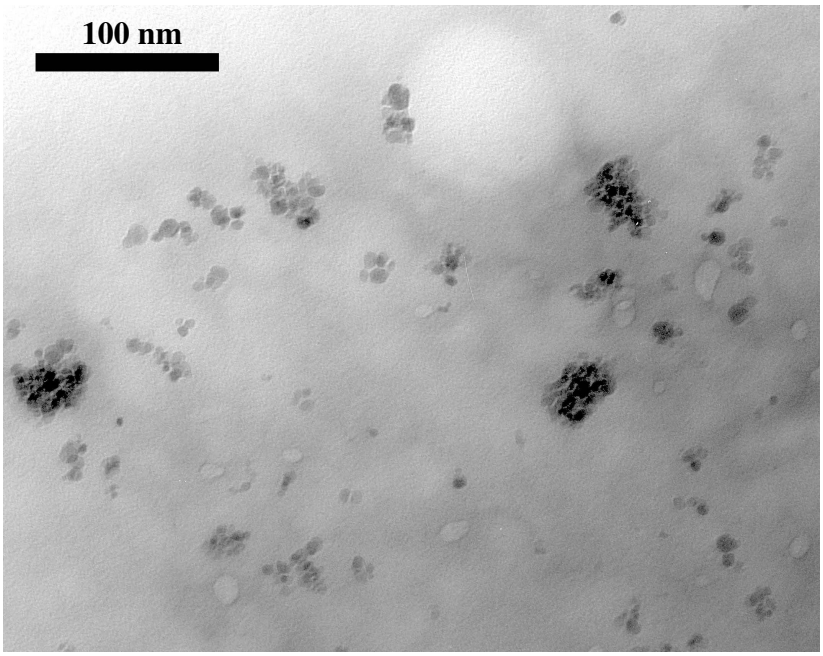

Figure 3.5. Low molecular weight PLGA nanospheres with 4% w/w of MOA theoretical loading. The black dots represent MOA entrapped in the PLGA nanoparticle.

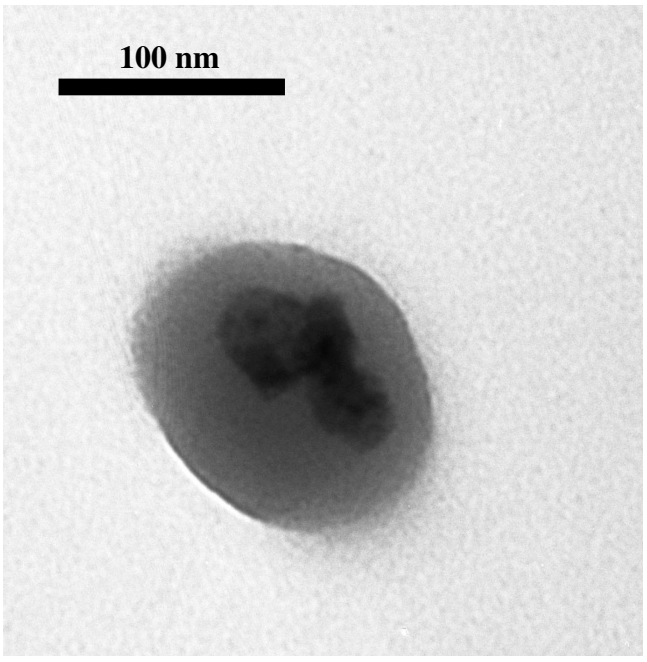

Figure 3.6. Medium molecular weight PLGA (40 to 75 kDa) nanosphere with 4% w/w of MOA theoretical loading. The magnetite is clearly showed in the center of this nanosphere by darker spots.

3.4.1.2. The Effect of Synthesis Parameters on Nanoparticle Physical Characteristics

- Surfactant concentration

The study of the surfactant concentration effect on the nanoparticle size was performed for the low molecular weight PLGA 5 to 15 kDa (Figure 3.7). Three distinctive regions were observed. Region A: For a SDS concentration lower than the critical micelle concentration (CMC), 1.2 mg/ml for SDS [27], the mean nanoparticle size decreased from 69.1 nm (0.4 mg/ml SDS) to 45.6 nm (1.2 mg/ml SDS). The polydispersity index (PI) decreased with increasing SDS concentration from 0.170 to 0.227 in the same range. The decrease in size and PI can be explained by the decrease in the surface tension with increasing surfactant concentrations up to the CMC. The availability of the surfactant molecules at higher concentrations, required for stabilization of the smaller emulsion droplets created during sonication, is another reason for the improved size and size distribution in this region. Region B: At SDS concentrations higher than CMC, smaller particles were formed as a result of SDS molecules availability, as well. Although the size decreased, the polydispersity index (PI) of the formed nanoparticles increased with increasing SDS concentration. The increase of the PI suggests that the excess SDS was responsible for aggregation of the nanoparticles by interactions between the SDS polar heads and cluster formation. Region C: Ultimately, the aggregation due to the excess surfactant was responsible for an increase in the size and the PI of the nanoparticles when the SDS concentration exceeded a threshold of 7 mg/ml (Figure 3.7).

Nanoparticle aggregation due to the excess surfactant was apparent in the nanoparticle size distribution curves (Figure 3.8) for a SDS concentration of 4.8 mg/ml (Figure 3.8-b) with PLGA of low molecular weight. The main peak was at 37 nm, a second peak (size range of 200 to 900 nm), and a third pick (over 4 μm) were present, which impacted the polydispersity index; whereas at SDS concentrations of 1.2 mg/ml a single peak was observed at 60 nm (Figure 3.8a) for PLGA with medium molecular weight.

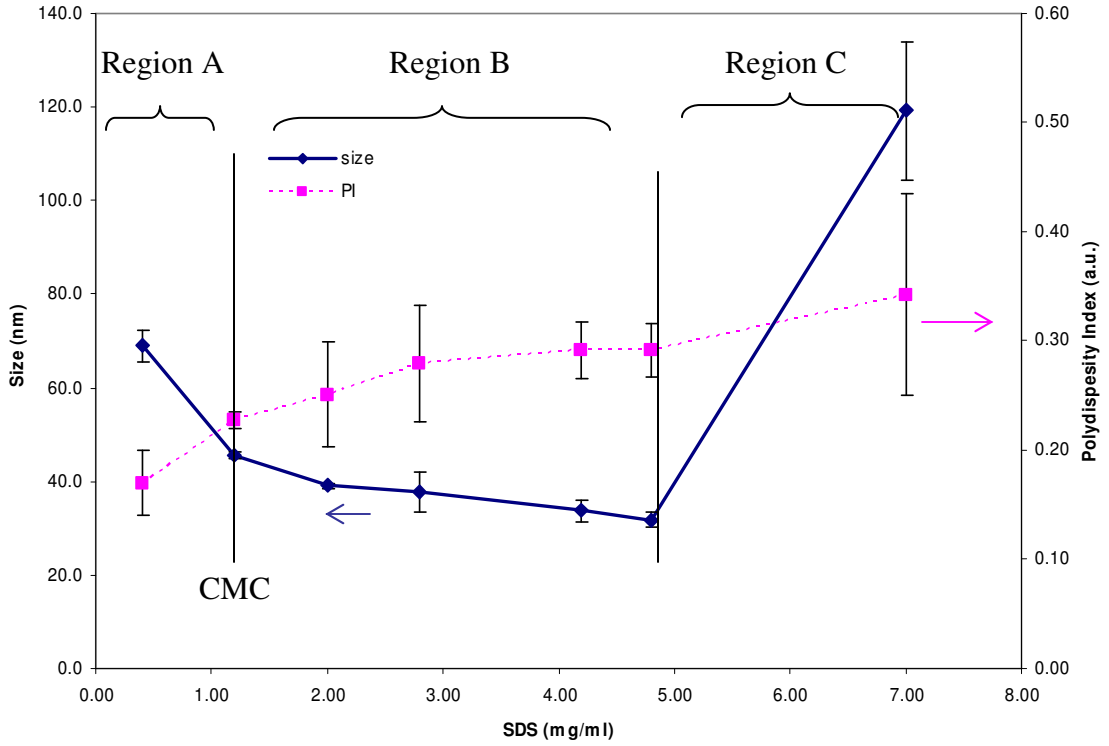

Figure 3.7. Effect of SDS concentration on the size and polydispersity index of PLGA nanospheres (PLGA 5% w/v, molecular weight of 5 to 10 kDa, and copolymer molar ratio of 50:50), n = 2

- PLGA concentration

The study of different PLGA concentrations was completed for low molecular weight PLGA (5 to 15 kDa). The increase from 5% to 15 % w/v in the PLGA concentration resulted in an increase in the nanoparticle size (Figure 3.9) for SDS concentrations of 2 mg/ml and 4 mg/ml. For a SDS concentration of 2% mg/ml, there was a slight increase in size from 38.6 nm to 52.7 nm, and for 4% SDS, the nanoparticle size increased from 36.1 to 41.6 nm. The increase in size, however small, suggested that the amount of surfactant was not enough to maintain the stability of the droplets and coalescence of the droplets occurred. The nanoparticle size improved when the SDS concentration increased from 2% to 4% w/v for all polymer concentrations tested (from 5 to 15% w/v). The results also showed that it was possible to increase the polymer concentration three fold (from 5 to 15 % w/v) without forming particles over 100 nm in size. This finding is important because an increase in the polymer concentration is directly related to an increase in the efficiency of the nanoparticle synthesis.

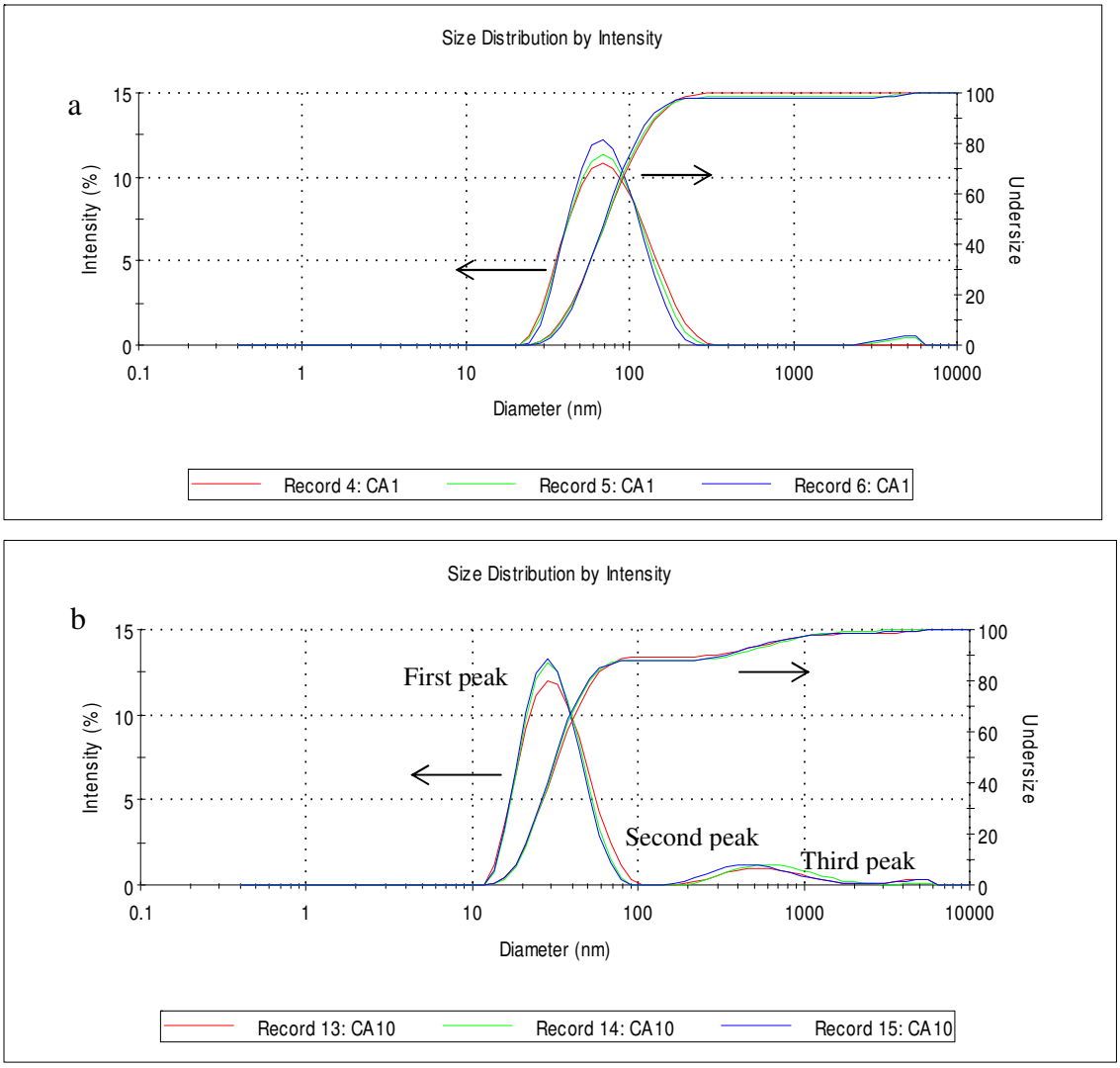

Figure 3.8. Size distribution and undersize curve for PLGA nanoparticles. Three runs at 25 °C with detector at 70°. a was PLGA 50:50 with molecular weight of 40 to 75 kDa and a SDS concentration of 1.2 mg/ml. b was PLGA 50:50 with molecular weight of 5 to 15 kDa and SDS concentration of 4.8 mg/ml

- Sonication amplitude

The sonication effect on size was evaluated with two different amplitudes at a SDS concentration of 2 mg/ml for naked PLGA nanoparticles. Amplitudes of 30% and 39% were evaluated (Table 3.1), showing a small decrease in the PLGA nanoparticles size for the three PLGA molecular weights tested.

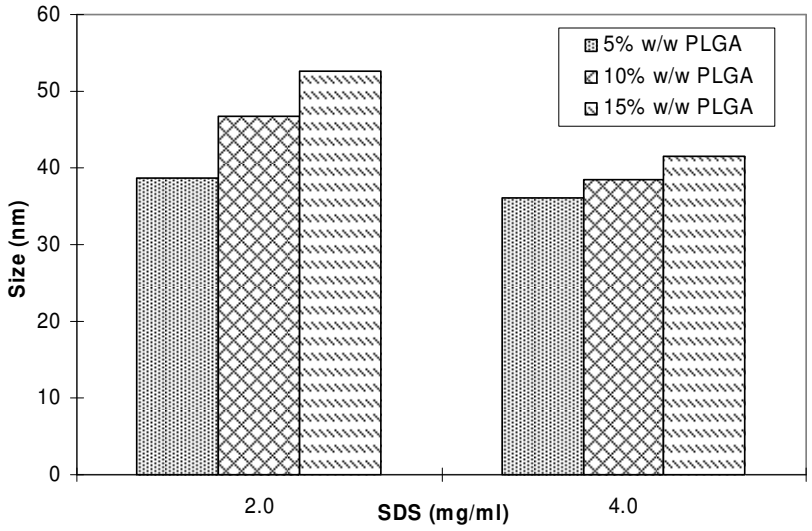

Figure 3.9. Effect of PLGA and SDS concentration on the nanospheres size (PLGA molecular weight of 5 to 10 kDa, copolymer molar ratio of 50:50)

The amplitude in sonication is defined as peak to peak displacement at the probe tip, which is maintained constant during sonication. The percentages of amplitude are in function of the maximum displacement. The random process of droplet disruption and fusion during sonication improved the nanoparticle size for all polymer molecular weights (amplitude 39%).

Table 3.1. Size of PLGA nanospheres as a function of sonication wave amplitude

	Sonicated with 30% amplitude			**Sonicated with 39% amplitude**		
MW (kDa)	5 to 15	40 to 75	90 to 126	5 to 15	40 to 75	90 to 126
(L:G ratio)	(50:50)	(50:50)	(75:25)	(50:50)	(50:50)	(75:25)
Size (nm)	39.4±1.7	66.8±1.8	70.6±0.3	38.6±0.2	63.3±0.3	67.1±0.5
PI	0.285±0.016	0.107±0.008	0.121±0.01	0.217±0.018	0.127±0.003	0.127±0.005
ζ (mV)	-28.0±3.7	-31.4±4.6	-39.7±2.9	-19.2±4.6	-26.3±1.3	-27.1±2.9

* n=3 for all samples

The nanoparticles size reduction with increasing the sonication amplitude was higher for the medium and high molecular weight (5.3% and 5%) as compared with the nanospheres of low molecular weight (2.03%). However, the decrease in size with increasing sonication amplitude was not significant for the three molecular weights tested (p values of 0.9768, 0.0542, and 0.3065 for low, medium and high PLGA molecular weight, respectively). Not only the size, but also the PI was affected by the sonication amplitude. A better PI was observed for the low molecular weight (5 to 15 kDa) PLGA

with increasing the sonication amplitude. The medium (40 to 75 kDa) and high (90 to 126 kDa) molecular weights had similar PIs (close to 0.1), and indicator of monodisperse suspension, for both sonication amplitudes.

- Effect of MOA size on the final MPNP size and size distribution

To evaluate the effect of MOA size on the final MPNPs size, MOA was sonicated before it was added to the nanosphere preparation. At constant amplitude of 39%, the sonication time tested was 2 and 10 minutes. The final size of MPNPs was affected (Table 3.2) by sonication time.

Table 3.2. Effect of sonication time of MOA on the PLGA nanosphere with magnetite entrapped in the polymeric matrix

	MOA sonicated for 2 min			**MOA sonicated for 10 min**		
Molecular	size	PI	Z	size	PI	ζ
weight (kDa)	nm	a.u.	mV	nm	a.u.	mV
4% magnetite						
5 to 15 (50:50)	109.2±2.4	0.321±0.024	-39.5±1.7	87.2±0.8	0.297±0.006	-28.5±3.9
40 to 75 (50:50)	87.5±4.1	0.270±0.019	-49.9±23.9	81.8±6.1	0.222±0.06	-26.9±2.9
90 to 126 (75:25)	84.0±0.7	0.234±0.006	-49.6±11.1	78.8±0.3	0.172±0.017	-33.6±1.9
8% magnetite						
5 to 15 (50:50)	138.7±10.5	0.299±0.076	-38.9±2.5	115.1±1.0	0.320±0.019	-36.1±4.4
40 to 75 (50:50)	100.0±1.9	0.268±0.008	-39.2±4.3	93.0±1.4	0.249±0.01	-34.1±3.2
90 to 126 (75:25)	96.8±1.3	0.258±0.003	-38.1±3.4	107.4±4.9	0.258±0.004	-37.6±3.1

* MOA suspension in ethyl acetate. n = 3, and the amplitude of sonication was 39%

The size of nanospheres with 4% of MOA theoretical loading was improved from 109.2 nm to 87.2 nm for the low molecular weight sample. The medium and high molecular weight showed a reduction in size of 5.7 nm and 6 nm, respectively. Moreover, the PI was lower for all 4% MOA preparations after 10 minutes of sonication. It was obvious that the size decrease in the MOA accomplished by increasing the sonication time, which was associated with an improvement in the final MPNP characteristics for low, medium, and high PLGA molecular weight at 4% of MOA.

When the nanospheres were prepared with 8% of MOA theoretical loading, with low molecular weight PLGA (5 to 15 kDa), the size was reduced from 138.7 nm to 115.1 nm. The MPNPs size decreased from 100 nm to 93 nm for the medium molecular weight PLGA (40 to 75 kDa). However, the size of the MPNPs formed with high molecular weight PLGA (90 to 126 kDa) increased by 10.6 nm, while the PI remained constant. In

general, a strong shear stress applied to the MOA suspension reduced the size the MOA clusters naturally occurring and therefore improved the MPNP size.

- Polymer molecular weight

The particle size, size distribution, and zeta potential were measured after nanoparticle formation for three PLGA molecular weights (MW): low MW 5-15 kDa, medium MW 40-75 kDa, and high MW 90-126 kDa (Table 3.3). The nanoparticle size was found to increase with the polymer molecular weight, from 38.6 nm to 67.1 nm. The size distribution improved for high MW PLGA (PI of 0.127) as compared to low MW PLGA (PI of 0.217). The results are consistent with the literature, where a direct relationship is defined between the polymer molecular weight and the nanoparticle size (for naked PLGA nanoparticles). The differences in nanoparticle size between low and medium PLGA molecular weight, and low and high PLGA molecular weight, were significant (both p values < 0.05 (0.0001)). The difference between medium and high PLGA molecular weight was not significant (p value > 0.05 (0.9455)).

- Magnetite concentration

The amount of magnetite entrapped in the polymeric matrix was found to affect the final mean size of the polymeric nanoparticle (Table 3.3). The addition of magnetite increased the size and size distribution of the nanoparticles (Figure 3.10).

When 4% magnetite was entrapped into the matrix, the size increased from 38.6 nm to 87.2 nm (for low MW) and from 67.1 to 78.8 nm (for high MW). The increase in the nanoparticle size was even more evident when 8% magnetite was entrapped into the polymeric matrix. The size increment was higher for low molecular weight PLGA as compared to the medium and high molecular weight PLGA, with a maximum size of 115.1 nm for low MW PLGA. The difference in size was significant for all combinations of MOA entrapped (0%, 4%, and 8%) and for all three PLGA molecular weights (P values < 0.05).

The increase in size observed for all MW PLGA can be explained by the hydrophobic interactions between the oleic acid tails belonging to two or more partially covered magnetic particles. These interactions could be responsible for magnetite clustering, and therefore could explain the increase in the particle size and size distribution.

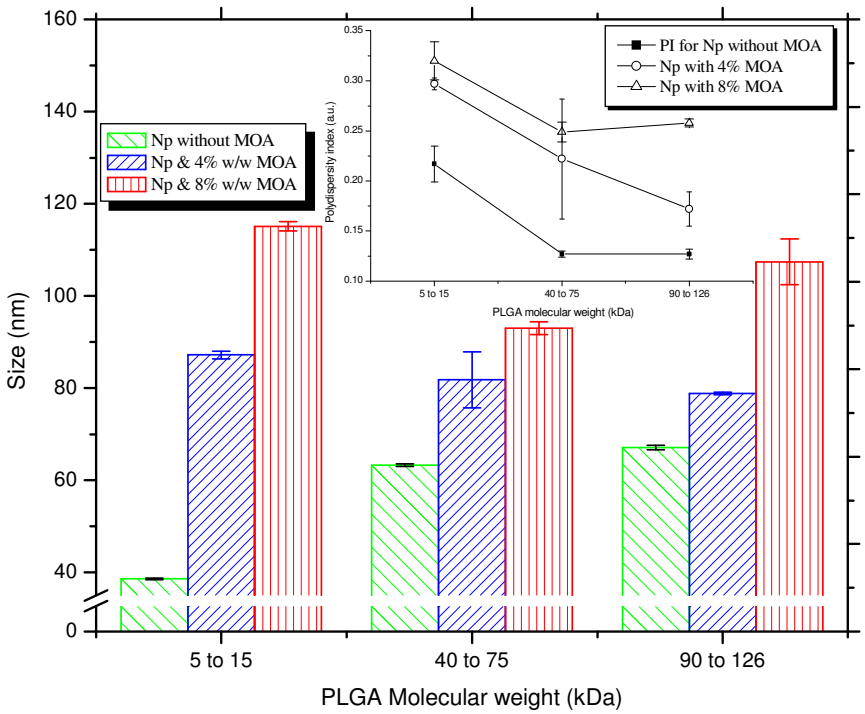

Figure 3.10. PLGA nanoparticles size and polydispersity measured by DLS (at 70°, 25 °C). n = 3

Table 3.3. Mean size, polydispersity index, and zeta potential of nanoparticles for different molecular weights and magnetite concentration BEFORE dialysis

MW (kDa)	Size (nm)	PI	ζ (mV)
0% magnetite			
5 to 15 (50:50)	38.6±0.2	0.217±0.018	-19.2±4.6
40 to 75 (50:50)	63.3±0.3	0.127±0.003	-26.3±1.3
90 to 126 (75:25)	67.1±0.5	0.127±0.005	-27.1±2.9
4% magnetite			
5 to 15 (50:50)	87.2±0.8	0.297±0.006	-28.5±3.9
40 to 75 (50:50)	81.8±6.1	0.222±0.060	-26.9±2.9
90 to 126 (75:25)	78.8±0.3	0.172±0.017	-33.6±1.9
8% magnetite			
5 to 15 (50:50)	115.1±1.0	0.320±0.019	-36.1±4.4
40 to 75 (50:50)	93.0±1.4	0.249±0.010	-34.1±3.2
90 to 126 (75:25)	107.4±4.9	0.258±0.004	-37.6±3.1

*All samples were run in triplicate, measured after three to four hours after formation

Table 3.4. Mean size, polydispersity index, and zeta potential of nanoparticles for different molecular weights and magnetite concentration AFTER dialysis

MW (kDa)	Size (nm)	PI	ζ (mV)
0% magnetite			
5 to 15 (50:50)	54.5±1.6	0.155±0.027	-33.2±7.3
40 to 75 (50:50)	68.5±0.8	0.146±0.014	-30.9±4.8
90 to 126 (75:25)	70.3±0.2	0.138±0.007	-33.5±4.6
4% magnetite			
5 to 15 (50:50)	82.9±1.6	0.261±0.003	-29.2±12.3
40 to 75 (50:50)	82.6±0.7	0.167±0.003	-30.8±3.3
90 to 126 (75:25)	82.8±0.7	0.169±0.007	-27.1±4.0
8% magnetite			
5 to 15 (50:50)	108.4±3.7	0.290±0.007	-42.2±7.4
40 to 75 (50:50)	95.8±1.1	0.238±0.006	-45.7±7.5
90 to 126 (75:25)	108.5±3.8	0.246±0.006	-37.7±9.3

*All samples were run in triplicate, measured after four to 10 hours after formation

The increase in size, most evident in the low molecular weight PLGA, was probably due to the limited coating of the magnetite by the polymer as compared to the higher molecular weight PLGA nanoparticles. The polydispersity of the modified magnetite could be another factor which could have negatively impacted the polydispersity of the system, which was observed when two different sonication times were applied to the MAO suspension before nanosphere preparation.

Medium (40 to 75 kDa) and high (90 to 126 kDa) molecular weight polymer proved to be more suitable for magnetite entrapment. The size of the particles only increased from 63.3 nm to 81.8 nm for medium M.W. and from 67.1 nm to 78.8 nm for high M.W., when 4% of MOA was entrapped. The higher lactide (a more hydrophobic component) present in the high M.W. polymer (75:25), as compared to 50:50 lactide:glycolide for medium M.W., may explain the smaller increase in size for the medium MW PLGA nanoparticles in the presence of MOA.

The nanoparticles were characterized before and after purification. An increase in the mean nanoparticle size from 38.6 nm to 54.5 nm (significant difference, p value <0.05) was detected after dialysis for the low MW PLGA nanoparticles without magnetite (Table 3.4), while the polydispersity index was improved from 0.217 to 0.155 due to the removal of small nanoparticles and MOA by dialysis. A similar effect, an increase in the mean particle size following dialysis, was observed for the medium and

high PLGA molecular weights, but the difference was not significant (p value >0.05).. The polydispersity index was improved for all samples due to the removal of SDS in excess and the SDS trapped over the nanoparticle surface, which limited the nanoparticle aggregation. In addition, losses of small nanoparticles during dialysis explain the increase in the PLGA nanoparticles mean size without MOA, and the PI improvement. When 4% w/w of MOA was added, the difference in size was not significant for the medium molecular weight PLGA. It was not conclusive whether the PLGA nanoparticle size was affected by dialysis (p value almost 0.05) for low and high PLGA molecular weight with 4% w/w of MOA. The difference in nanoparticle mean size before and after dialysis was not significant when 8% w/w of MOA was added (p value > 0.05).

3.4.1.3. Yield of Nanoparticles, Entrapment Efficiency of MOA, Remaining SDS, and Oleic Acid Amount over Magnetite

The amount of MOA in the PLGA matrix was measured by a colorimetric method, and the SDS left in the sample was calculated from TGA data (Figure 3.11a and 3.11b) combined with data collected from the colorimetric method (Table 3.5). The residue after 600 °C obtained by TGA analysis for the MPNPs was composed of magnetite, sulfate, and sodium (from SDS). The SDS residue was determined by subtracting the amount of magnetite obtained from the colorimetric method (Table 3.5) from the total residue amount obtained by TGA. From Figure 3.11a, a relation between SDS residue and total SDS can be obtained (The sodium and sulfate groups are 24.75 wt.% of SDS). The entrapment efficiency (final weight ratio of MOA in lyophilized MPNPs measured by colorimetric method divided by the initial amount of MOA added in the formation process) varied from 57.36% to 91.9% for the PLGA with low and high PLGA molecular weight nanoparticles, respectively. The differences in the entrapment efficiency were not significant between the 4 and 8 %w/w MOA samples for all molecular weights (p values > 0.05).

The medium molecular weight (40 to 75 kDa) PLGA nanoparticles showed similar entrapment efficiency for 4% and 8% of MOA theoretical loading, 77.34% and 78.75%, respectively. The low (5 to 15 kDa) and high (40 to 75 kDa) molecular weight PLGA MPNPs presented different entrapment efficiencies for 4 and 8% w/w MOA theoretical loading. The entrapment efficiency of MPNPs formed with 5 to 15 kDa PLGA

M.W. was 57.36% and 76.27% for 4 and 8% w/w of MOA theoretical loading, respectively.

Table 3.5. Entrapment of magnetite oleic acid and SDS residue in nanoparticles

	Magnetite with oleic acid (MOA)			Surfactant	
Nanoparticle molecular weight kDa	Theoretical loading[1] wt%	Nanosphere yield[2] %	Entrapment efficiency[3] %	SDS residue[4] wt%	SDS removed[5] %
PLGA 5 to 15	4%	66.8±3.6	57.36±6.8	5.95±1.3	55.34%
PLGA 5 to 15	8%	61.6±1.8	76.27±11.7	6.59±2.5	48.90%
PLGA 40 to 75	4%	58.9±9.3	77.34±8.50	1.50±0.4	88.77%
PLGA 40 to 75	8%	62.7±3.9	78.75±3.80	6.32±1.7	51.02%
PLGA 90 to 126	4%	66.6±2.6	70.23±18.5	4.80±2.6	64.00%
PLGA 90 to 126	8%	56.2±3.7	91.90±31.8	4.71±3.1	63.48%

*All samples in triplicate

1. Theoretical loading: Initial amount of MOA added to the nanoparticle formation process (wt%)
2. Nanosphere yield: final weight of sample after freeze drying (mg)/initial weight of sample (mg)
3. Entrapment efficiency: MOA in samples (wt%)/theoretical loading (wt%)
4. SDS residue: Total residue (wt%) (from TGA) – magnetite (wt%) (from colorimetric method)
5. SDS removed: SDS residue (wt%)/total SDS added in the nanoparticle formation process (wt%)

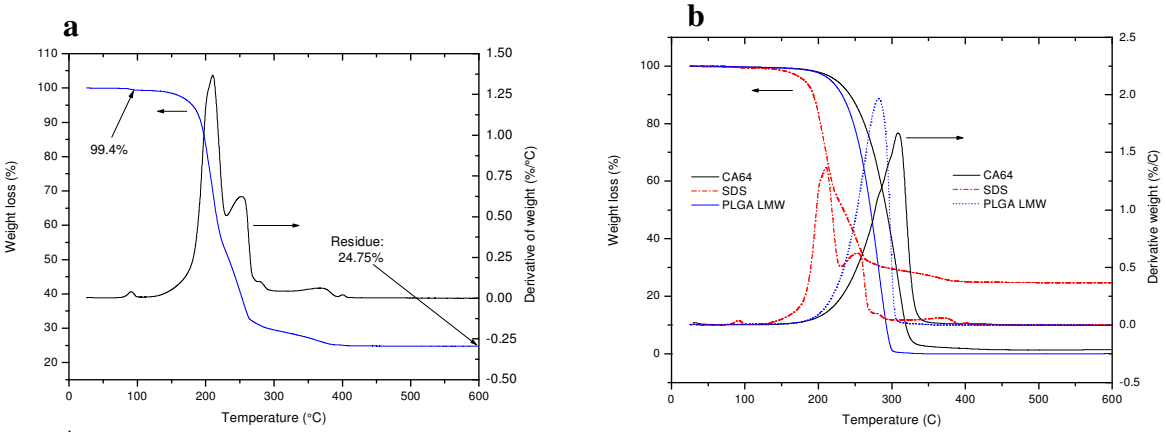

Figure 3.11. a. SDS profiles acquired by TGA. Temperature was varied from 25 to 600 °C. A residue of 24.75% composed of sulfate and sodium group of the SDS molecule was found at 600 ºC. This residue present in all samples was used to calculate the amount of SDS remaining in the nanoparticles. b. A typical curve for the MPNPs formed with low molecular weight PLGA (CA64). The residue at 600 °C was due to the sodium and sulfate groups of SDS, and magnetite.

The medium molecular weight (40 to 75 kDa) PLGA nanoparticles showed similar entrapment efficiency for 4% and 8% of MOA theoretical loading, 77.34% and 78.75%, respectively. The low (5 to 15 kDa) and high (40 to 75 kDa) molecular weight PLGA MPNPs presented different entrapment efficiencies for 4 and 8% w/w MOA theoretical loading. The entrapment efficiency of MPNPs formed with 5 to 15 kDa PLGA

M.W. was 57.36% and 76.27% for 4 and 8% w/w of MOA theoretical loading, respectively

The MPNPs yield ranged from 56.2% to 66.8% due to losses during dialysis and freeze drying. This data suggested that the dialysis membrane cutoff was high, or compatibility between nanoparticles and membrane promoted adsorption of PLGA nanoparticles with entrapped MOA on the surface of the dialysis membrane. All membranes presented surface areas visibly brown in color (membrane is white prior to use) after the samples were removed. No visual difference was observed between MPNPs prepared with 4% and 8% of MOA.

The SDS amount removed by the three washes varied from 51.02% to 88.77%. No obvious relationship was found between the SDS removed and the PLGA molecular weights, or amount of magnetite added.

- Oleic acid on magnetite

The amount of oleic acid was measured by thermogravimetric analysis (TGA) (Figure 3.12).

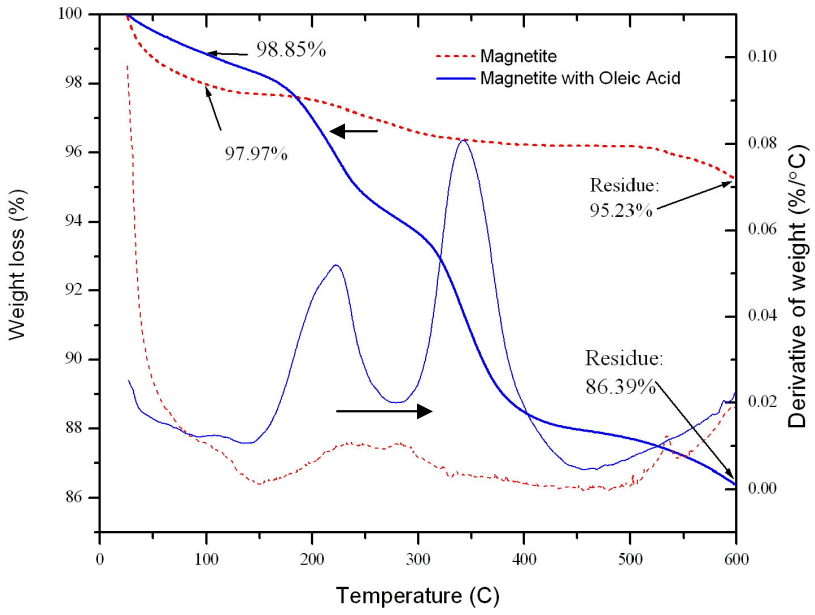

Figure 3.12. TGA data for magnetite and MOA (magnetite plus oleic acid). The initial decrease was due to the presence of water (approximately 2 wt% for magnetite and 1.15% for MOA). The 2.74 wt% and 3.64 wt% remaining could be explained by ammonium used in the magnetite formulation.

The TGA residue for MOA at 600 °C was 86.39 wt%. The TGA residue for normal magnetite was 95.23%. The 8.84 wt% difference was associated with the oleic acid presence. This data correlated well with the colorimetric method for iron detection, in which the oleic acid content detected was 10.24 wt% with an error of 0.03 wt%.

3.5. Conclusions

Surface modification of magnetite with oleic acid was a useful approach to ensure the entrapment of magnetite into a hydrophobic polymer (PLGA) with high entrapment efficiency. MPNPs with a final mean size under 100 nm were obtained, at 4% w/w MOA theoretical loading. When MOA theoretical loading was increased to 8% w/w, nanoparticles mean size under 120 nm were formed. The entrapment efficiency was highly different for the low (57%) and high PLGA molecular weight (92%).

The emulsion evaporation method was a suitable synthesis method for the formation of nanoparticles with a mean size under 100 nm. The SDS concentration played a critical role in controlling the nanoparticle size. The size and uniformity of the MOA suspension was found critical in forming small and uniform MPNPs. With the method proposed, it was possible to increase the PLGA concentration by at least three times without increasing the nanoparticle size over 100 nm. Stability of MPNPs was improved by applying a purification step quickly after synthesis. Dialysis was used as a purification step to remove the excess of SDS and avoid aggregation.

3.6. References

1. Nakache, E., Poulain, N., Candau, F., Orecchioni, A.M., and Irache, J.M., In the Handbook of nanostructured materials and nanotechnology. (E. Nalwa, H.S. ed.), Academic Press, v 5, 577-635 (2000).

2. Tartaj, P., Morales, M.P, Veintemillas-Verdaguer, S., Gonzalez-Carreno, T., and Serna, C.J., The preparation of magnetic nanoparticles for applications in biomedicine. Journal of Physics D: Applied Physics, R182-R197 (2003).

3. Gao, H., Zhao, Y., Fu, S., Li, B., and Li, M., Preparation of a novel polymeric fluorescent nanoparticle. Colloid and Polymer Science, **280** (7), 653-660 (2002).

4. Bucak, S., Jones, D.A., Laibinis, P.E., and Hatton T.A., Protein separations using colloidal magnetic nanoparticles. Biotechnology Progress, **19**, 477-484 (2003).

5. Jordan, A., Scholz, R., Wust, P., Fahling, H., and Felix, R., Magnetic fluid hyperthermia (MFH): cancer treatment with AC magnetic field induced excitation

of biocompatible superparamagnetic nanoparticles. Journal of Magnetism and Magnetic Materials, **201**, 413-419 (1999).

6. Pankhurst, Q., Connolly, J., Jones, S., and Dobson J., Applications of magnetic nanoparticles in biomedicine. Journal of Physics D: Applied Physics, **36**, R167-R181 (2003).

7. Barrat, G., Courraze, G., Couvreur, C., Fattal, E., Gref, R., Labarre D., Legrand, P., Ponchel, G., Vauthier, C., Polymeric Micro- and Nanoparticles as drug Carriers. In Polymeric Biomaterials, second ed. (S. Dumitriu, ed.). Marcel Dekker Inc., New York, 753-781 (2000).

8. Levy, L., Sahoo, Y., Kim, K. S., Bergey, E. J., Prasad, P.N., Nanochemistry: Synthesis and characterization of multifunctional nanoclinics for biological applications. Chemistry of Materials, **14**, 3715-3721 (2002).

9. Brigger, I; Dubernet, C. Couvreur, P., Nanoparticles in cancer therapy and diagnosis. Advanced Drug Delivery Reviews, **54**:631-651 (2002).

10. De Jaeghere, F., Doelker, E., Gurny, R., In the Encyclopedia of control drug delivery. (E. Mathiowitz ed.) John Wiley & Sons, Inc. New York, v. 2: p. 641-664 (1999).

11. Hans, M.L., Lowman, A.M., Biodegradable nanoparticles for drug delivery and targeting. Current Opinion Solid State Matter Science, **6**, 319-327 (2002).

12. Kreuter, J. 1994. Colloidal drug delivery systems. (J. Kreuter, ed.) Marcel Dekker, Inc. New York, p. 219-342 (1994).

13. Blanco MD., Alonso, MJ., Development and characterization of protein-loaded poly(lactide-co-glycolide) nanospheres. European Journal of Pharmaceutics and Biopharmaceutics, **43**, 287-294 (1997).

14. Panyam, J., and Labhasetwar V., Biodegradable nanoparticles for drug and gene delivery to cells and tissue. Advanced Drug Delivery Reviews, **55**, 329-347 (2003).

15. Ravi Kumar, M.N.V., Bakowsky, U., Lehr, C.M., Preparation and characterization of cationic PLGA nanospheres as DNA carriers. Biomaterials, **25**, 1771-1777 (2004).

16. Oster, C.G., Wittmar, M., Unger, F., Barbu-Tudoran, L., Schaper, A.K., and Kissel, T., Design of amine-modified graft polyesters for effective gene delivery using DNA-loaded nanoparticles. Pharmaceutical Research, **21**(6), 927-931 (2004).

17. Vinogradov, S., Batrakova, E., Kabanov, A., Poly(ethylene glycol)-polyethyleneimine nanogel particles: novel drug delivery systems for antisense oligonucleotidos. Colloids and surfaces B: Biointerfaces, **16**: 291-304 (1999).

18. Kouassi, G.K., Irudayaraj, J., McCarty, G., Activity of glucose oxidase functionalized onto magnetic nanoparticles. Biomagnetic Research and Technology, **3**, 1-10 (2005).

19. Anderson, J.M., Shive, M.S., Biodegradation and biocompatibility of PLA and PLGA microspheres. Advanced Drug Delivery Reviews, **28**, 5-24 (1997).

20. Govender, T. Stolnik, S., Garnett, M.C., Illum, L., and Davis, S.S., PLGA nanoparticles prepared by nanoprecipitation: drug loading and release studies of a water soluble drug. Journal of Controlled Release, **57**, 171-185 (1999).

21. Jeong, J.R., Lee, S.J., Kim, J.D., and Shin, S.C., Magnetic properties of Fe_3O_4 nanoparticles encapsulated with poly(D,L Lactide-co-Glycolide). IEEE Transaction on Magnetics, **40** (4), 3015-3017 (2004).

22. Lee, S.J., Jeong, J.R., Shin, S.C., Kim, J.C., Chang, Y.H., Chang, Y.M., and Kim, J.D., Nanoparticles of magnetic ferric oxides encapsulated with poly(D,L Lactide-co-Glycolide) and their applications to magnetic resonance imaging contrast agent. Journal of Magnetism and Magnetic Materials, **272-276**, 2432-2433 (2004).

23. Mu, L., and Feng, S.S., A novel controlled release formulation for anticancer drug paclitaxel (Taxol®): PLGA nanoparticles containing vitamin E. TPGS. Journal of Controlled Release, **86**, 33-48 (2003).

24. Panyam, J., and Labhasetwar V., Dynamics of endocytosis and exocytosis of poly(D,L-lactide-co-glycolide) nanoparticles in vascular smooth muscle cells. Pharmaceutical Research, **20**(2), 212-220 (2003).

25. Yan, P., Huiying, Z., Hui, X., Gang, W., Jinsong, H., and Junming, Z., Effect of experimental parameters on the encapsulation of insulin-loaded poly(lactide-co-glycolide) nanoparticles prepared by a double emulsion method. Journal of Chinese Pharmaceutical Science, **11**(1), 38-40 (2002).

26. Song, C.X., Labhasetwar, V., Murphy, H., Qu X., Humphrey W.R., Shebuski, R.J., Levy, R.J., Formulation and characterization of biodegradable nanoparticles for intravascular local drug delivery. Journal of Controlled Release, **43**: 197-212 (1997).

27. Desgouilles, S., Vauthier, C., Bazile, D., Vacus, J., Grossiord, JL., The design of nanoparticles obtained by solvent evaporation: a comprehensive study. Journal of American Chemical Society, **19**:9504-9510 (2003).

CHAPTER 4. CONCLUSIONS

Magnetite was successfully entrapped into PLGA nanoparticles while maintaining their size under 100 nm, for 4% w/w MOA theoretical loading. The SDS concentration and MOA size and size distribution were found to be the critical factors in controlling the nanoparticle size. The entrapment efficiency varied between 57% for low MW PLGA and 92% for high MW PLGA. Entrapment of magnetite can be coupled with the entrapment and delivery of active components (cancer drug, peptides, DNA, and others) to the target by the developed MPNPs.

It was found that an increase in the PLGA concentration (batch of production) by three times was possible with the proposed method, while keeping the nanosphere size less than 100 nm. This finding is significant, considering that commercial application of the synthesis method is strongly dependent on the nanoparticle yield formation, directly proportional to polymer concentration. Lastly, it was found that synthesis must be followed by a purification step (i.e. dialysis) to avoid aggregation of the nanoparticles due to excess of surfactant in the suspension.

CHAPTER 5. FUTURE WORK

The main target of the thesis research was to synthesize nanoparticles less than 100 nm in size, with entrapped magnetite in the polymeric matrix. The study of technologies available and the main parameters affecting the final PLGA nanoparticle size were the two main parts of this research. Although significant progress was made toward understanding the system developed, other areas of research should be addressed before the developed MPNPs could be successfully implemented in the drug delivery field. The future work should address the following aspects:

- Test the MPNP system with a suitable drug. The hydrophilic and hydrophobic drugs have different behaviors affecting the process parameters and size of the nanospheres. Although, the hydrophobic drugs are suitable for single emulsion evaporation method, the hydrophilic drugs should be tested. This requires switching from the single emulsion-evaporation to double emulsion-evaporation method. Some limitations should be addressed for the double emulsion - evaporation method, such as formation of bigger nanoparticles with lower drug entrapment efficiency (losses of active component in the continuous phase due to hydrophilic behavior of active component). The addition of some additives can improve the entrapment efficiency (i.e. higher viscosity, cationic-anionic interaction).
- Remove or replace SDS by other surfactants. SDS can not be administrated by parenteral route. To overcome this limitation two approaches can be followed:
    - Purification of the nanoparticles suspension to remove the SDS associated with the nanoparticles. Dialysis is an adequate method for elimination of SDS, but ultra-filtration can be used, and it should be tested.
    - Synthesis of a suitable surfactant with high hydrophilic-lipophilic balance (HLB) value (over 20), biodegradable, biocompatible, good packing number (less than 0.3), and small molecular size to replace SDS. The advantage of SDS is the use of electrostatic and steric forces to form small micelles that are used to form small nanoparticles.

- Optimize the SDS concentration, PLGA concentration, sonication time, entrapment efficiency of active component, and purification steps to obtain the optimum nanoparticle size by factorial design.
- Study the effect of sonication on the structure of the LGA chains, especially for high molecular weight. The size reduction of polymer chains can affect the possible release profiles of the active component entrapped.
- Conduct stability studies. The aggregation profile should be measured over time at different pHs. The nanoparticles aggregation must be avoided at corporal pH (neutral) for parenteral administration.
- Study the release profile of drugs entrapped in the MPNPs, an important step for further uses in vivo.
- Test the cellular uptake of PLGA-SDS nanoparticles to find the toxicity levels, and the advantages/disadvantages of the system. This is related with the active component bio-distribution, mechanism of cellular uptake and action (i.e. the negative and positive charges over the surface of the particle play an important role in the cellular uptake of PLGA nanoparticles).
- Conduct targeting studies required to find the minimum amount of magnetite that should be entrapped in the MPNP to obtain a suitable drug delivery system.

APPENDIX A. AUTHORIZATION FOR REPRODUCTIONS

Dear Dr. Astete,

Regarding your permission request to reprint the following material: "Synthesis and characterization of PLGA nanoparticles: a review" in your thesis, we grant you non-exclusive world rights free of charge provided full credit acknowledgement will be given to Brill Academic Publishers.

With best regard,

Sabine Steenbeek
Publishing Assistant STM
Brill Academic Publishers

- Permissions for pictures

Dear Ms Williams

We hereby grant you permission to reproduce the material detailed below in your thesis at no charge subject to the following conditions:
1. If any part of the material to be used (for example, figures) has appeared in our publication with credit or acknowledgement to another source, permission must also be sought from that source. If such permission is not obtained then that material may not be included in your publication/copies.
2. Suitable acknowledgment to the source must be made, either as a footnote or in a reference list at the end of your publication, as follows:
"Reprinted from Publication title, Vol number, Author(s), Title of article, Pages No., Copyright (Year), with permission from Elsevier".
3. Reproduction of this material is confined to the purpose for which permission is hereby given.
4. This permission is granted for non-exclusive world English rights only. For other languages please reapply separately for each one required. Permission excludes use in an electronic form. Should you have a specific electronic project in mind please reapply for permission.
5. This includes permission for UMI to supply single copies, on demand, of the complete thesis. Should your thesis be published commercially, please reapply for permission.
Yours sincerely,
<<...OLE_Obj...>>
Natalie David
Rights Assistant

-----Original Message-----
From: lwill44@lsu.edu [mailto:lwill44@lsu.edu <mailto:lwill44@lsu.edu>]
Sent: 01 November 2005 22:15
To: permissions@elsevier.com
Subject: Obtain Permission

This Email was sent from the Elsevier Corporate Web Site and is related to Obtain Permission form:

Product: Customer Support
Component: Obtain Permission
Web server: http://www.elsevier.com <http://www.elsevier.com>

IP address: 10.10.24.148
Client: Mozilla/5.0 (Windows; U; Windows NT 5.1; en-US; rv:1.7.8) Gecko/20050511 Firefox/1.0.4
Invoked from:
http://www.elsevier.com/wps/find/obtainpermissionform.cws_home?isSubmitted=yes&navigateXmlFileName=/store/prod_webcache_act/framework_support/obtainpermission.xml
<http://www.elsevier.com/wps/find/obtainpermissionform.cws_home?isSubmitted=yes&navigateXmlFileName=/store/prod_webcache_act/framework_support/obtainpermission.xml>

Request From:
Student Worker Lauren Williams
LSU, BAE Department
141 E. B. Doran
70803
Baton Rouge
United States

Contact Details:
Telephone: (225) 578-1055
Fax: (225) 578-3492
Email Address: lwill44@lsu.edu

To use the following material:
ISSN/ISBN:
Title: Journal of Controlled Release
Author(s): C. X. Song et al.
Volume: 43
Issue: None
Year: 1997
Pages: 197 - 212
Article title: Form & char biodegr nanopart for intravas drug del

How much of the requested material is to be used:
Fig 5 and caption: Efficiency of drug (U-86983) entrapment into PLGA nanoparticles by changing the pH of the aqueous phase from neutral to basic.
Are you the author: No
Author at institute: Yes
How/where will the requested material be used: [how_used]
Details:

Title: Synthesis of Poly(DL-Lactide-Co-Glycolide) Nanoparticles with Entrapped Magnetite; Author: Carlos Astete; Masters Thesis

Additional Info:
- end -
For further info regarding this automatic email, please contact:
WEB APPLICATIONS TEAM (esweb.admin@elsevier.co.uk)

Dear Ms Williams

We hereby grant you permission to reproduce the material detailed below in your thesis at no charge subject to the following conditions:
1. If any part of the material to be used (for example, figures) has appeared in our publication with credit or acknowledgement to another source, permission must also be sought from that source. If such permission is not obtained then that material may not be included in your publication/copies.
2. Suitable acknowledgment to the source must be made, either as a footnote or in a reference list at the end of your publication, as follows:
"Reprinted from Publication title, Vol number, Author(s), Title of article, Pages No., Copyright (Year), with permission from Elsevier".
3. Reproduction of this material is confined to the purpose for which permission is hereby given.
4. This permission is granted for non-exclusive world English rights only. For other languages please reapply separately for each one required. Permission excludes use in an electronic form. Should you have a specific electronic project in mind please reapply for permission.
5. This includes permission for UMI to supply single copies, on demand, of the complete thesis. Should your thesis be published commercially, please reapply for permission.

Yours sincerely,
<<...OLE_Obj...>>
Natalie David
Rights Assistant

-----Original Message-----
From: lwill44@lsu.edu [mailto:lwill44@lsu.edu <mailto:lwill44@lsu.edu>]
Sent: 25 October 2005 23:43
To: permissions@elsevier.com
Subject: Obtain Permission

This Email was sent from the Elsevier Corporate Web Site and is related to Obtain Permission form:

Product: Customer Support
Component: Obtain Permission

Web server: http://www.elsevier.com <http://www.elsevier.com>
IP address: 10.10.24.148
Client: Mozilla/5.0 (Windows; U; Windows NT 5.1; en-US; rv:1.7.8) Gecko/20050511 Firefox/1.0.4
Invoked from:
http://www.elsevier.com/wps/find/obtainpermissionform.cws_home?isSubmitted=yes&navigateXmlFileName=/store/prod_webcache_act/framework_support/obtainpermission.xml
<http://www.elsevier.com/wps/find/obtainpermissionform.cws_home?isSubmitted=yes&navigateXmlFileName=/store/prod_webcache_act/framework_support/obtainpermission.xml>

Request From:
student worker Lauren Williams
LSu, BAE Department
141 E. B. Doran
70803
Baton Rouge
United States

Contact Details:
Telephone: (225) 578-1055
Fax: (225) 578-3492
Email Address: lwill44@lsu.edu

To use the following material:
ISSN/ISBN:
Title: International Journal of Pharmaceutics
Author(s): Y. N. Konan et al.
Volume: 233
Issue: none
Year: 2002
Pages: 239 - 252
Article title: Prep & Char sterile & freezedried sub-200 nanopart

How much of the requested material is to be used:
Are you the author: No
Author at institute: Yes
How/where will the requested material be used: [how_used]

Details:

Title: Synthesis of Poly(DL-Lactide-Co-Glycolide) Nanoparticles with Entrapped Magnetite; Author: Carlos Astete; Masters Thesis

Additional Info:
- end -
For further info regarding this automatic email, please contact:
WEB APPLICATIONS TEAM (esweb.admin@elsevier.co.uk)

Dear Dr Williams

We hereby grant you permission to reproduce the material detailed below in your thesis at no charge subject to the following conditions:
1. If any part of the material to be used (for example, figures) has appeared in our publication with credit or acknowledgement to another source, permission must also be sought from that source. If such permission is not obtained then that material may not be included in your publication/copies.
2. Suitable acknowledgment to the source must be made, either as a footnote or in a reference list at the end of your publication, as follows:
"Reprinted from Publication title, Vol number, Author(s), Title of article, Pages No., Copyright (Year), with permission from Elsevier".
3. Reproduction of this material is confined to the purpose for which permission is hereby given.
4. This permission is granted for non-exclusive world English rights only. For other languages please reapply separately for each one required. Permission excludes use in an electronic form. Should you have a specific electronic project in mind please reapply for permission.
5. This includes permission for UMI to supply single copies, on demand, of the complete thesis. Should your thesis be published commercially, please reapply for permission.
Yours sincerely,
<<...OLE_Obj...>>
Natalie David
Rights Assistant

-----Original Message-----
From: lwill44@lsu.edu [mailto:lwill44@lsu.edu <mailto:lwill44@lsu.edu>]

Sent: 25 October 2005 22:40
To: permissions@elsevier.com
Subject: Obtain Permission

This Email was sent from the Elsevier Corporate Web Site and is related to
Obtain Permission form:

Product: Customer Support
Component: Obtain Permission
Web server: http://www.elsevier.com <http://www.elsevier.com>
IP address: 10.10.24.148
Client: Mozilla/5.0 (Windows; U; Windows NT 5.1; en-US; rv:1.7.8)
Gecko/20050511 Firefox/1.0.4
Invoked from:
http://www.elsevier.com/wps/find/obtainpermissionform.cws_home?isSubmitted=y
es&navigateXmlFileName=/store/prod_webcache_act/framework_support/obtainperm
ission.xml
<http://www.elsevier.com/wps/find/obtainpermissionform.cws_home?isSubmitted=
yes&navigateXmlFileName=/store/prod_webcache_act/framework_support/obtainper
mission.xml>

Request From:
Student Worker Lauren Williams
LSU, BAE Department
141 E. B. Doran
70803
Baton Rouge
United States

Contact Details:
Telephone: (225) 578-1055
Fax: (225) 578-3492
Email Address: lwill44@lsu.edu

To use the following material:
ISSN/ISBN:
Title: Colloids & Surfaces A: Physiochemical & Eng Aspects
Author(s): Hye-Young Kwon et al.
Volume: 182
Issue: None
Year: 2001
Pages: 123 - 130
Article title: Prep PLGA Nanopart contain estrogen by emul-diff

How much of the requested material is to be used:
Figs 2, 4, 5 & captions read as follows:Fig 2: The influence of surfactant on mean size of PLGA nanoparticles. Fig 4: Surface Tension of DMAB & PVA soln as a func of conc (wt%). Fig 5: Effect of PLGA conc on mean particle size of PLGA nanoparticles.
Are you the author: No
Author at institute: Yes

How/where will the requested material be used: [how_used]

Details:

Title: Synthesis of Poly(DL-Lactide-Co-Glycolide) Nanoparticles with Entrapped Magnetite, Masters Thesis, Author: Caslos Astete

Additional Info:
- end -
For further info regarding this automatic email, please contact:
WEB APPLICATIONS TEAM (esweb.admin@elsevier.co.uk)

republication
<republication@wiley.com>

11/01/2005 05:37 PM

Please respond to republication <republication@wiley.com>

To <republication@wiley.com>
cc
bcc
Subject Republication/Electronic Request Form

A01_First_Name: Lauren
A02_Last_Name: Williams
A03_Company_Name: LSU, BAE Department
A04_Address: 141 E. B. Doran
A05_City: Baton Rouge
A06_State: Louisiana
A07_Zip: 70803
A08_Country: United States
A09_Contact_Phone_Number: (225) 578-1055
A10_Fax: (225) 578-3492
A11_Emails: lwill44@lsu.edu
A12_Reference: None
A13_Book_Title: Journal of Applied Polymer Science Wiley Stm.
A40_Book_or_Journal: Journal
A14_Book_Author:
A15_Book_ISBN:
A16_Journal_Month: None
A17_Journal_Year: 2001
A18_Journal_Volume: 80
A19_Journal_Issue_Number: None
A20_Copy_Pages: Fig 2 on pg. 2231 of "Preparation of Poly (DL-lactide-co-gylcolide) Nanoparticles without Surfactant" by Young-Il Jeong et al. and caption: Scanning Electron microphotographs of 50:50 PLGA nanoparticles prepared from a) DMAC or b) acetone as a function of the initial solvent
A21_Maximum_Copies: Don't Know
A22_Your_Publisher: None
A23_Your_Title: Synthesis of Poly(DL-Lactide-Co-Glycolide) Nanoparticles with Entrapped Magnetite
A24_Publication_Date: None
A25_Format: print
A31_Print_Run_Size:
A41_Ebook_Reader_Type:
A26_If_WWW_URL:
A27_If_WWW_From_Adopted_Book:
A28_If_WWW_Password_Access: No
A45_WWW_Users:
A29_If_WWW_Material_Posted_From:
A30_If_WWW_Material_Posted_To:
A42_If_Intranet_URL:
A32_If_Intranet_From_Adopted_Book:
A33_If_Intranet_Password_Access: No
A48_Intranet_Users:
A34_If_Intranet_Material_Posted_From:
A35_If_Intranet_Material_Posted_To:
A36_If_Software_Print_Run:
A37_Comments_For_Request: The request is for Carlos Astetes's Masters Thesis.

PERMISSION GRANTED
BY: _____ 11/02/05
Legal Department, John Wiley & Sons, Inc.

NOTE: No rights are granted to use content that appears in the work with credit to another source.

/03/2005 16:20 FAX 2027768112

)V 02 2005 5:22PM HP LASERJET 3200

ACS PUBLICATIONS DIVISION
NOV - 3 2005
COPYRIGHT OFFICE

PERMISSION REQUEST FORM FOR FIGURES AND TABLES

Date: 11/2/05

To: Copyright Office
Publications Division
American Chemical Society
1155 Sixteenth Street, N.W.
Washington, DC 20036

FAX: 202-776-8112

From: Dr. Cristina Sabliov
LSU, BAE Department
141 E.B. Doran
Baton Rouge, LA 70803

Your Phone No. (225)-578-1055
Your Fax No. (225)-578-3492

I am preparing a paper entitled:
Synthesis of Poly(DL-lactide-Co-Glycolide) Nanoparticles with Entrapped Magnetite
to appear in a (circle one) book, magazine, journal, proceedings, other Master's Thesis
entitled: N/A

to be published by: N/A

I would appreciate your permission to use the following ACS material in print and other formats with the understanding that the required ACS copyright credit line will appear with each item and that this permission is for only the requested work listed above:

From ACS journals or magazines (for ACS magazines, also include issue no.):

ACS Publication Title	Issue Date	Vol.	No.	Page(s)	Material to be used*
Biomacromolecules	2005	6	1	274	"PLGA:Poloxamer and PLGA:Poloxamine Blend Nanoparticles: New Carriers for Gene Delivery"; Fig 2 and caption on Pg. 274

From ACS books: include ACS book title, series name and number, year, page(s), book editor's name(s), chapter author's name(s), and material to be used, such as Figs. 2 & 3, full text, etc.*

* If you use more than three figures/tables from any article and/or chapter, the author's permission will also be required.

Questions? Please call Arleen Cou

This space is reserved for ACS Copyright Office Use

PERMISSION TO REPRINT IS GRANTED BY THE AMERICAN CHEMICAL SOCIETY

ACS CREDIT LINE REQUIRED. Please follow this sample: Reprinted with permission from (reference citation). Copyright (year) American Chemical Society.

APPROVED BY: *C. Arleen Courtney* 11/3/05
ACS Copyright Office

☐ If box is checked, author permission is also required. See original article for address.

12/3/99

APPENDIX B. STANDARD CURVE FOR IRON DETECTION

Iron determination based on Prussian blue reaction. The wavelength used was at 700 nm. The digestion was made with Hydrochloric acid at 6 N.

The standard curve was prepared with iron (III) oxide, 99.999% of purity.

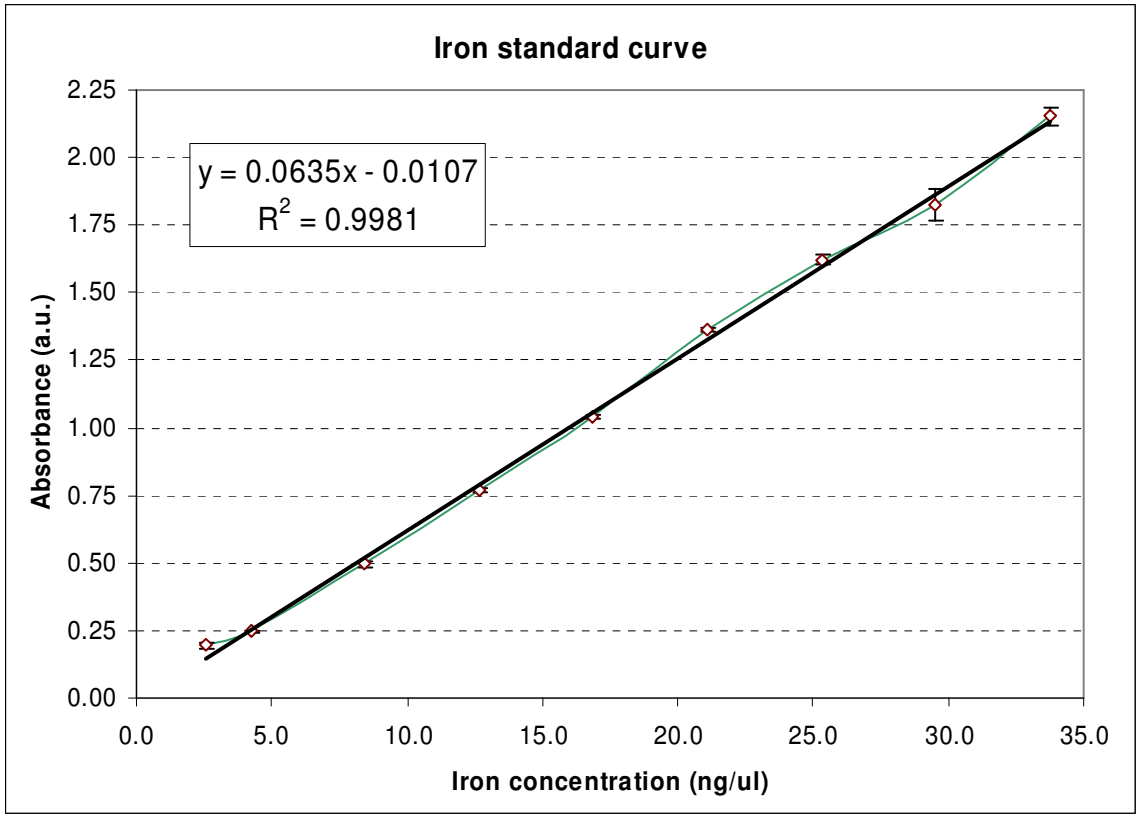

APPENDIX C. SIZE MEASUREMENTS WITH DLS (MALVERN ZETASIZER NANOSERIES)

There were prepared a lot of sample to define the important parameters to obtain nanoparticle under 100 nm. The tables presented in this appendix showed the diversity of nanoparticle size in function of the parameters tested. Many experiments were design to test some theories and procedures.

Double emulsion method without second sonication (CAR 140, CAR 132), and all other parameters were maintained constant. CAR 131 is the standard single emulsion evaporation method, but the magnetite entrapped was without oleic acid surface modification. CAR 133 was double emulsion method with second sonication. CAR 135 and CAR 136 were different evaporation rates with single emulsion method (PLGA of LMW). The evaporation procedure tested were without injection of nitrogen and high vacuum (40 cm Hg), and without nitrogen injection and high vacuum (40 cm Hg). The sample CAR 138 was with low vacuum (100 cm Hg) and nitrogen injection. All other samples are explained in the table.

Record	Type	Sample	Date	T (°C)	Z-Ave (nm)	PDI	ZP (mV)	Cond (mS/cm)
1	Size	CAR140 DE w/o II sonic	01/26/05	25	201.2	0.212		
2	Size	CAR140 DE w/o II sonic	01/26/05	25	204.8	0.198		
3	Size	CAR140 DE w/o II sonic	01/26/05	25	204.6	0.226		
4	Size	CAR131 Standard Mgn	01/26/05	25	171.6	0.263		
5	Size	CAR131 Standard Mgn	01/26/05	25	115.1	0.527		
6	Size	CAR131 Standard Mgn	01/26/05	25	100.5	0.598		
7	Size	CAR131 Standard Mgn 2pick	01/26/05	25	89.05	0.762		
8	Size	CAR131 Standard Mgn 2pick	01/26/05	25	91.3	0.801		
9	Size	CAR131 Standard Mgn 2pick	01/26/05	25	99.11	0.512		
10	Size	CAR132 DEWOS	01/26/05	25	124	0.364		
11	Size	CAR132 DEWOS	01/26/05	25	125.6	0.281		
12	Size	CAR132 DEWOS	01/26/05	25	122.8	0.281		
13	Size	CAR133 DEWS	01/26/05	25	110.4	0.42		
14	Size	CAR133 DEWS	01/26/05	25	99.45	0.524		
15	Size	CAR133 DEWS	01/26/05	25	100.9	0.461		
16	Size	CAR133 DEWS 2picks	01/26/05	25	93.49	0.464		
17	Size	CAR133 DEWS 2picks	01/26/05	25	87.23	0.434		
18	Size	CAR133 DEWS 2picks	01/26/05	25	93.32	0.604		
19	Size	CAR134 stdb liposurf	01/26/05	25	172.1	0.265		

20	Size	CAR134 stdb liposurf	01/26/05	25	124.3	0.393
21	Size	CAR134 stdb liposurf	01/26/05	25	94.34	0.686
22	Size	CAR134 stdb liposurf 2pick	01/26/05	25	90.47	0.498
23	Size	CAR134 stdb liposurf 2pick	01/26/05	25	85.02	0.625
24	Size	CAR134 stdb liposurf 2pick	01/26/05	25	92.21	0.502
25	Size	CAR 135 Ev rate	01/26/05	25	41.43	0.342
26	Size	CAR 135 Ev rate	01/26/05	25	41.39	0.302
27	Size	CAR 135 Ev rate	01/26/05	25	39.95	0.322
28	Size	CAR 136 Ev rate	01/26/05	25	58.02	0.414
29	Size	CAR 136 Ev rate	01/26/05	25	57.96	0.418
30	Size	CAR 136 Ev rate	01/26/05	25	56.94	0.41
31	Size	CAR 137 DEWOS VE	01/26/05	25	193.2	0.7
32	Size	CAR 137 DEWOS VE	01/26/05	25	136.9	0.959
33	Size	CAR 137 DEWOS VE	01/26/05	25	140.2	0.957
34	Size	CAR 137 DEWOS VE 2pick	01/26/05	25	77.14	0.759
35	Size	CAR 137 DEWOS VE 2pick	01/26/05	25	80.67	0.521
36	Size	CAR 137 DEWOS VE 2pick	01/26/05	25	88.12	0.493
37	Size	CAR 138 Ev Rate low vac	01/26/05	25	66.34	0.212
38	Size	CAR 138 Ev Rate low vac	01/26/05	25	42.57	0.402
39	Size	CAR 138 Ev Rate low vac	01/26/05	25	42.34	0.367
40	Size	CAR 139 DEWOS VE MMW	01/26/05	25	71.66	0.393
41	Size	CAR 139 DEWOS VE MMW	01/26/05	25	70.43	0.388
42	Size	CAR 139 DEWOS VE MMW	01/26/05	25	72.11	0.365
43	Size	CAR Mgn lipo	01/26/05	25	175.3	0.4
44	Size	CAR Mgn lipo	01/26/05	25	179.3	0.417
45	Size	CAR Mgn lipo	01/26/05	25	176.6	0.392
46	Size	CAR Mgn lipo 2pick	01/26/05	25	329.9	0.695
47	Size	CAR Mgn lipo 2pick	01/26/05	25	297	0.535
48	Size	CAR Mgn lipo 2pick	01/26/05	25	248.2	0.664
49	Size	CAR Mgn	01/26/05	25	270.5	0.359
50	Size	CAR Mgn	01/26/05	25	241.9	0.431
51	Size	CAR Mgn	01/26/05	25	237.8	0.418
52	Size	CAR 134 waste	01/26/05	25	51.6	0.443
53	Size	CAR 134 waste	01/26/05	25	50.64	0.416
54	Size	CAR 134 waste	01/26/05	25	48.25	0.418
55	Size	CAR 131 waste	01/26/05	25	67.18	0.463
56	Size	CAR 131 waste	01/26/05	25	67.55	0.464
57	Size	CAR 131 waste	01/26/05	25	65.2	0.478
58	Size	CAR 131 waste 2pick	01/26/05	25	66.86	0.49
59	Size	CAR 131 waste 2pick	01/26/05	25	63.78	0.469
60	Size	CAR 131 waste 2pick	01/26/05	25	67.85	0.464
61	Size	water	01/26/05	25	1639	0.776
62	Size	water 2	01/26/05	25	2609	1
63	Size	water 2	01/26/05	25	1274	0.617
64	Size	water 2	01/26/05	25	875.1	0.568
65	Size	water 2 fitered	01/26/05	25	426.9	0.382

Sample CAR 185 and CAR 186 were prepared with different amounts of PLGA. The sample CAR 178, CAR 179, and CAR181 were with high molecular weight PLGA. The samples CAR 168, CAR 172, CAR 182 and CAR 180 were prepared with more surfactant (35 mg). CAR 173 and CAR 174 were formed with medium PLGA molecular weight (MMW). In all samples presented in this table, the aqueous phase was prepared with a buffer solution (pH 8). They showed a strong precipitation after two hour ended the formation process. Strong aggregation was present, which was reflected in the higher size measured.

Record	Type	Sample Name	Date	T (°C)	Z-Ave (nm)	PDI	ZP (mV)	Cond (mS/cm)
1	Size	Car185-100mg	May 20, 2005	25	74.43	0.124		
2	Size	Car185-100mg	May 20, 2005	25	74.11	0.137		
3	Size	Car185-100mg	May 20, 2005	25	74.72	0.126		
4	Size	Car184-150mg	May 20, 2005	25	65.02	0.171		
5	Size	Car184-150mg	May 20, 2005	25	65.36	0.143		
6	Size	Car184-150mg	May 20, 2005	25	65.16	0.175		
7	Size	Car178-HMW	May 20, 2005	25	149.8	0.504		
8	Size	Car178-HMW	May 20, 2005	25	148.5	0.495		
9	Size	Car178-HMW	May 20, 2005	25	149.5	0.502		
10	Size	Car181-HMW	May 20, 2005	25	122.6	0.417		
11	Size	Car181-HMW	May 20, 2005	25	123	0.427		
12	Size	Car181-HMW	May 20, 2005	25	123.8	0.433		
13	Size	Car182-HMW35mg	May 20, 2005	25	118.4	0.473		
14	Size	Car182-HMW35mg	May 20, 2005	25	115.7	0.456		
15	Size	Car182-HMW35mg	May 20, 2005	25	118.4	0.422		
16	Size	Car180-HMW35mg	May 20, 2005	25	148.2	0.55		
17	Size	Car180-HMW35mg	May 20, 2005	25	154.6	0.522		
18	Size	Car180-HMW35mg	May 20, 2005	25	154.9	0.521		
19	Size	Car179-HMW	May 20, 2005	25	142.2	0.492		
20	Size	Car179-HMW	May 20, 2005	25	138.3	0.499		
21	Size	Car179-HMW	May 20, 2005	25	142.6	0.49		
22	Size	Car172-MMW35mg	May 20, 2005	25	171	0.523		
23	Size	Car172-MMW35mg	May 20, 2005	25	173.7	0.537		
24	Size	Car172-MMW35mg	May 20, 2005	25	166.5	0.584		
25	Size	Car173-MMW	May 20, 2005	25	211.6	1		
26	Size	Car173-MMW	May 20, 2005	25	208.7	1		
27	Size	Car173-MMW	May 20, 2005	25	209.1	1		
28	Size	Car174-MMW	May 20, 2005	25	215.8	1		
29	Size	Car174-MMW	May 20, 2005	25	214.8	1		
30	Size	Car174-MMW	May 20, 2005	25	209.4	0.985		
31	Size	Car166-LMW	May 20, 2005	25	297.2	0.667		
32	Size	Car166-LMW	May 20, 2005	25	233.7	1		
33	Size	Car166-LMW	May 20, 2005	25	287.1	0.655		
34	Size	Car168-LMW35mg	May 20, 2005	25	201.5	0.637		

35	Size	Car168-LMW35mg	May 20, 2005	25	196.2	0.619		
36	Size	Car168-LMW35mg	May 20, 2005	25	200.7	0.64		
37	Size	Car167-LMW	May 20, 2005	25	188.1	0.597		
38	Size	Car167-LMW	May 20, 2005	25	192	0.603		
39	Size	Car167-LMW	May 20, 2005	25	191.7	0.594		
40	Size	Car-MAO	May 20, 2005	25	200.6	0.242		
41	Size	Car-MAO	May 20, 2005	25	198.9	0.225		
42	Size	Car-MAO	May 20, 2005	25	202.6	0.239		
43	Zeta	Car-184Z	May 20, 2005	25			-98.5	0.8654
44	Zeta	Car-184Z	May 20, 2005	25			-99.18	0.9144
45	Zeta	Car-184Z	May 20, 2005	25			-101.5	0.9352
46	Zeta	Car-184Zdup	May 20, 2005	25			-99.1	0.8952
47	Zeta	Car-184Zdup	May 20, 2005	25			-99.85	0.9099
48	Zeta	Car-184Zdup	May 20, 2005	25			-98.01	0.9187

The samples CAR 250, CAR 256, CAR 262 were formed with poly(vinyl alcohol) (PVA). All other samples were for magnetite entrapment by emulsion evaporation (single emulsion).

Record	Type	Sample Name	Date	T (°C)	Z-Ave (nm)	PDI	ZP (mV)	Cond (mS/cm)
1	Size	CAR250pva	May 25, 2005	25	117.8	0.161		
2	Size	CAR250pva	May 25, 2005	25	120.6	0.16		
3	Size	CAR250pva	May 25, 2005	25	121.2	0.18		
4	Size	CAR250pva	May 25, 2005	25	121.6	0.164		
5	Size	CAR256pva	May 25, 2005	25	135.8	0.135		
6	Size	CAR256pva	May 25, 2005	25	137.4	0.127		
7	Size	CAR256pva	May 25, 2005	25	138.1	0.068		
8	Size	CAR262pva	May 25, 2005	25	149.3	0.073		
9	Size	CAR262pva	May 25, 2005	25	148.2	0.093		
10	Size	CAR262pva	May 25, 2005	25	147.3	0.058		
11	Size	CAR196magLMW	May 25, 2005	25	110.1	0.395		
12	Size	CAR196magLMW	May 25, 2005	25	107.3	0.433		
13	Size	CAR196magLMW	May 25, 2005	25	108.7	0.396		
14	Size	CAR197magLMW	May 25, 2005	25	146	0.269		
15	Size	CAR197magLMW	May 25, 2005	25	145.3	0.281		
16	Size	CAR197magLMW	May 25, 2005	25	142.1	0.28		
17	Size	CAR198magLMW	May 25, 2005	25	130.4	0.281		
18	Size	CAR198magLMW	May 25, 2005	25	128.1	0.271		
19	Size	CAR198magLMW	May 25, 2005	25	130.6	0.28		
20	Size	CAR199magLMW	May 25, 2005	25	149.2	0.229		
21	Size	CAR199magLMW	May 25, 2005	25	147.1	0.241		
22	Size	CAR199magLMW	May 25, 2005	25	145.7	0.234		
23	Size	CAR200magLMW	May 25, 2005	25	91.23	0.371		

24	Size	CAR200magLMW	May 25, 2005	25	90.09	0.361
25	Size	CAR200magLMW	May 25, 2005	25	89.59	0.373
26	Size	CAR201magLMW	May 25, 2005	25	146.7	0.253
27	Size	CAR201magLMW	May 25, 2005	25	145.8	0.241
28	Size	CAR201magLMW	May 25, 2005	25	144.1	0.246
29	Size	CAR202magMMW	May 25, 2005	25	84.67	0.295
30	Size	CAR202magMMW	May 25, 2005	25	82.7	0.284
31	Size	CAR202magMMW	May 25, 2005	25	82.19	0.284
32	Size	CAR203magMMW	May 25, 2005	25	144.1	0.284
33	Size	CAR203magMMW	May 25, 2005	25	140.6	0.214
34	Size	CAR203magMMW	May 25, 2005	25	139.3	0.207
35	Size	CAR204magMMW	May 25, 2005	25	89.9	0.381
36	Size	CAR204magMMW	May 25, 2005	25	89.31	0.387
37	Size	CAR204magMMW	May 25, 2005	25	86.9	0.374
38	Size	CAR208magHMW	May 25, 2005	25	77.04	0.325
39	Size	CAR208magHMW	May 25, 2005	25	77.1	0.257
40	Size	CAR208magHMW	May 25, 2005	25	75.78	0.263
41	Size	CAR209magHMW	May 25, 2005	25	83.38	0.341
42	Size	CAR209magHMW	May 25, 2005	25	81.91	0.337
43	Size	CAR209magHMW	May 25, 2005	25	81.28	0.327
44	Size	CAR210magHMW	May 25, 2005	25	83.44	0.397
45	Size	CAR210magHMW	May 25, 2005	25	82.5	0.403
46	Size	CAR210magHMW	May 25, 2005	25	79.15	0.365
47	Size	CAR205HmagMMW	May 25, 2005	25	101.5	0.285
48	Size	CAR205HmagMMW	May 25, 2005	25	102.4	0.299
49	Size	CAR205HmagMMW	May 25, 2005	25	101.8	0.281
50	Size	CAR211HmagHMW	May 25, 2005	25	99.01	0.356
51	Size	CAR211HmagHMW	May 25, 2005	25	95.27	0.371
52	Size	CAR211HmagHMW	May 25, 2005	25	94.68	0.387

All sample were prepared with emulsion evaporation method (SDS of 2 mg/ml), and with the three PLGA molecular weight used in this research.

Record	Type	Sample Name	Date	T (℃)	Z-Ave (nm)	PDI	ZP (mV)	Cond (mS/cm)
1	Size	CAR238LMWLS	May 26, 2005	25	37.91	0.301		
2	Size	CAR238LMWLS	May 26, 2005	25	39.13	0.304		
3	Size	CAR238LMWLS	May 26, 2005	25	39.12	0.299		
4	Size	CAR238LMWLSB	May 26, 2005	25	39.42	0.3		
5	Size	CAR238LMWLSB	May 26, 2005	25	39.77	0.274		
6	Size	CAR238LMWLSB	May 26, 2005	25	39.55	0.255		
7	Size	CAR239LMWLS	May 26, 2005	25	37.89	0.293		
8	Size	CAR239LMWLS	May 26, 2005	25	38.27	0.296		
9	Size	CAR239LMWLS	May 26, 2005	25	38.16	0.262		
10	Size	CAR240MMWLS	May 26, 2005	25	41.15	0.288		
11	Size	CAR240MMWLS	May 26, 2005	25	41.53	0.261		

12	Size	CAR240MMWLS	May 26, 2005	25	41.38	0.257		
13	Size	CAR241MMWLS	May 26, 2005	25	67.16	0.106		
14	Size	CAR241MMWLS	May 26, 2005	25	67.49	0.111		
15	Size	CAR241MMWLS	May 26, 2005	25	66.86	0.111		
16	Size	CAR242MMWLS	May 26, 2005	25	68.02	0.097		
17	Size	CAR242MMWLS	May 26, 2005	25	68.38	0.096		
18	Size	CAR242MMWLS	May 26, 2005	25	68.86	0.1		
19	Size	CAR244HMWLS	May 26, 2005	25	69.83	0.132		
20	Size	CAR244HMWLS	May 26, 2005	25	70.4	0.113		
21	Size	CAR244HMWLS	May 26, 2005	25	70.71	0.114		
22	Size	CAR245HMWLS	May 26, 2005	25	71.7	0.132		
23	Size	CAR245HMWLS	May 26, 2005	25	70.53	0.129		
24	Size	CAR245HMWLS	May 26, 2005	25	69.66	0.134		
25	Size	CAR270LMWLS	May 26, 2005	25	111.4	0.315		
26	Size	CAR270LMWLS	May 26, 2005	25	112.5	0.312		
27	Size	CAR270LMWLS	May 26, 2005	25	111.9	0.313		
28	Size	CAR271LMWLS	May 26, 2005	25	110.3	0.314		
29	Size	CAR271LMWLS	May 26, 2005	25	103	0.422		
30	Size	CAR271LMWLS	May 26, 2005	25	108.3	0.306		
31	Size	CAR272LMWLS	May 26, 2005	25	108.3	0.304		
32	Size	CAR272LMWLS	May 26, 2005	25	109.8	0.303		
33	Size	CAR272LMWLS	May 26, 2005	25	107.6	0.298		
34	Size	CAR250LMWPVACentA	May 26, 2005	25	131.3	0.19		
35	Size	CAR250LMWPVACentA	May 26, 2005	25	129.4	0.165		
36	Size	CAR250LMWPVACentA	May 26, 2005	25	129.9	0.188		
37	Size	CAR250LMWPVACentB	May 26, 2005	25	134.9	0.218		
38	Size	CAR250LMWPVACentB	May 26, 2005	25	132.9	0.191		
39	Size	CAR250LMWPVACentB	May 26, 2005	25	133.7	0.205		
40	Zeta	CAR238	May 26, 2005	25			-27.01	0.04717
41	Zeta	CAR238	May 26, 2005	25			-31.68	0.04591
42	Zeta	CAR238	May 26, 2005	25			-28.26	0.04641
43	Zeta	CAR239	May 26, 2005	25			-0.419	0.02604
44	Zeta	CAR239	May 26, 2005	25			-0.39	0.03365
45	Zeta	CAR239	May 26, 2005	25			-0.007	0.02787
46	Zeta	CAR240	May 26, 2005	25			-32.73	0.04691
47	Zeta	CAR240	May 26, 2005	25			-34.34	0.05291
48	Zeta	CAR240	May 26, 2005	25			-25.87	0.04898
49	Zeta	CAR241	May 26, 2005	25			-37.32	0.05661
50	Zeta	CAR241	May 26, 2005	25			-32.94	0.05253
51	Zeta	CAR241	May 26, 2005	25			-28.45	0.0505
52	Zeta	CAR242	May 26, 2005	25			-33.32	0.04405
53	Zeta	CAR242	May 26, 2005	25			-36.94	0.04596
54	Zeta	CAR242	May 26, 2005	25			-35.23	0.04512
55	Zeta	CAR244	May 26, 2005	25			-37.73	0.04893
56	Zeta	CAR244	May 26, 2005	25			-38.21	0.05791
57	Zeta	CAR244	May 26, 2005	25			-33.36	0.05458
58	Zeta	CAR245	May 26, 2005	25			-40.82	0.05726
59	Zeta	CAR245	May 26, 2005	25			-48.45	0.05051
60	Zeta	CAR245	May 26, 2005	25			-36.99	0.04983
61	Zeta	CAR239good	May 26, 2005	25			-26.67	0.0492

62	Zeta	CAR239good	May 26, 2005	25	-24.14	0.05313
63	Zeta	CAR239good	May 26, 2005	25	-20.9	0.05301
64	Zeta	CAR270	May 26, 2005	25	-38.42	0.04357
65	Zeta	CAR270	May 26, 2005	25	-39.54	0.04467
66	Zeta	CAR270	May 26, 2005	25	-41.52	0.05614
67	Zeta	CAR271	May 26, 2005	25	-40.02	0.05087
68	Zeta	CAR271	May 26, 2005	25	-34.48	0.04217
69	Zeta	CAR271	May 26, 2005	25	-38.64	0.04197
70	Zeta	CAR272	May 26, 2005	25	-39.71	0.05134
71	Zeta	CAR272	May 26, 2005	25	-40.38	0.04539
72	Zeta	CAR272	May 26, 2005	25	-42.87	0.04933
73	Zeta	CAR250	May 26, 2005	25	-23.5	0.01789
74	Zeta	CAR250	May 26, 2005	25	-24.4	0.03051
75	Zeta	CAR250	May 26, 2005	25	-22.29	0.01175
76	Zeta	CAR197	May 26, 2005	25	-35.26	0.09469
77	Zeta	CAR197	May 26, 2005	25	-36.1	0.094
78	Zeta	CAR197	May 26, 2005	25	-35.72	0.0928

All sample were prepared with emulsion evaporation method (SDS of 2 mg/ml), and with the three PLGA molecular weight used in this research.

Record	Type	Sample Name	Date	T (°C)	Z-Ave (nm)	PDI	ZP (mV)	Cond (mS/cm)
1	Size	CAR280LMW12S	May 27, 2005	25	40.42	0.344		
2	Size	CAR280LMW12S	May 27, 2005	25	39.79	0.328		
3	Size	CAR280LMW12S	May 27, 2005	25	39.37	0.319		
4	Size	CAR282LMW08S	May 27, 2005	25	39.94	0.268		
5	Size	CAR282LMW08S	May 27, 2005	25	40.68	0.296		
6	Size	CAR282LMW08S	May 27, 2005	25	41.49	0.3		
7	Size	CAR283LMW12Smag	May 27, 2005	25	120.7	0.382		
8	Size	CAR283LMW12Smag	May 27, 2005	25	121.6	0.366		
9	Size	CAR283LMW12Smag	May 27, 2005	25	122.8	0.376		
10	Size	CAR273MMWmag	May 27, 2005	25	90.06	0.312		
11	Size	CAR273MMWmag	May 27, 2005	25	91.53	0.269		
12	Size	CAR273MMWmag	May 27, 2005	25	90.49	0.266		
13	Size	CAR274MMWmag	May 27, 2005	25	90.13	0.262		
14	Size	CAR274MMWmag	May 27, 2005	25	88.95	0.308		
15	Size	CAR274MMWmag	May 27, 2005	25	87.93	0.271		
16	Size	CAR276HMWmag	May 27, 2005	25	84.14	0.228		
17	Size	CAR276HMWmag	May 27, 2005	25	84.36	0.242		
18	Size	CAR276HMWmag	May 27, 2005	25	82.73	0.226		
19	Size	CAR277HMWmag	May 27, 2005	25	84.36	0.251		
20	Size	CAR277HMWmag	May 27, 2005	25	85.37	0.239		
21	Size	CAR277HMWmag	May 27, 2005	25	84.65	0.233		
22	Zeta	CAR280	May 27, 2005	25			-23.61	0.05224
23	Zeta	CAR280	May 27, 2005	25			-35.74	0.04815

24	Zeta	CAR280	May 27, 2005	25			-29.58	0.05152
25	Zeta	CAR282	May 27, 2005	25			-20.9	0.045
26	Zeta	CAR282	May 27, 2005	25			-26.71	0.05282
27	Zeta	CAR282	May 27, 2005	25			-26.43	0.04728
28	Zeta	CAR283	May 27, 2005	25			-47.24	0.04702
29	Zeta	CAR283	May 27, 2005	25			-46.15	0.05155
30	Zeta	CAR283	May 27, 2005	25			-43.66	0.04594
31	Zeta	CAR273	May 27, 2005	25			-38.31	0.04669
32	Zeta	CAR273	May 27, 2005	25			-40.96	0.05421
33	Zeta	CAR273	May 27, 2005	25			-42.22	0.04773
34	Zeta	CAR274	May 27, 2005	25			-78.11	0.2119
35	Zeta	CAR274	May 27, 2005	25			-81.23	0.2167
36	Zeta	CAR274	May 27, 2005	25			-72.12	0.2184
37	Zeta	CAR276	May 27, 2005	25			-47.2	0.06435
38	Zeta	CAR276	May 27, 2005	25			-48.1	0.06122
39	Zeta	CAR276	May 27, 2005	25			-53.9	0.06464
40	Zeta	CAR277	May 27, 2005	25			-65.88	0.1229
41	Zeta	CAR277	May 27, 2005	25			-54.92	0.1237
42	Zeta	CAR277	May 27, 2005	25			-61.07	0.1224
43	Size	car280B	May 27, 2005	25	39.05	0.312		
44	Size	car280B	May 27, 2005	25	39.54	0.28		
45	Size	car280B	May 27, 2005	25	38.87	0.257		
46	Size	CAR206MMW8mag	May 27, 2005	25	96.61	0.365		
47	Size	CAR206MMW8mag	May 27, 2005	25	98.76	0.289		
48	Size	CAR206MMW8mag	May 27, 2005	25	98.99	0.281		
49	Size	CAR207MMW8mag	May 27, 2005	25	89.24	0.274		
50	Size	CAR207MMW8mag	May 27, 2005	25	90.53	0.273		
51	Size	CAR207MMW8mag	May 27, 2005	25	90.69	0.279		
52	Size	CAR212HMW8mag	May 27, 2005	25	101	0.288		
53	Size	CAR212HMW8mag	May 27, 2005	25	97.37	0.354		
54	Size	CAR212HMW8mag	May 27, 2005	25	97.06	0.363		
55	Size	CAR213HMW8mag	May 27, 2005	25	101	0.366		
56	Size	CAR213HMW8mag	May 27, 2005	25	101	0.382		
57	Size	CAR213HMW8mag	May 27, 2005	25	102.2	0.371		

All sample were prepared with emulsion evaporation method (SDS of 2 mg/ml), and with the three PLGA molecular weight used in this research.

Record	Type	Sample	Date	T (°C)	Z-Ave (nm)	PDI	ZP (mV)	Cond (mS/cm)
1	Size	car284	June 1, 2005	25	39.74	0.329		
2	Size	car284	June 1, 2005	25	41.02	0.285		
3	Size	car284	June 1, 2005	25	41.49	0.338		
4	Size	car285	June 1, 2005	25	36.79	0.271		
5	Size	car285	June 1, 2005	25	36.64	0.265		
6	Size	car285	June 1, 2005	25	35.83	0.252		

7	Size	car286	June 1, 2005	25	35.72	0.31		
8	Size	car286	June 1, 2005	25	35.26	0.314		
9	Size	car286	June 1, 2005	25	34.92	0.305		
10	Size	car287	June 1, 2005	25	33.74	0.328		
11	Size	car287	June 1, 2005	25	32.87	0.312		
12	Size	car287	June 1, 2005	25	32.13	0.287		
13	Size	car227	June 1, 2005	25	59.69	0.136		
14	Size	car227	June 1, 2005	25	59.28	0.13		
15	Size	car227	June 1, 2005	25	59.34	0.129		
16	Size	car228	June 1, 2005	25	58.51	0.128		
17	Size	car228	June 1, 2005	25	58.64	0.147		
18	Size	car228	June 1, 2005	25	58.8	0.126		
19	Size	car230	June 1, 2005	25	54.29	0.146		
20	Size	car230	June 1, 2005	25	54.66	0.156		
21	Size	car230	June 1, 2005	25	54.99	0.147		
22	Size	car231	June 1, 2005	25	56.23	0.157		
23	Size	car231	June 1, 2005	25	55.54	0.154		
24	Size	car231	June 1, 2005	25	56.38	0.136		
25	Size	car233	June 1, 2005	25	65.26	0.145		
26	Size	car233	June 1, 2005	25	66.01	0.143		
27	Size	car233	June 1, 2005	25	65.86	0.106		
28	Size	car234	June 1, 2005	25	64.64	0.13		
29	Size	car234	June 1, 2005	25	64.35	0.138		
30	Size	car234	June 1, 2005	25	64.62	0.098		
31	Size	car236	June 1, 2005	25	62.64	0.113		
32	Size	car236	June 1, 2005	25	61.84	0.123		
33	Size	car236	June 1, 2005	25	62	0.118		
34	Size	car237	June 1, 2005	25	62.67	0.108		
35	Size	car237	June 1, 2005	25	62.66	0.123		
36	Size	car237	June 1, 2005	25	62.81	0.119		
37	Zeta	CAR227	June 1, 2005	25			-42.25	0.05356
38	Zeta	CAR227	June 1, 2005	25			-39.85	0.04572
39	Zeta	CAR227	June 1, 2005	25			-48.49	0.04773
40	Zeta	CAR228	June 1, 2005	25			-26.31	0.04532
41	Zeta	CAR228	June 1, 2005	25			-32.21	0.05414
42	Zeta	CAR228	June 1, 2005	25			-40.24	0.05379
43	Zeta	CAR230	June 1, 2005	25			-38.04	0.05605
44	Zeta	CAR230	June 1, 2005	25			-46.52	0.05541
45	Zeta	CAR230	June 1, 2005	25			-33.7	0.04612
46	Zeta	CAR231	June 1, 2005	25			-39.71	0.0532
47	Zeta	CAR231	June 1, 2005	25			-30.69	0.05288
48	Zeta	CAR231	June 1, 2005	25			-40.24	0.04728
49	Zeta	CAR233	June 1, 2005	25			-37.77	0.05128
50	Zeta	CAR233	June 1, 2005	25			-37.49	0.04805
51	Zeta	CAR233	June 1, 2005	25			-34.04	0.04194
52	Zeta	CAR234	June 1, 2005	25			-41.83	0.05085
53	Zeta	CAR234	June 1, 2005	25			-37.96	0.05366
54	Zeta	CAR234	June 1, 2005	25			-40.49	0.05513
55	Zeta	CAR236	June 1, 2005	25			-44.75	0.04805
56	Zeta	CAR236	June 1, 2005	25			-43.62	0.05331

57	Zeta	CAR236	June 1, 2005	25	-41.81	0.04469
58	Zeta	CAR237	June 1, 2005	25	-40.27	0.04468
59	Zeta	CAR237	June 1, 2005	25	-30.79	0.05193
60	Zeta	CAR237	June 1, 2005	25	-44.99	0.05545

All sample were prepared with emulsion evaporation method (SDS of 2 mg/ml), and with the three PLGA molecular weight used in this research.

Record	Type	Sample Name	Date	T (°C)	Z-Ave (nm)	PDI	ZP (mV)	Cond (mS/cm)
1	Size	car305	June 3, 2005	25	42.45	0.245		
2	Size	car305	June 3, 2005	25	42.28	0.235		
3	Size	car305	June 3, 2005	25	41.65	0.219		
4	Size	car306	June 3, 2005	25	45.82	0.226		
5	Size	car306	June 3, 2005	25	46.19	0.227		
6	Size	car306	June 3, 2005	25	45.95	0.211		
7	Size	car307	June 3, 2005	25	50.31	0.214		
8	Size	car307	June 3, 2005	25	50.59	0.208		
9	Size	car307	June 3, 2005	25	50.33	0.206		
10	Size	car308	June 3, 2005	25	71.61	0.146		
11	Size	car308	June 3, 2005	25	71.68	0.16		
12	Size	car308	June 3, 2005	25	71.17	0.141		
13	Size	car220	June 3, 2005	25	50.43	0.43		
14	Size	car220	June 3, 2005	25	50.43	0.407		
15	Size	car220	June 3, 2005	25	50.6	0.381		
16	Size	car221	June 3, 2005	25	46.06	0.338		
17	Size	car221	June 3, 2005	25	45.73	0.338		
18	Size	car221	June 3, 2005	25	45.37	0.326		
19	Size	car222	June 3, 2005	25	54.98	0.4		
20	Size	car222	June 3, 2005	25	55.29	0.409		
21	Size	car222	June 3, 2005	25	54.93	0.404		
22	Size	car223	June 3, 2005	25	45.21	0.329		
23	Size	car223	June 3, 2005	25	45.2	0.326		
24	Size	car223	June 3, 2005	25	44.5	0.326		
25	Size	car224	June 3, 2005	25	48.13	0.363		
26	Size	car224	June 3, 2005	25	48.15	0.368		
27	Size	car224	June 3, 2005	25	47.93	0.36		
28	Size	car225	June 3, 2005	25	45.7	0.347		
29	Size	car225	June 3, 2005	25	44.92	0.337		
30	Size	car225	June 3, 2005	25	45.98	0.298		
31	Size	car278	June 3, 2005	25	85.09	0.239		
32	Size	car278	June 3, 2005	25	82.13	0.215		
33	Size	car278	June 3, 2005	25	83.19	0.232		
34	Size	car298	June 3, 2005	25	94.42	0.255		
35	Size	car298	June 3, 2005	25	97.01	0.27		
36	Size	car298	June 3, 2005	25	94.58	0.253		

37	Size	car246B	June 3, 2005	25	71.21	0.109		
38	Size	car246B	June 3, 2005	25	70.77	0.109		
39	Size	car246B	June 3, 2005	25	70.7	0.119		
40	Zeta	305	June 3, 2005	25			-22.79	0.04735
41	Zeta	305	June 3, 2005	25			-21.41	0.04462
42	Zeta	305	June 3, 2005	25			-30.68	0.04621
43	Zeta	306	June 3, 2005	25			-30.49	0.04179
44	Zeta	306	June 3, 2005	25			-33.5	0.04166
45	Zeta	306	June 3, 2005	25			-28.08	0.04476
46	Zeta	307	June 3, 2005	25			-34.34	0.04706
47	Zeta	307	June 3, 2005	25			-31.02	0.04254
48	Zeta	307	June 3, 2005	25			-38.75	0.04664
49	Zeta	308	June 3, 2005	25			-28.79	0.03723
50	Zeta	308	June 3, 2005	25			-28.87	0.04204
51	Zeta	308	June 3, 2005	25			-28.89	0.04493
52	Zeta	220	June 3, 2005	25			-29.28	0.05139
53	Zeta	220	June 3, 2005	25			-30.57	0.0493
54	Zeta	220	June 3, 2005	25			-29.12	0.05355
55	Zeta	221	June 3, 2005	25			-43.6	0.05563
56	Zeta	221	June 3, 2005	25			-36.31	0.05485
57	Zeta	221	June 3, 2005	25			-32.76	0.04848
58	Zeta	221	June 3, 2005	25			-37.38	0.05555
59	Zeta	221	June 3, 2005	25			-45.27	0.05616
60	Zeta	221	June 3, 2005	25			-47.66	0.05769
61	Zeta	car222	June 3, 2005	25			-28.31	0.05764
62	Zeta	car222	June 3, 2005	25			-31.09	0.0509
63	Zeta	car222	June 3, 2005	25			-32.73	0.05893
64	Zeta	car224	June 3, 2005	25			-41.64	0.06209
65	Zeta	car224	June 3, 2005	25			-38.75	0.05962
66	Zeta	car224	June 3, 2005	25			-36.83	0.05459
67	Zeta	car225	June 3, 2005	25			-33.29	0.0526
68	Zeta	car225	June 3, 2005	25			-35.63	0.05361
69	Zeta	car225	June 3, 2005	25			-31.65	0.06025
70	Zeta	car278	June 3, 2005	25			-39.8	0.05376
71	Zeta	car278	June 3, 2005	25			-37.75	0.05196
72	Zeta	car278	June 3, 2005	25			-37.74	0.04382
73	Zeta	car298	June 3, 2005	25			-40.16	0.04919
74	Zeta	car298	June 3, 2005	25			-42.54	0.04754
75	Zeta	car298	June 3, 2005	25			-41.52	0.05034
76	Zeta	car246B	June 3, 2005	25			-41.94	0.06332
77	Zeta	car246B	June 3, 2005	25			-42.72	0.06383
78	Zeta	car246B	June 3, 2005	25			-37.01	0.06173
79	Zeta	car290	June 3, 2005	25			-39.09	0.05605
80	Zeta	car290	June 3, 2005	25			-40.2	0.05033
81	Zeta	car290	June 3, 2005	25			-37.92	0.04803
82	Zeta	car291	June 3, 2005	25			-35.57	0.04945
83	Zeta	car291	June 3, 2005	25			-36.68	0.0434
84	Zeta	car291	June 3, 2005	25			-36.67	0.04517
85	Zeta	car292	June 3, 2005	25			-41.85	0.04898
86	Zeta	car292	June 3, 2005	25			-39.76	0.04906

87	Zeta	car292	June 3, 2005	25	-42.32	0.04582
88	Zeta	car294	June 3, 2005	25	-36.1	0.05677
89	Zeta	car294	June 3, 2005	25	-35.98	0.05735
90	Zeta	car294	June 3, 2005	25	-41.99	0.05419
91	Zeta	car295	June 3, 2005	25	-36.26	0.04908
92	Zeta	car295	June 3, 2005	25	-36.45	0.05581
93	Zeta	car295	June 3, 2005	25	-34.19	0.04544
94	Zeta	car281	June 3, 2005	25	-16.26	0.05288
95	Zeta	car281	June 3, 2005	25	-22.89	0.05259
96	Zeta	car281	June 3, 2005	25	-27.3	0.05847
97	Zeta	car284	June 3, 2005	25	-46.72	0.05927
98	Zeta	car284	June 3, 2005	25	-48.39	0.06012
99	Zeta	car284	June 3, 2005	25	-47.27	0.06056
100	Zeta	car297	June 3, 2005	25	-39.78	0.06191
101	Zeta	car297	June 3, 2005	25	-39.57	0.0657
102	Zeta	car297	June 3, 2005	25	-35.74	0.06543
103	Zeta	car267D	June 3, 2005	25	-21	0.01114
104	Zeta	car267D	June 3, 2005	25	-22.63	0.03553
105	Zeta	car267D	June 3, 2005	25	-22.16	0.03242
106	Zeta	car285	June 3, 2005	25	-22.37	0.05831
107	Zeta	car285	June 3, 2005	25	-21.55	0.05001
108	Zeta	car285	June 3, 2005	25	-19.88	0.05926
109	Zeta	car286	June 3, 2005	25	-20.47	0.07439
110	Zeta	car286	June 3, 2005	25	-21.63	0.0766
111	Zeta	car286	June 3, 2005	25	-33.98	0.0734
112	Zeta	car287	June 3, 2005	25	-28.58	0.07888
113	Zeta	car287	June 3, 2005	25	-15.81	0.07966
114	Zeta	car287	June 3, 2005	25	-23.97	0.08622

All sample were prepared with emulsion evaporation method (SDS of 2 mg/ml), and with the three PLGA molecular weight used in this research. The symbol D in the samples name means after dialysis.

Record	Type	Sample Name	Date	T (°C)	Z-Ave (nm)	PDI	ZP (mV)	Cond (mS/cm)
1	Size	car309	June 7, 2005	25	46.32	0.22		
2	Size	car309	June 7, 2005	25	46.99	0.223		
3	Size	car309	June 7, 2005	25	47	0.229		
4	Size	car310	June 7, 2005	25	38.39	0.239		
5	Size	car310	June 7, 2005	25	38.38	0.249		
6	Size	car310	June 7, 2005	25	38.49	0.251		
7	Size	car311	June 7, 2005	25	41.53	0.242		
8	Size	car311	June 7, 2005	25	41.48	0.239		
9	Size	car311	June 7, 2005	25	41.82	0.225		
10	Size	car312	June 7, 2005	25	52.67	0.199		
11	Size	car312	June 7, 2005	25	52.38	0.213		
12	Size	car312	June 7, 2005	25	52.95	0.196		

13	Size	car310B	June 7, 2005	25	38.26	0.243
14	Size	car310B	June 7, 2005	25	38.52	0.242
15	Size	car310B	June 7, 2005	25	38.45	0.236
16	Size	car295B	June 7, 2005	25	98.2	0.269
17	Size	car295B	June 7, 2005	25	98.71	0.274
18	Size	car295B	June 7, 2005	25	96.59	0.238
19	Size	car322	June 7, 2005	25	80.42	0.257
20	Size	car322	June 7, 2005	25	81.54	0.268
21	Size	car322	June 7, 2005	25	81.39	0.287
22	Size	car323	June 7, 2005	25	81.14	0.254
23	Size	car323	June 7, 2005	25	79.85	0.227
24	Size	car323	June 7, 2005	25	79.63	0.212
25	Size	car227	June 7, 2005	25	65.8	0.212
26	Size	car227	June 7, 2005	25	65.6	0.209
27	Size	car227	June 7, 2005	25	65.02	0.215
28	Size	car292	June 7, 2005	25	119.4	0.252
29	Size	car292	June 7, 2005	25	120.1	0.248
30	Size	car292	June 7, 2005	25	119.2	0.255
31	Size	car291	June 7, 2005	25	116.8	0.237
32	Size	car291	June 7, 2005	25	118.2	0.262
33	Size	car291	June 7, 2005	25	116.9	0.252
34	Size	car271	June 7, 2005	25	105.3	0.291
35	Size	car271	June 7, 2005	25	104.9	0.287
36	Size	car271	June 7, 2005	25	104.8	0.296
37	Size	car270	June 7, 2005	25	107.3	0.291
38	Size	car270	June 7, 2005	25	106.4	0.28
39	Size	car270	June 7, 2005	25	106.8	0.276
40	Size	car293	June 7, 2005	25	96.1	0.216
41	Size	car293	June 7, 2005	25	96.24	0.19
42	Size	car293	June 7, 2005	25	94.16	0.213
43	Size	car236D	June 7, 2005	25	68.75	0.119
44	Size	car236D	June 7, 2005	25	68.51	0.115
45	Size	car236D	June 7, 2005	25	68.8	0.095
46	Size	car294D	June 7, 2005	25	95.97	0.213
47	Size	car294D	June 7, 2005	25	96.29	0.198
48	Size	car294D	June 7, 2005	25	94.67	0.211
49	Size	car274D	June 7, 2005	25	87.45	0.198
50	Size	car274D	June 7, 2005	25	87.02	0.187
51	Size	car274D	June 7, 2005	25	85.13	0.207
52	Size	car297	June 7, 2005	25	87.44	0.193
53	Size	car297	June 7, 2005	25	86.63	0.193
54	Size	car297	June 7, 2005	25	87.34	0.197
55	Size	car226D	June 7, 2005	25	67.08	0.15
56	Size	car226D	June 7, 2005	25	67.89	0.119
57	Size	car226D	June 7, 2005	25	67.55	0.103
58	Size	car290D	June 7, 2005	25	111.4	0.247
59	Size	car290D	June 7, 2005	25	111.9	0.256
60	Size	car290D	June 7, 2005	25	113.6	0.241
61	Size	car276D	June 7, 2005	25	81.97	0.177
62	Size	car276D	June 7, 2005	25	81.43	0.197

63	Size	car276D	June 7, 2005	25	81.94	0.192		
64	Size	car244D	June 7, 2005	25	75.07	0.115		
65	Size	car244D	June 7, 2005	25	75.11	0.104		
66	Size	car244D	June 7, 2005	25	75.16	0.123		
67	Size	car240D	June 7, 2005	25	50.51	0.31		
68	Size	car240D	June 7, 2005	25	50.85	0.269		
69	Size	car240D	June 7, 2005	25	50.55	0.276		
70	Size	car277D	June 7, 2005	25	80.06	0.194		
71	Size	car277D	June 7, 2005	25	79.45	0.18		
72	Size	car277D	June 7, 2005	25	78.07	0.187		
73	Size	car243D	June 7, 2005	25	70.89	0.183		
74	Size	car243D	June 7, 2005	25	70.18	0.176		
75	Size	car243D	June 7, 2005	25	70.6	0.17		
76	Zeta	car295B	June 7, 2005	25			-44.34	0.05961
77	Zeta	car295B	June 7, 2005	25			-44.42	0.05544
78	Zeta	car295B	June 7, 2005	25			-45.08	0.05587
79	Zeta	car323	June 7, 2005	25			-41.11	0.04982
80	Zeta	car323	June 7, 2005	25			-39.99	0.04692
81	Zeta	car323	June 7, 2005	25			-36.61	0.05343
82	Zeta	car227D	June 7, 2005	25			-38.45	0.01142
83	Zeta	car227D	June 7, 2005	25			-36.13	0.03206
84	Zeta	car227D	June 7, 2005	25			-30.63	0.03136
85	Zeta	car292D	June 7, 2005	25			-30.87	0.0338
86	Zeta	car292D	June 7, 2005	25			-32.12	0.03201
87	Zeta	car292D	June 7, 2005	25			-32.89	0.03613
88	Zeta	car271D	June 7, 2005	25			-35.94	0.0408
89	Zeta	car271D	June 7, 2005	25			-45.65	0.0403
90	Zeta	car271D	June 7, 2005	25			-31.3	0.03191
91	Zeta	car240D	June 7, 2005	25			-38.86	0.01368
92	Zeta	car240D	June 7, 2005	25			-24.2	0.02971
93	Zeta	car240D	June 7, 2005	25			-26.85	0.02055
94	Zeta	car243D	June 7, 2005	25			-41.66	0.03599
95	Zeta	car243D	June 7, 2005	25			-48.75	0.0348
96	Zeta	car243D	June 7, 2005	25			-38.25	0.03574
97	Zeta	car226D	June 7, 2005	25			-29.73	0.0322
98	Zeta	car226D	June 7, 2005	25			-29.31	0.03894
99	Zeta	car226D	June 7, 2005	25			-32.48	0.02884
100	Zeta	car310	June 7, 2005	25			-45.63	0.1611
101	Zeta	car310	June 7, 2005	25			-43.63	0.1635
102	Zeta	car310	June 7, 2005	25			-46.17	0.168
103	Zeta	car312	June 7, 2005	25			-39.38	0.05628
104	Zeta	car312	June 7, 2005	25			-36.82	0.05124
105	Zeta	car312	June 7, 2005	25			-37.6	0.04674
106	Zeta	car249D	June 7, 2005	25			-39.44	0.02625
107	Zeta	car249D	June 7, 2005	25			-40.31	0.03019
108	Zeta	car249D	June 7, 2005	25			-42.8	0.02894
109	Zeta	car277D	June 7, 2005	25			-41.84	0.06295
110	Zeta	car277D	June 7, 2005	25			-33.74	0.05501
111	Zeta	car277D	June 7, 2005	25			-38.54	0.05573

All sample were prepared with emulsion evaporation method (SDS of 2 mg/ml), and with the three PLGA molecular weight used in this research. The amplitude used was 39%. The evaporation time was 7 min. The amount of MOA was 4% w/w and 8%w/w.

Record	Type	Sample	Date	T (℃)	Z-Ave (nm)	PDI	ZP (mV)	Cond (mS/cm)
1	Size	CA64	July 5, 2005	25	38.81	0.233		
2	Size	CA64	July 5, 2005	25	39.01	0.212		
3	Size	CA64	July 5, 2005	25	38.86	0.214		
4	Size	CA65	July 5, 2005	25	38.47	0.226		
5	Size	CA65	July 5, 2005	25	38.62	0.245		
6	Size	CA65	July 5, 2005	25	38.61	0.23		
7	Size	CA66	July 5, 2005	25	52.72	0.385		
8	Size	CA66	July 5, 2005	25	53.59	0.364		
9	Size	CA66	July 5, 2005	25	54.77	0.399		
10	Size	CA67	July 5, 2005	25	63.61	0.135		
11	Size	CA67	July 5, 2005	25	63.39	0.132		
12	Size	CA67	July 5, 2005	25	63.74	0.121		
13	Size	CA68	July 5, 2005	25	63.35	0.117		
14	Size	CA68	July 5, 2005	25	63.05	0.118		
15	Size	CA68	July 5, 2005	25	62.91	0.148		
16	Size	CA69	July 5, 2005	25	63.55	0.119		
17	Size	CA69	July 5, 2005	25	62.94	0.126		
18	Size	CA69	July 5, 2005	25	62.92	0.124		
19	Size	CA70	July 5, 2005	25	66.06	0.13		
20	Size	CA70	July 5, 2005	25	66.58	0.117		
21	Size	CA70	July 5, 2005	25	66.75	0.128		
22	Size	CA71	July 5, 2005	25	67.65	0.125		
23	Size	CA71	July 5, 2005	25	67.27	0.118		
24	Size	CA71	July 5, 2005	25	66.87	0.127		
25	Size	CA72	July 5, 2005	25	68.05	0.156		
26	Size	CA72	July 5, 2005	25	66.95	0.13		
27	Size	CA72	July 5, 2005	25	67.47	0.111		
28	Size	CAR324B	July 5, 2005	25	83.27	0.169		
29	Size	CAR324B	July 5, 2005	25	84.46	0.165		
30	Size	CAR324B	July 5, 2005	25	84.95	0.204		
31	Size	CAR324Bd	July 5, 2005	25	76.41	0.17		
32	Size	CAR324Bd	July 5, 2005	25	76.97	0.164		
33	Size	CAR324Bd	July 5, 2005	25	76.41	0.154		
34	Size	CAR325B	July 5, 2005	25	92.94	0.168		
35	Size	CAR325B	July 5, 2005	25	92.32	0.203		
36	Size	CAR325B	July 5, 2005	25	90.89	0.183		
37	Size	CAR325Bd	July 5, 2005	25	87.11	0.21		
38	Size	CAR325Bd	July 5, 2005	25	86.32	0.207		
39	Size	CAR325Bd	July 5, 2005	25	85.56	0.202		
40	Zeta	CA64	July 5, 2005	25			-12.91	0.06245

41	Zeta	CA64	July 5, 2005	25	-9.807	0.06122
42	Zeta	CA64	July 5, 2005	25	-23.13	0.06295
43	Zeta	CA65	July 5, 2005	25	-20.57	0.05185
44	Zeta	CA65	July 5, 2005	25	-15.61	0.0536
45	Zeta	CA65	July 5, 2005	25	-18.51	0.05874
46	Zeta	CA66	July 5, 2005	25	-21.27	0.05534
47	Zeta	CA66	July 5, 2005	25	-25.83	0.05911
48	Zeta	CA66	July 5, 2005	25	-25.59	0.06282
49	Zeta	CA67	July 5, 2005	25	-25.64	0.06076
50	Zeta	CA67	July 5, 2005	25	-18.51	0.05591
51	Zeta	CA67	July 5, 2005	25	-30.33	0.05918
52	Zeta	CA68	July 5, 2005	25	-21.49	0.05441
53	Zeta	CA68	July 5, 2005	25	-30.42	0.0583
54	Zeta	CA68	July 5, 2005	25	-30.31	0.05497
55	Zeta	CA69	July 5, 2005	25	-25.83	0.05436
56	Zeta	CA69	July 5, 2005	25	-26.66	0.05299
57	Zeta	CA69	July 5, 2005	25	-27.58	0.06211
58	Zeta	CA70	July 5, 2005	25	-33.42	0.06064
59	Zeta	CA70	July 5, 2005	25	-29.55	0.0613
60	Zeta	CA70	July 5, 2005	25	-24.87	0.06363
61	Zeta	CA71	July 5, 2005	25	-26.76	0.05636
62	Zeta	CA71	July 5, 2005	25	-22.09	0.05531
63	Zeta	CA71	July 5, 2005	25	-22.4	0.06397
64	Zeta	CA72	July 5, 2005	25	-32.47	0.05571
65	Zeta	CA72	July 5, 2005	25	-27.75	0.06102
66	Zeta	CA72	July 5, 2005	25	-24.19	0.05908
67	Zeta	CAR324B	July 5, 2005	25	-34.2	0.04592
68	Zeta	CAR324B	July 5, 2005	25	-39.53	0.04942
69	Zeta	CAR324B	July 5, 2005	25	-38.91	0.04601
70	Zeta	CAR324Bd	July 5, 2005	25	-25.59	0.03581
71	Zeta	CAR324Bd	July 5, 2005	25	-24.94	0.03331
72	Zeta	CAR324Bd	July 5, 2005	25	-22.89	0.02498
73	Zeta	CAR325B	July 5, 2005	25	-40.11	0.04227
74	Zeta	CAR325B	July 5, 2005	25	-37.64	0.04801
75	Zeta	CAR325B	July 5, 2005	25	-38.79	0.03533
76	Zeta	CAR325Bd	July 5, 2005	25	-34.66	0.02218
77	Zeta	CAR325Bd	July 5, 2005	25	-22.75	0.03844
78	Zeta	CAR325Bd	July 5, 2005	25	-36.66	0.02003

All sample were prepared with emulsion evaporation method (SDS of 2 mg/ml), and with the three PLGA molecular weight used in this research. The amplitude used was 39%. The evaporation time was 7 min. The amount of MOA was 4% w/w and 8%w/w.

Record	Type	Sample	Date	T (°C)	Z-Ave (nm)	PDI	ZP (mV)	Cond (mS/cm)
1	Size	CA46	July 12, 2005	25	87.85	0.312		
2	Size	CA46	July 12, 2005	25	86.56	0.297		
3	Size	CA46	July 12, 2005	25	84.91	0.298		
4	Size	CA47	July 12, 2005	25	86.7	0.299		
5	Size	CA47	July 12, 2005	25	87.94	0.297		
6	Size	CA47	July 12, 2005	25	86.36	0.296		
7	Size	CA48	July 12, 2005	25	88.3	0.295		
8	Size	CA48	July 12, 2005	25	86.79	0.288		
9	Size	CA48	July 12, 2005	25	89.19	0.291		
10	Size	CA52	July 12, 2005	25	89.39	0.295		
11	Size	CA52	July 12, 2005	25	88.59	0.306		
12	Size	CA52	July 12, 2005	25	88.42	0.272		
13	Size	CA53	July 12, 2005	25	80.98	0.198		
14	Size	CA53	July 12, 2005	25	78.88	0.188		
15	Size	CA53	July 12, 2005	25	78.12	0.181		
16	Size	CA54	July 12, 2005	25	77.05	0.195		
17	Size	CA54	July 12, 2005	25	77.6	0.183		
18	Size	CA54	July 12, 2005	25	77.37	0.18		
19	Size	CA58	July 12, 2005	25	78.76	0.173		
20	Size	CA58	July 12, 2005	25	79.56	0.188		
21	Size	CA58	July 12, 2005	25	79.07	0.166		
22	Size	CA59	July 12, 2005	25	77.95	0.168		
23	Size	CA59	July 12, 2005	25	79.16	0.139		
24	Size	CA59	July 12, 2005	25	78.96	0.154		
25	Size	CA60	July 12, 2005	25	79.37	0.189		
26	Size	CA60	July 12, 2005	25	78.3	0.19		
27	Size	CA60	July 12, 2005	25	78.15	0.181		
28	Size	CA64	July 12, 2005	25	53.38	0.154		
29	Size	CA64	July 12, 2005	25	53.68	0.153		
30	Size	CA64	July 12, 2005	25	53.47	0.154		
31	Size	CA65	July 12, 2005	25	54.11	0.118		
32	Size	CA65	July 12, 2005	25	53.35	0.142		
33	Size	CA65	July 12, 2005	25	53.58	0.129		
34	Size	CA66	July 12, 2005	25	57.22	0.192		
35	Size	CA66	July 12, 2005	25	56.08	0.185		
36	Size	CA66	July 12, 2005	25	55.61	0.172		
37	Size	CA67AD	July 12, 2005	25	68.46	0.149		
38	Size	CA67AD	July 12, 2005	25	68.31	0.137		
39	Size	CA67AD	July 12, 2005	25	68.44	0.128		
40	Size	CA68AD	July 12, 2005	25	70.21	0.153		
41	Size	CA68AD	July 12, 2005	25	69.44	0.166		
42	Size	CA68AD	July 12, 2005	25	68.55	0.169		
43	Size	CA69AD	July 12, 2005	25	69.03	0.138		
44	Size	CA69AD	July 12, 2005	25	67.28	0.127		
45	Size	CA69AD	July 12, 2005	25	66.88	0.147		
46	Size	CA70AD	July 12, 2005	25	70.89	0.14		
47	Size	CA70AD	July 12, 2005	25	69.61	0.128		
48	Size	CA70AD	July 12, 2005	25	69.98	0.12		

49	Size	CA71AD	July 12, 2005	25	70.83	0.137		
50	Size	CA71AD	July 12, 2005	25	70.45	0.143		
51	Size	CA71AD	July 12, 2005	25	70.21	0.148		
52	Size	CA72AD	July 12, 2005	25	70.6	0.143		
53	Size	CA72AD	July 12, 2005	25	70.11	0.143		
54	Size	CA72AD	July 12, 2005	25	69.99	0.136		
55	Size	CA46AD	July 12, 2005	25	81.3	0.272		
56	Size	CA46AD	July 12, 2005	25	82.33	0.255		
57	Size	CA46AD	July 12, 2005	25	82.19	0.255		
58	Size	CA47AD	July 12, 2005	25	85.85	0.262		
59	Size	CA47AD	July 12, 2005	25	84.95	0.263		
60	Size	CA47AD	July 12, 2005	25	83.37	0.268		
61	Size	CA48AD	July 12, 2005	25	81.71	0.259		
62	Size	CA48AD	July 12, 2005	25	81.62	0.259		
63	Size	CA48AD	July 12, 2005	25	82.88	0.257		
64	Size	CA52AD	July 12, 2005	25	83.3	0.181		
65	Size	CA52AD	July 12, 2005	25	83.74	0.17		
66	Size	CA52AD	July 12, 2005	25	83.27	0.15		
67	Size	CA53AD	July 12, 2005	25	82.29	0.157		
68	Size	CA53AD	July 12, 2005	25	82.69	0.176		
69	Size	CA53AD	July 12, 2005	25	81.56	0.175		
70	Size	CA54AD	July 12, 2005	25	81.68	0.174		
71	Size	CA54AD	July 12, 2005	25	82.68	0.146		
72	Size	CA54AD	July 12, 2005	25	82.13	0.172		
73	Size	CA58AD	July 12, 2005	25	82.57	0.181		
74	Size	CA58AD	July 12, 2005	25	82.35	0.164		
75	Size	CA58AD	July 12, 2005	25	82.47	0.164		
76	Size	CA59AD	July 12, 2005	25	81.44	0.172		
77	Size	CA59AD	July 12, 2005	25	82.92	0.16		
78	Size	CA59AD	July 12, 2005	25	82.58	0.153		
79	Size	CA60AD	July 12, 2005	25	84.64	0.182		
80	Size	CA60AD	July 12, 2005	25	83.04	0.175		
81	Size	CA60AD	July 12, 2005	25	82.88	0.171		
82	Zeta	CA64AD	July 12, 2005	25			-29.52	0.03673
83	Zeta	CA64AD	July 12, 2005	25			-31.71	0.03312
84	Zeta	CA64AD	July 12, 2005	25			-33.99	0.02105
85	Zeta	CA65AD	July 12, 2005	25			-28.67	0.03486
86	Zeta	CA65AD	July 12, 2005	25			-25.85	0.02822
87	Zeta	CA65AD	July 12, 2005	25			-25.55	0.02596
88	Zeta	CA66AD	July 12, 2005	25			-41.61	0.01139
89	Zeta	CA66AD	July 12, 2005	25			-38.18	0.03504
90	Zeta	CA66AD	July 12, 2005	25			-43.41	0.03109
91	Zeta	CA67AD	July 12, 2005	25			-32.31	0.02989
92	Zeta	CA67AD	July 12, 2005	25			-32.16	0.01203
93	Zeta	CA67AD	July 12, 2005	25			-31.04	0.03462
94	Zeta	CA68AD	July 12, 2005	25			-34.72	0.0114
95	Zeta	CA68AD	July 12, 2005	25			-33.48	0.02884
96	Zeta	CA68AD	July 12, 2005	25			-36.98	0.03461
97	Zeta	CA69AD	July 12, 2005	25			-23.02	0.01207
98	Zeta	CA69AD	July 12, 2005	25			-29.77	0.02555

99	Zeta	CA69AD	July 12, 2005	25	-24.23	0.0297
100	Zeta	CA70AD	July 12, 2005	25	-25.97	0.03194
101	Zeta	CA70AD	July 12, 2005	25	-31.58	0.01207
102	Zeta	CA70AD	July 12, 2005	25	-33.4	0.01913
103	Zeta	CA71AD	July 12, 2005	25	-36.35	0.01369
104	Zeta	CA71AD	July 12, 2005	25	-39.24	0.02446
105	Zeta	CA71AD	July 12, 2005	25	-40.65	0.02406
106	Zeta	CA72AD	July 12, 2005	25	-34.67	0.03526
107	Zeta	CA72AD	July 12, 2005	25	-26.06	0.03188
108	Zeta	CA72AD	July 12, 2005	25	-33.2	0.01604
109	Zeta	CA46AD	July 12, 2005	25	-23.52	0.01603
110	Zeta	CA46AD	July 12, 2005	25	-24.21	0.0302
111	Zeta	CA46AD	July 12, 2005	25	-24.1	0.01675
112	Zeta	CA47AD	July 12, 2005	25	-43.38	0.03603
113	Zeta	CA47AD	July 12, 2005	25	-42.63	0.03764
114	Zeta	CA47AD	July 12, 2005	25	-43.82	0.02526

All sample were prepared with emulsion evaporation method (SDS of 2 mg/ml), and with the three PLGA molecular weight used in this research. The amplitude used was 39%. The evaporation time was 7 min. The amount of MOA was 4% w/w and 8%w/w.

Record	Type	Sample	Date	T (°C)	Z-Ave (nm)	PDI	ZP (mV)	Cond (mS/cm)
1	Size	CA49	July 15, 2005	24	118	0.309		
2	Size	CA49	July 15, 2005	24	115.2	0.365		
3	Size	CA49	July 15, 2005	24	115.3	0.297		
4	Size	CA50	July 15, 2005	24	113.6	0.342		
5	Size	CA50	July 15, 2005	24	114.8	0.367		
6	Size	CA50	July 15, 2005	24	115.7	0.304		
7	Size	CA51	July 15, 2005	24	115	0.306		
8	Size	CA51	July 15, 2005	24	114.3	0.298		
9	Size	CA51	July 15, 2005	24	113.8	0.296		
10	Size	CA49AD	July 15, 2005	24	106.7	0.285		
11	Size	CA49AD	July 15, 2005	24	106.9	0.277		
12	Size	CA49AD	July 15, 2005	24	106.2	0.286		
13	Size	CA50AD	July 15, 2005	24	113.9	0.291		
14	Size	CA50AD	July 15, 2005	24	112.2	0.295		
15	Size	CA50AD	July 15, 2005	24	111.6	0.291		
16	Size	CA51AD	July 15, 2005	24	107.7	0.296		
17	Size	CA51AD	July 15, 2005	24	104.4	0.302		
18	Size	CA51AD	July 15, 2005	24	105.6	0.288		
19	Size	CA55	July 15, 2005	24	92.62	0.23		
20	Size	CA55	July 15, 2005	24	91.51	0.242		
21	Size	CA55	July 15, 2005	24	91.91	0.241		
22	Size	CA56	July 15, 2005	24	92.61	0.265		
23	Size	CA56	July 15, 2005	24	92.29	0.25		

24	Size	CA56	July 15, 2005	24	92.18	0.239		
25	Size	CA57	July 15, 2005	24	94.65	0.259		
26	Size	CA57	July 15, 2005	24	94.7	0.257		
27	Size	CA57	July 15, 2005	24	94.32	0.257		
28	Size	CA55AD	July 15, 2005	24	96.65	0.249		
29	Size	CA55AD	July 15, 2005	24	95.45	0.224		
30	Size	CA55AD	July 15, 2005	24	93.38	0.234		
31	Size	CA56AD	July 15, 2005	24	97.31	0.242		
32	Size	CA56AD	July 15, 2005	24	93.97	0.236		
33	Size	CA56AD	July 15, 2005	24	94.27	0.219		
34	Size	CA57AD	July 15, 2005	24	97.76	0.257		
35	Size	CA57AD	July 15, 2005	24	97.17	0.246		
36	Size	CA57AD	July 15, 2005	24	96.12	0.231		
37	Size	CA61	July 15, 2005	24	111.2	0.251		
38	Size	CA61	July 15, 2005	24	111.3	0.257		
39	Size	CA61	July 15, 2005	24	111.5	0.254		
40	Size	CA62	July 15, 2005	24	102.1	0.258		
41	Size	CA62	July 15, 2005	24	102.1	0.262		
42	Size	CA62	July 15, 2005	24	101.4	0.255		
43	Size	CA63	July 15, 2005	24	110.9	0.267		
44	Size	CA63	July 15, 2005	24	108.6	0.256		
45	Size	CA63	July 15, 2005	24	107.2	0.263		
46	Size	CA61AD	July 15, 2005	24	110.1	0.228		
47	Size	CA61AD	July 15, 2005	24	109.1	0.25		
48	Size	CA61AD	July 15, 2005	24	108.7	0.239		
49	Size	CA62AD	July 15, 2005	24	105.3	0.248		
50	Size	CA62AD	July 15, 2005	24	105.2	0.255		
51	Size	CA62AD	July 15, 2005	24	102.7	0.244		
52	Size	CA63AD	July 15, 2005	24	110.6	0.259		
53	Size	CA63AD	July 15, 2005	24	112	0.246		
54	Size	CA63AD	July 15, 2005	24	112.9	0.245		
55	Size	CA63ADT	July 15, 2005	25	115.1	0.261		
56	Size	CA63ADT	July 15, 2005	25	115.6	0.258		
57	Size	CA63ADT	July 15, 2005	25	113.1	0.255		
58	Zeta	CA49	July 15, 2005	25			-28.87	0.04323
59	Zeta	CA49	July 15, 2005	25			-31.17	0.04672
60	Zeta	CA49	July 15, 2005	25			-34.76	0.04642
61	Zeta	CA50	July 15, 2005	25			-34.93	0.05304
62	Zeta	CA50	July 15, 2005	25			-36.48	0.05332
63	Zeta	CA50	July 15, 2005	25			-37.35	0.05282
64	Zeta	CA51	July 15, 2005	25			-40.45	0.04901
65	Zeta	CA51	July 15, 2005	25			-41.48	0.04936
66	Zeta	CA51	July 15, 2005	25			-39.01	0.05645
67	Zeta	CA49AD	July 15, 2005	25			-41.38	0.02754
68	Zeta	CA49AD	July 15, 2005	25			-43.95	0.03569
69	Zeta	CA49AD	July 15, 2005	25			-41.24	0.02272
70	Zeta	CA50AD	July 15, 2005	25			-34.82	0.0348
71	Zeta	CA50AD	July 15, 2005	25			-35.08	0.03603
72	Zeta	CA50AD	July 15, 2005	25			-34.41	0.01709
73	Zeta	CA51AD	July 15, 2005	25			-49.81	0.01232
74	Zeta	CA51AD	July 15, 2005	25			-49.2	0.0168
75	Zeta	CA51AD	July 15, 2005	25			-49.76	0.03254

76	Zeta	CA55	July 15, 2005	25	-29.59	0.04544
77	Zeta	CA55	July 15, 2005	25	-31.16	0.03277
78	Zeta	CA55	July 15, 2005	25	-30.48	0.0339
79	Zeta	CA56	July 15, 2005	25	-36.54	0.04697
80	Zeta	CA56	July 15, 2005	25	-33.83	0.03484
81	Zeta	CA56	July 15, 2005	25	-36.25	0.03411
82	Zeta	CA57	July 15, 2005	25	-35.92	0.04955
83	Zeta	CA57	July 15, 2005	25	-33.4	0.05804
84	Zeta	CA57	July 15, 2005	25	-39.5	0.05686
85	Zeta	CA55D	July 15, 2005	25	-42.79	0.03703
86	Zeta	CA55D	July 15, 2005	25	-44.05	0.01857
87	Zeta	CA55D	July 15, 2005	25	-48.3	0.03593
88	Zeta	CA56D	July 15, 2005	25	-52.03	0.03032
89	Zeta	CA56D	July 15, 2005	25	-51.25	0.02136
90	Zeta	CA56D	July 15, 2005	25	-57.2	0.01252
91	Zeta	CA57D	July 15, 2005	25	-37.83	0.01333
92	Zeta	CA57D	July 15, 2005	25	-39.23	0.03353
93	Zeta	CA57D	July 15, 2005	25	-38.38	0.01364
94	Zeta	CA61	July 15, 2005	25	-41.51	0.03602
95	Zeta	CA61	July 15, 2005	25	-37.65	0.0474
96	Zeta	CA61	July 15, 2005	25	-44.16	0.04636
97	Zeta	CA62	July 15, 2005	25	-34.9	0.04585
98	Zeta	CA62	July 15, 2005	25	-35.7	0.04746
99	Zeta	CA62	July 15, 2005	25	-36.08	0.04751
100	Zeta	CA63	July 15, 2005	25	-37.74	0.04386
101	Zeta	CA63	July 15, 2005	25	-35.24	0.04193
102	Zeta	CA63	July 15, 2005	25	-35.28	0.04543
103	Zeta	CA61d	July 15, 2005	25	-26.78	0.03368
104	Zeta	CA61d	July 15, 2005	25	-27.03	0.01376
105	Zeta	CA61d	July 15, 2005	25	-27.08	0.02994
106	Zeta	CA62d	July 15, 2005	25	-41.93	0.03316
107	Zeta	CA62d	July 15, 2005	25	-39.23	0.01798
108	Zeta	CA62d	July 15, 2005	25	-48.8	0.01908
109	Zeta	CA63d	July 15, 2005	25	-40.16	0.03061
110	Zeta	CA63d	July 15, 2005	25	-44.62	0.0335
111	Zeta	CA63d	July 15, 2005	25	-43.7	0.03591
112	Zeta	CA48d	July 15, 2005	25	-18.73	0.03706
113	Zeta	CA48d	July 15, 2005	25	-20.29	0.036
114	Zeta	CA48d	July 15, 2005	25	-22.26	0.03334
115	Zeta	CA52d	July 15, 2005	25	-29.83	0.02918
116	Zeta	CA52d	July 15, 2005	25	-31.95	0.01571
117	Zeta	CA52d	July 15, 2005	25	-29.56	0.01591
118	Zeta	CA53d	July 15, 2005	25	-34.32	0.03804
119	Zeta	CA53d	July 15, 2005	25	-32.85	0.03811
120	Zeta	CA53d	July 15, 2005	25	-35.72	0.03805
121	Zeta	CA54d	July 15, 2005	25	-31.29	0.03255
122	Zeta	CA54d	July 15, 2005	25	-24.45	0.01913
123	Zeta	CA54d	July 15, 2005	25	-27.42	0.03508
124	Zeta	CA58d	July 15, 2005	25	-28.33	0.01526
125	Zeta	CA58d	July 15, 2005	25	-21.29	0.01581
126	Zeta	CA58d	July 15, 2005	25	-29.2	0.03316
127	Zeta	CA59d	July 15, 2005	25	-33.44	0.0172

128	Zeta	CA59d	July 15, 2005	25	-31.54	0.02946
129	Zeta	CA59d	July 15, 2005	25	-29.23	0.03231
130	Zeta	CA60d	July 15, 2005	25	-26.36	0.03619
131	Zeta	CA60d	July 15, 2005	25	-21.51	0.01768
132	Zeta	CA60d	July 15, 2005	25	-22.77	0.02739
133	Zeta	CA46	July 15, 2005	25	-23.53	0.05858
134	Zeta	CA46	July 15, 2005	25	-26.56	0.06197
135	Zeta	CA46	July 15, 2005	25	-24.98	0.06733
136	Zeta	CA47	July 15, 2005	25	-26.51	0.05669
137	Zeta	CA47	July 15, 2005	25	-28.95	0.05978
138	Zeta	CA47	July 15, 2005	25	-27.72	0.05673
139	Zeta	CA48	July 15, 2005	25	-27.56	0.05657
140	Zeta	CA48	July 15, 2005	25	-36.56	0.06527
141	Zeta	CA48	July 15, 2005	25	-33.94	0.06606
142	Zeta	CA52	July 15, 2005	25	-28.73	0.06249
143	Zeta	CA52	July 15, 2005	25	-29.87	0.05929
144	Zeta	CA52	July 15, 2005	25	-31.98	0.05971
145	Zeta	CA53	July 15, 2005	25	-25.2	0.09448
146	Zeta	CA53	July 15, 2005	25	-26.15	0.09667
147	Zeta	CA53	July 15, 2005	25	-23.58	0.09639
148	Zeta	CA54	July 15, 2005	25	-25.46	0.05217
149	Zeta	CA54	July 15, 2005	25	-25.27	0.05263
150	Zeta	CA54	July 15, 2005	25	-25.78	0.05351
151	Zeta	CA58	July 15, 2005	25	-34.38	0.05817
152	Zeta	CA58	July 15, 2005	25	-32.91	0.05886
153	Zeta	CA58	July 15, 2005	25	-31.59	0.06233
154	Zeta	CA59	July 15, 2005	25	-38.18	0.07735
155	Zeta	CA59	July 15, 2005	25	-34.96	0.07765
156	Zeta	CA59	July 15, 2005	25	-34.03	0.078
157	Zeta	CA60	July 15, 2005	25	-31.96	0.05438
158	Zeta	CA60	July 15, 2005	25	-31.93	0.05455
159	Zeta	CA60	July 15, 2005	25	-32.56	0.0565

All sample were prepared with emulsion evaporation method (SDS of 2 mg/ml), and with the three PLGA molecular weight used in this research. The amplitude used was 39%. The evaporation time was 7 min. The amount of MOA was 4% w/w and 8%w/w.

Record	Type	Sample	Date	T (°C)	Z-Ave (nm)	PDI	ZP (mV)	Cond (mS/cm)
1	Size	CA66b	July 26, 2005	25	42.36	0.136		
2	Size	CA66b	July 26, 2005	25	36.85	0.247		
3	Size	CA66b	July 26, 2005	25	36.13	0.212		
4	Size	CA1	July 26, 2005	25	66.14	0.18		
5	Size	CA1	July 26, 2005	25	67.14	0.201		
6	Size	CA1	July 26, 2005	25	66.68	0.192		
7	Size	CA4	July 26, 2005	25	45.64	0.234		

8	Size	CA4	July 26, 2005	25	44.97	0.232		
9	Size	CA4	July 26, 2005	25	44.76	0.234		
10	Size	CA7	July 26, 2005	25	34.2	0.243		
11	Size	CA7	July 26, 2005	25	34.98	0.242		
12	Size	CA7	July 26, 2005	25	34.99	0.24		
13	Size	CA10	July 26, 2005	25	32.52	0.274		
14	Size	CA10	July 26, 2005	25	32.13	0.27		
15	Size	CA10	July 26, 2005	25	31.8	0.274		
16	Size	CA13	July 26, 2005	25	31.23	0.294		
17	Size	CA13	July 26, 2005	25	30.68	0.271		
18	Size	CA13	July 26, 2005	25	30.24	0.258		
19	Size	TCA1	July 26, 2005	25	87.18	0.218		
20	Size	TCA1	July 26, 2005	25	87.28	0.21		
21	Size	TCA1	July 26, 2005	25	85.15	0.211		
22	Size	TCA2	July 26, 2005	25	81.43	0.191		
23	Size	TCA2	July 26, 2005	25	79.26	0.195		
24	Size	TCA2	July 26, 2005	25	79.52	0.199		
25	Size	TCA3	July 26, 2005	25	95.33	0.391		
26	Size	TCA3	July 26, 2005	25	94.86	0.309		
27	Size	TCA3	July 26, 2005	25	94.08	0.391		
28	Size	CA62RS	July 26, 2005	25	872.2	0.703		
29	Size	CA62RS	July 26, 2005	25	850	0.683		
30	Size	CA62RS	July 26, 2005	25	937.3	0.764		
31	Size	CA62TRS	July 26, 2005	25	1036	0.666		
32	Size	CA62TRS	July 26, 2005	25	1165	0.673		
33	Size	CA62TRS	July 26, 2005	25	1239	0.805		
34	Size	CA65RS	July 26, 2005	25	976.5	0.779		
35	Size	CA65RS	July 26, 2005	25	801.5	0.661		
36	Size	CA65RS	July 26, 2005	25	429.9	0.641		
37	Size	CA65TRS	July 26, 2005	25	2103	1		
38	Size	CA65TRS	July 26, 2005	25	1363	0.848		
39	Size	CA65TRS	July 26, 2005	25	687	0.642		
40	Size	CA65RS2	July 26, 2005	25	981.8	0.757		
41	Size	CA65RS2	July 26, 2005	25	1011	0.789		
42	Size	CA65RS2	July 26, 2005	25	414.9	0.741		
43	Zeta	CA66b	July 26, 2005	25			-27.31	0.04447
44	Zeta	CA66b	July 26, 2005	25			-35.92	0.03059
45	Zeta	CA66b	July 26, 2005	25			-29.38	0.04481
46	Zeta	CA1	July 26, 2005	25			-32.02	0.02929
47	Zeta	CA1	July 26, 2005	25			-28.15	0.03035
48	Zeta	CA1	July 26, 2005	25			-35.93	0.01985
49	Zeta	CA4	July 26, 2005	25			-27.53	0.02218
50	Zeta	CA4	July 26, 2005	25			-29.69	0.02354
51	Zeta	CA4	July 26, 2005	25			-22.71	0.04021
52	Zeta	CA7	July 26, 2005	25			-38.59	0.03356
53	Zeta	CA7	July 26, 2005	25			-48.12	0.04156
54	Zeta	CA7	July 26, 2005	25			-38.45	0.04042
55	Zeta	CA10	July 26, 2005	25			-36.28	0.03359
56	Zeta	CA10	July 26, 2005	25			-30.14	0.04715
57	Zeta	CA10	July 26, 2005	25			-48.55	0.03741

58	Zeta	CA13	July 26, 2005	25	-32.16	0.05517
59	Zeta	CA13	July 26, 2005	25	-27.43	0.0535
60	Zeta	CA13	July 26, 2005	25	-30.97	0.05652
61	Zeta	TCA1	July 26, 2005	25	-24.26	0.03499
62	Zeta	TCA1	July 26, 2005	25	-23.23	0.04819
63	Zeta	TCA1	July 26, 2005	25	-24.41	0.0491
64	Zeta	TCA2	July 26, 2005	25	-22.07	0.03822
65	Zeta	TCA2	July 26, 2005	25	-21.93	0.03767
66	Zeta	TCA2	July 26, 2005	25	-22.34	0.04373
67	Zeta	TCA3	July 26, 2005	25	-23.85	0.04753
68	Zeta	TCA3	July 26, 2005	25	-22.39	0.03561
69	Zeta	TCA3	July 26, 2005	25	-23.49	0.03684
70	Zeta	CA62RS	July 26, 2005	25	-41.4	0.02966
71	Zeta	CA62RS	July 26, 2005	25	-41.5	0.02326
72	Zeta	CA62RS	July 26, 2005	25	-37.58	0.02265
73	Zeta	CA62TRS	July 26, 2005	25	-43.33	0.02563
74	Zeta	CA62TRS	July 26, 2005	25	-47.49	0.0171
75	Zeta	CA62TRS	July 26, 2005	25	-48.52	0.03385
76	Zeta	CA65RS	July 26, 2005	25	-32.12	0.02134
77	Zeta	CA65RS	July 26, 2005	25	-35.79	0.03574
78	Zeta	CA65RS	July 26, 2005	25	-37.82	0.03545
79	Zeta	CA65TRS	July 26, 2005	25	-50.64	0.02522
80	Zeta	CA65TRS	July 26, 2005	25	-48.32	0.01853
81	Zeta	CA65TRS	July 26, 2005	25	-64.5	0.03354

APPENDIX D. STATISTICS ANALYSIS OF DATA

Analysis by SAS software using proc mixed procedure ($\alpha = 0.05$). The results showed the effect of active component (AC), PLGA molecular weight (MW), and dialysis (Dys) in nanoparticle size is significant.

Randomize complete design (one-way anova)
Effect of PLGA molecular weight, MOA, and dialysis in Np size
List of Data **SIN GROUP DIALSYSIS**

Obs	Size	Dys	AC	MW	Rep
1	38.9	1	1	1	1
2	38.6	1	1	1	2
3	38.4	1	1	1	3
4	63.6	1	1	2	1
5	63.1	1	1	2	2
6	63.1	1	1	2	3
7	66.5	1	1	3	1
8	67.3	1	1	3	2
9	67.5	1	1	3	3
10	86.4	1	2	1	1
11	87.0	1	2	1	2
12	88.1	1	2	1	3
13	88.8	1	2	2	1
14	79.3	1	2	2	2
15	77.3	1	2	2	3
16	79.1	1	2	3	1
17	78.7	1	2	3	2
18	78.6	1	2	3	3
19	116.2	1	3	1	1
20	114.7	1	3	1	2
21	114.4	1	3	1	3
22	92.0	1	3	2	1
23	92.4	1	3	2	2
24	94.6	1	3	2	3
25	111.3	1	3	3	1
26	101.9	1	3	3	2
27	108.9	1	3	3	3
28	53.5	2	1	1	1
29	53.7	2	1	1	2
30	56.3	2	1	1	3
31	68.4	2	1	2	1
32	69.4	2	1	2	2
33	67.7	2	1	2	3
34	70.2	2	1	3	1
35	70.5	2	1	3	2
36	70.2	2	1	3	3
37	81.9	2	2	1	1
38	84.7	2	2	1	2
39	82.1	2	2	1	3
40	88.8	2	2	2	1
41	82.2	2	2	2	2
42	82.2	2	2	2	3
43	82.5	2	2	3	1
44	82.3	2	2	3	2
45	83.5	2	2	3	3
46	106.6	2	3	1	1

47	112.6	2	3	1	2
48	105.9	2	3	1	3
49	95.2	2	3	2	1
50	95.2	2	3	2	2
51	97.0	2	3	2	3
52	109.3	2	3	3	1
53	104.4	2	3	3	2
54	111.8	2	3	3	3

Randomize complete design (one-way anova)
effect of PLGA molecular weight, MOA, and dialysis in Np size
CRD with proc mixed **SIN GROUP DIALSYSIS**

The Mixed Procedure

Model Information

Data Set	WORK.NANOPARTICLES
Dependent Variable	Size
Covariance Structure	Variance Components
Estimation Method	REML
Residual Variance Method	Profile
Fixed Effects SE Method	Model-Based
Degrees of Freedom Method	Containment

Class Level Information

Class	Levels	Values
AC	3	1 2 3
MW	3	1 2 3
Dys	2	1 2
Rep	3	1 2 3

Dimensions

Covariance Parameters	2
Columns in X	48
Columns in Z	27
Subjects	1
Max Obs Per Subject	54

Number of Observations

Number of Observations Read	54
Number of Observations Used	54
Number of Observations Not Used	0

Iteration History

Iteration	Evaluations	-2 Res Log Like	Criterion
0	1	188.74031456	
1	1	178.18514374	0.00000000

Convergence criteria met.

Covariance Parameter Estimates

Cov Parm	Estimate
Rep(AC*MW)	4.2600
Residual	2.1356

Fit Statistics

-2 Res Log Likelihood	178.2
AIC (smaller is better)	182.2
AICC (smaller is better)	182.5
BIC (smaller is better)	184.8

Type 3 Tests of Fixed Effects

Effect	Num DF	Den DF	F Value	Pr > F
AC	2	18	829.10	<.0001
MW	2	18	12.37	0.0004
AC*MW	4	18	59.33	<.0001
Dys	1	18	44.21	<.0001
AC*Dys	2	18	48.56	<.0001
MW*Dys	2	18	1.97	0.1684
AC*MW*Dys	4	18	31.21	<.0001

Least Squares Means

Effect	AC	MW	Dys	Estimate	Standard Error	DF	t Value	Pr > |t|
AC	1			60.3833	0.7694	18	78.48	<.0001
AC	2			82.9722	0.7694	18	107.84	<.0001
AC	3			104.69	0.7694	18	136.07	<.0001
MW		1		81.1111	0.7694	18	105.42	<.0001
MW		2		81.1278	0.7694	18	105.44	<.0001
MW		3		85.8056	0.7694	18	111.52	<.0001
AC*MW	1	1		46.5667	1.3326	18	34.94	<.0001
AC*MW	1	2		65.8833	1.3326	18	49.44	<.0001
AC*MW	1	3		68.7000	1.3326	18	51.55	<.0001
AC*MW	2	1		85.0333	1.3326	18	63.81	<.0001
AC*MW	2	2		83.1000	1.3326	18	62.36	<.0001
AC*MW	2	3		80.7833	1.3326	18	60.62	<.0001
AC*MW	3	1		111.73	1.3326	18	83.84	<.0001
AC*MW	3	2		94.4000	1.3326	18	70.84	<.0001
AC*MW	3	3		107.93	1.3326	18	80.99	<.0001
Dys			1	81.3593	0.4867	18	167.17	<.0001
Dys			2	84.0037	0.4867	18	172.60	<.0001
AC*Dys	1		1	56.3333	0.8430	18	66.83	<.0001
AC*Dys	1		2	64.4333	0.8430	18	76.44	<.0001
AC*Dys	2		1	82.5889	0.8430	18	97.97	<.0001
AC*Dys	2		2	83.3556	0.8430	18	98.88	<.0001
AC*Dys	3		1	105.16	0.8430	18	124.74	<.0001
AC*Dys	3		2	104.22	0.8430	18	123.64	<.0001
MW*Dys		1	1	80.3000	0.8430	18	95.26	<.0001
MW*Dys		1	2	81.9222	0.8430	18	97.18	<.0001
MW*Dys		2	1	79.3556	0.8430	18	94.14	<.0001
MW*Dys		2	2	82.9000	0.8430	18	98.34	<.0001
MW*Dys		3	1	84.4222	0.8430	18	100.15	<.0001
MW*Dys		3	2	87.1889	0.8430	18	103.43	<.0001

AC*MW*Dys	1	1	1	38.6333	1.4601	18	26.46	<.0001
AC*MW*Dys	1	1	2	54.5000	1.4601	18	37.33	<.0001
AC*MW*Dys	1	2	1	63.2667	1.4601	18	43.33	<.0001
AC*MW*Dys	1	2	2	68.5000	1.4601	18	46.92	<.0001
AC*MW*Dys	1	3	1	67.1000	1.4601	18	45.96	<.0001
AC*MW*Dys	1	3	2	70.3000	1.4601	18	48.15	<.0001
AC*MW*Dys	2	1	1	87.1667	1.4601	18	59.70	<.0001
AC*MW*Dys	2	1	2	82.9000	1.4601	18	56.78	<.0001
AC*MW*Dys	2	2	1	81.8000	1.4601	18	56.02	<.0001
AC*MW*Dys	2	2	2	84.4000	1.4601	18	57.80	<.0001
AC*MW*Dys	2	3	1	78.8000	1.4601	18	53.97	<.0001
AC*MW*Dys	2	3	2	82.7667	1.4601	18	56.69	<.0001
AC*MW*Dys	3	1	1	115.10	1.4601	18	78.83	<.0001
AC*MW*Dys	3	1	2	108.37	1.4601	18	74.22	<.0001
AC*MW*Dys	3	2	1	93.0000	1.4601	18	63.69	<.0001
AC*MW*Dys	3	2	2	95.8000	1.4601	18	65.61	<.0001
AC*MW*Dys	3	3	1	107.37	1.4601	18	73.53	<.0001
AC*MW*Dys	3	3	2	108.50	1.4601	18	74.31	<.0001

Differences of Least Squares Means

Effect	AC	MW	Dys	_AC	_MW	_Dys	Estimate	Standard Error	DF	t Value	Pr > |t|	Adjustment	Adj P
AC	1			2			-22.5889	1.0881	18	-20.76	<.0001	Tukey	<.0001
AC	1			3			-44.3056	1.0881	18	-40.72	<.0001	Tukey	<.0001
AC	2			3			-21.7167	1.0881	18	-19.96	<.0001	Tukey	<.0001
MW		1			2		-0.01667	1.0881	18	-0.02	0.9879	Tukey	0.9999
MW		1			3		-4.6944	1.0881	18	-4.31	0.0004	Tukey	0.0012
MW		2			3		-4.6778	1.0881	18	-4.30	0.0004	Tukey	0.0012
AC*MW	1	1		1	2		-19.3167	1.8846	18	-10.25	<.0001	Tukey	<.0001
AC*MW	1	1		1	3		-22.1333	1.8846	18	-11.74	<.0001	Tukey	<.0001
AC*MW	1	1		2	1		-38.4667	1.8846	18	-20.41	<.0001	Tukey	<.0001
AC*MW	1	1		2	2		-36.5333	1.8846	18	-19.38	<.0001	Tukey	<.0001
AC*MW	1	1		2	3		-34.2167	1.8846	18	-18.16	<.0001	Tukey	<.0001
AC*MW	1	1		3	1		-65.1667	1.8846	18	-34.58	<.0001	Tukey	<.0001
AC*MW	1	1		3	2		-47.8333	1.8846	18	-25.38	<.0001	Tukey	<.0001
AC*MW	1	1		3	3		-61.3667	1.8846	18	-32.56	<.0001	Tukey	<.0001
AC*MW	1	2		1	3		-2.8167	1.8846	18	-1.49	0.1524	Tukey	0.8442
AC*MW	1	2		2	1		-19.1500	1.8846	18	-10.16	<.0001	Tukey	<.0001
AC*MW	1	2		2	2		-17.2167	1.8846	18	-9.14	<.0001	Tukey	<.0001
AC*MW	1	2		2	3		-14.9000	1.8846	18	-7.91	<.0001	Tukey	<.0001
AC*MW	1	2		3	1		-45.8500	1.8846	18	-24.33	<.0001	Tukey	<.0001
AC*MW	1	2		3	2		-28.5167	1.8846	18	-15.13	<.0001	Tukey	<.0001
AC*MW	1	2		3	3		-42.0500	1.8846	18	-22.31	<.0001	Tukey	<.0001
AC*MW	1	3		2	1		-16.3333	1.8846	18	-8.67	<.0001	Tukey	<.0001
AC*MW	1	3		2	2		-14.4000	1.8846	18	-7.64	<.0001	Tukey	<.0001
AC*MW	1	3		2	3		-12.0833	1.8846	18	-6.41	<.0001	Tukey	0.0001
AC*MW	1	3		3	1		-43.0333	1.8846	18	-22.83	<.0001	Tukey	<.0001
AC*MW	1	3		3	2		-25.7000	1.8846	18	-13.64	<.0001	Tukey	<.0001
AC*MW	1	3		3	3		-39.2333	1.8846	18	-20.82	<.0001	Tukey	<.0001
AC*MW	2	1		2	2		1.9333	1.8846	18	1.03	0.3186	Tukey	0.9779
AC*MW	2	1		2	3		4.2500	1.8846	18	2.26	0.0368	Tukey	0.4145
AC*MW	2	1		3	1		-26.7000	1.8846	18	-14.17	<.0001	Tukey	<.0001
AC*MW	2	1		3	2		-9.3667	1.8846	18	-4.97	<.0001	Tukey	0.0025
AC*MW	2	1		3	3		-22.9000	1.8846	18	-12.15	<.0001	Tukey	<.0001
AC*MW	2	2		2	3		2.3167	1.8846	18	1.23	0.2348	Tukey	0.9390
AC*MW	2	2		3	1		-28.6333	1.8846	18	-15.19	<.0001	Tukey	<.0001
AC*MW	2	2		3	2		-11.3000	1.8846	18	-6.00	<.0001	Tukey	0.0003
AC*MW	2	2		3	3		-24.8333	1.8846	18	-13.18	<.0001	Tukey	<.0001
AC*MW	2	3		3	1		-30.9500	1.8846	18	-16.42	<.0001	Tukey	<.0001
AC*MW	2	3		3	2		-13.6167	1.8846	18	-7.23	<.0001	Tukey	<.0001
AC*MW	2	3		3	3		-27.1500	1.8846	18	-14.41	<.0001	Tukey	<.0001
AC*MW	3	1		3	2		17.3333	1.8846	18	9.20	<.0001	Tukey	<.0001
AC*MW	3	1		3	3		3.8000	1.8846	18	2.02	0.0589	Tukey	0.5519
AC*MW	3	2		3	3		-13.5333	1.8846	18	-7.18	<.0001	Tukey	<.0001
Dys			1			2	-2.6444	0.3977	18	-6.65	<.0001	Tukey-Kramer	<.0001
AC*Dys	1		1	1		2	-8.1000	0.6889	18	-11.76	<.0001	Tukey-Kramer	<.0001
AC*Dys	1		1	2		1	-26.2556	1.1922	18	-22.02	<.0001	Tukey-Kramer	<.0001

AC*Dys	1		1	2		2	-27.0222	1.1922	18	-22.67	<.0001	Tukey-Kramer	<.0001
AC*Dys	1		1	3		1	-48.8222	1.1922	18	-40.95	<.0001	Tukey-Kramer	<.0001
AC*Dys	1		1	3		2	-47.8889	1.1922	18	-40.17	<.0001	Tukey-Kramer	<.0001
AC*Dys	1		2	2		1	-18.1556	1.1922	18	-15.23	<.0001	Tukey-Kramer	<.0001
AC*Dys	1		2	2		2	-18.9222	1.1922	18	-15.87	<.0001	Tukey-Kramer	<.0001
AC*Dys	1		2	3		1	-40.7222	1.1922	18	-34.16	<.0001	Tukey-Kramer	<.0001
AC*Dys	1		2	3		2	-39.7889	1.1922	18	-33.38	<.0001	Tukey-Kramer	<.0001
AC*Dys	2		1	2		2	-0.7667	0.6889	18	-1.11	0.2804	Tukey-Kramer	0.8698
AC*Dys	2		1	3		1	-22.5667	1.1922	18	-18.93	<.0001	Tukey-Kramer	<.0001
AC*Dys	2		1	3		2	-21.6333	1.1922	18	-18.15	<.0001	Tukey-Kramer	<.0001
AC*Dys	2		2	3		1	-21.8000	1.1922	18	-18.29	<.0001	Tukey-Kramer	<.0001
AC*Dys	2		2	3		2	-20.8667	1.1922	18	-17.50	<.0001	Tukey-Kramer	<.0001
AC*Dys	3		1	3		2	0.9333	0.6889	18	1.35	0.1922	Tukey-Kramer	0.7518
MW*Dys		1	1		1	2	-1.6222	0.6889	18	-2.35	0.0301	Tukey-Kramer	0.2237
MW*Dys		1	1		2	1	0.9444	1.1922	18	0.79	0.4386	Tukey-Kramer	0.9653
MW*Dys		1	1		2	2	-2.6000	1.1922	18	-2.18	0.0427	Tukey-Kramer	0.2933
MW*Dys		1	1		3	1	-4.1222	1.1922	18	-3.46	0.0028	Tukey-Kramer	0.0285
MW*Dys		1	1		3	2	-6.8889	1.1922	18	-5.78	<.0001	Tukey-Kramer	0.0002
MW*Dys		1	2		2	1	2.5667	1.1922	18	2.15	0.0451	Tukey-Kramer	0.3057
MW*Dys		1	2		2	2	-0.9778	1.1922	18	-0.82	0.4228	Tukey-Kramer	0.9599
MW*Dys		1	2		3	1	-2.5000	1.1922	18	-2.10	0.0504	Tukey-Kramer	0.3317
MW*Dys		1	2		3	2	-5.2667	1.1922	18	-4.42	0.0003	Tukey-Kramer	0.0038
MW*Dys		2	1		2	2	-3.5444	0.6889	18	-5.15	<.0001	Tukey-Kramer	0.0008
MW*Dys		2	1		3	1	-5.0667	1.1922	18	-4.25	0.0005	Tukey-Kramer	0.0054
MW*Dys		2	1		3	2	-7.8333	1.1922	18	-6.57	<.0001	Tukey-Kramer	<.0001
MW*Dys		2	2		3	1	-1.5222	1.1922	18	-1.28	0.2179	Tukey-Kramer	0.7933
MW*Dys		2	2		3	2	-4.2889	1.1922	18	-3.60	0.0021	Tukey-Kramer	0.0214
MW*Dys		3	1		3	2	-2.7667	0.6889	18	-4.02	0.0008	Tukey-Kramer	0.0089
AC*MW*Dys	1	1	1	1	1	2	-15.8667	1.1932	18	-13.30	<.0001	Tukey-Kramer	<.0001
AC*MW*Dys	1	1	1	1	2	1	-24.6333	2.0649	18	-11.93	<.0001	Tukey-Kramer	<.0001
AC*MW*Dys	1	1	1	1	2	2	-29.8667	2.0649	18	-14.46	<.0001	Tukey-Kramer	<.0001
AC*MW*Dys	1	1	1	1	3	1	-28.4667	2.0649	18	-13.79	<.0001	Tukey-Kramer	<.0001
AC*MW*Dys	1	1	1	1	3	2	-31.6667	2.0649	18	-15.34	<.0001	Tukey-Kramer	<.0001
AC*MW*Dys	1	1	1	2	1	1	-48.5333	2.0649	18	-23.50	<.0001	Tukey-Kramer	<.0001
AC*MW*Dys	1	1	1	2	1	2	-44.2667	2.0649	18	-21.44	<.0001	Tukey-Kramer	<.0001
AC*MW*Dys	1	1	1	2	2	1	-43.1667	2.0649	18	-20.91	<.0001	Tukey-Kramer	<.0001
AC*MW*Dys	1	1	1	2	2	2	-45.7667	2.0649	18	-22.16	<.0001	Tukey-Kramer	<.0001
AC*MW*Dys	1	1	1	2	3	1	-40.1667	2.0649	18	-19.45	<.0001	Tukey-Kramer	<.0001
AC*MW*Dys	1	1	1	2	3	2	-44.1333	2.0649	18	-21.37	<.0001	Tukey-Kramer	<.0001
AC*MW*Dys	1	1	1	3	1	1	-76.4667	2.0649	18	-37.03	<.0001	Tukey-Kramer	<.0001
AC*MW*Dys	1	1	1	3	1	2	-69.7333	2.0649	18	-33.77	<.0001	Tukey-Kramer	<.0001
AC*MW*Dys	1	1	1	3	2	1	-54.3667	2.0649	18	-26.33	<.0001	Tukey-Kramer	<.0001
AC*MW*Dys	1	1	1	3	2	2	-57.1667	2.0649	18	-27.69	<.0001	Tukey-Kramer	<.0001
AC*MW*Dys	1	1	1	3	3	1	-68.7333	2.0649	18	-33.29	<.0001	Tukey-Kramer	<.0001
AC*MW*Dys	1	1	1	3	3	2	-69.8667	2.0649	18	-33.84	<.0001	Tukey-Kramer	<.0001
AC*MW*Dys	1	1	2	1	2	1	-8.7667	2.0649	18	-4.25	0.0005	Tukey-Kramer	0.0326
AC*MW*Dys	1	1	2	1	2	2	-14.0000	2.0649	18	-6.78	<.0001	Tukey-Kramer	0.0002
AC*MW*Dys	1	1	2	1	3	1	-12.6000	2.0649	18	-6.10	<.0001	Tukey-Kramer	0.0008
AC*MW*Dys	1	1	2	1	3	2	-15.8000	2.0649	18	-7.65	<.0001	Tukey-Kramer	<.0001
AC*MW*Dys	1	1	2	2	1	1	-32.6667	2.0649	18	-15.82	<.0001	Tukey-Kramer	<.0001
AC*MW*Dys	1	1	2	2	1	2	-28.4000	2.0649	18	-13.75	<.0001	Tukey-Kramer	<.0001

AC*MW*Dys	1	1	2	2	2	1	-27.3000	2.0649	18	-13.22	<.0001	Tukey-Kramer	<.0001
AC*MW*Dys	1	1	2	2	2	2	-29.9000	2.0649	18	-14.48	<.0001	Tukey-Kramer	<.0001
AC*MW*Dys	1	1	2	2	3	1	-24.3000	2.0649	18	-11.77	<.0001	Tukey-Kramer	<.0001
AC*MW*Dys	1	1	2	2	3	2	-28.2667	2.0649	18	-13.69	<.0001	Tukey-Kramer	<.0001
AC*MW*Dys	1	1	2	3	1	1	-60.6000	2.0649	18	-29.35	<.0001	Tukey-Kramer	<.0001
AC*MW*Dys	1	1	2	3	1	2	-53.8667	2.0649	18	-26.09	<.0001	Tukey-Kramer	<.0001
AC*MW*Dys	1	1	2	3	2	1	-38.5000	2.0649	18	-18.65	<.0001	Tukey-Kramer	<.0001
AC*MW*Dys	1	1	2	3	2	2	-41.3000	2.0649	18	-20.00	<.0001	Tukey-Kramer	<.0001
AC*MW*Dys	1	1	2	3	3	1	-52.8667	2.0649	18	-25.60	<.0001	Tukey-Kramer	<.0001
AC*MW*Dys	1	1	2	3	3	2	-54.0000	2.0649	18	-26.15	<.0001	Tukey-Kramer	<.0001
AC*MW*Dys	1	2	1	1	2	2	-5.2333	1.1932	18	-4.39	0.0004	Tukey-Kramer	0.0248
AC*MW*Dys	1	2	1	1	3	1	-3.8333	2.0649	18	-1.86	0.0798	Tukey-Kramer	0.8954
AC*MW*Dys	1	2	1	1	3	2	-7.0333	2.0649	18	-3.41	0.0031	Tukey-Kramer	0.1524
AC*MW*Dys	1	2	1	2	1	1	-23.9000	2.0649	18	-11.57	<.0001	Tukey-Kramer	<.0001
AC*MW*Dys	1	2	1	2	1	2	-19.6333	2.0649	18	-9.51	<.0001	Tukey-Kramer	<.0001
AC*MW*Dys	1	2	1	2	2	1	-18.5333	2.0649	18	-8.98	<.0001	Tukey-Kramer	<.0001

Randomize complete design (one-way anova)
effect of PLGA molecular weight, MOA, and dialysis in Np size
 CRD with proc mixed

The Mixed Procedure

Differences of Least Squares Means

Effect	AC	MW	Dys	_AC	_MW	_Dys	Estimate	Standard Error	DF	t Value	Pr > |t|	Adjustment	Adj P
AC*MW*Dys	1	2	1	2	2	2	-21.1333	2.0649	18	-10.23	<.0001	Tukey-Kramer	<.0001
AC*MW*Dys	1	2	1	2	3	1	-15.5333	2.0649	18	-7.52	<.0001	Tukey-Kramer	<.0001
AC*MW*Dys	1	2	1	2	3	2	-19.5000	2.0649	18	-9.44	<.0001	Tukey-Kramer	<.0001
AC*MW*Dys	1	2	1	3	1	1	-51.8333	2.0649	18	-25.10	<.0001	Tukey-Kramer	<.0001
AC*MW*Dys	1	2	1	3	1	2	-45.1000	2.0649	18	-21.84	<.0001	Tukey-Kramer	<.0001
AC*MW*Dys	1	2	1	3	2	1	-29.7333	2.0649	18	-14.40	<.0001	Tukey-Kramer	<.0001
AC*MW*Dys	1	2	1	3	2	2	-32.5333	2.0649	18	-15.76	<.0001	Tukey-Kramer	<.0001
AC*MW*Dys	1	2	1	3	3	1	-44.1000	2.0649	18	-21.36	<.0001	Tukey-Kramer	<.0001
AC*MW*Dys	1	2	1	3	3	2	-45.2333	2.0649	18	-21.91	<.0001	Tukey-Kramer	<.0001
AC*MW*Dys	1	2	2	1	3	1	1.4000	2.0649	18	0.68	0.5064	Tukey-Kramer	1.0000
AC*MW*Dys	1	2	2	1	3	2	-1.8000	2.0649	18	-0.87	0.3948	Tukey-Kramer	1.0000
AC*MW*Dys	1	2	2	2	1	1	-18.6667	2.0649	18	-9.04	<.0001	Tukey-Kramer	<.0001
AC*MW*Dys	1	2	2	2	1	2	-14.4000	2.0649	18	-6.97	<.0001	Tukey-Kramer	0.0002
AC*MW*Dys	1	2	2	2	2	1	-13.3000	2.0649	18	-6.44	<.0001	Tukey-Kramer	0.0004
AC*MW*Dys	1	2	2	2	2	2	-15.9000	2.0649	18	-7.70	<.0001	Tukey-Kramer	<.0001
AC*MW*Dys	1	2	2	2	3	1	-10.3000	2.0649	18	-4.99	<.0001	Tukey-Kramer	0.0075
AC*MW*Dys	1	2	2	2	3	2	-14.2667	2.0649	18	-6.91	<.0001	Tukey-Kramer	0.0002
AC*MW*Dys	1	2	2	3	1	1	-46.6000	2.0649	18	-22.57	<.0001	Tukey-Kramer	<.0001
AC*MW*Dys	1	2	2	3	1	2	-39.8667	2.0649	18	-19.31	<.0001	Tukey-Kramer	<.0001
AC*MW*Dys	1	2	2	3	2	1	-24.5000	2.0649	18	-11.87	<.0001	Tukey-Kramer	<.0001
AC*MW*Dys	1	2	2	3	2	2	-27.3000	2.0649	18	-13.22	<.0001	Tukey-Kramer	<.0001
AC*MW*Dys	1	2	2	3	3	1	-38.8667	2.0649	18	-18.82	<.0001	Tukey-Kramer	<.0001
AC*MW*Dys	1	2	2	3	3	2	-40.0000	2.0649	18	-19.37	<.0001	Tukey-Kramer	<.0001
AC*MW*Dys	1	3	1	1	3	2	-3.2000	1.1932	18	-2.68	0.0152	Tukey-Kramer	0.4501
AC*MW*Dys	1	3	1	2	1	1	-20.0667	2.0649	18	-9.72	<.0001	Tukey-Kramer	<.0001
AC*MW*Dys	1	3	1	2	1	2	-15.8000	2.0649	18	-7.65	<.0001	Tukey-Kramer	<.0001
AC*MW*Dys	1	3	1	2	2	1	-14.7000	2.0649	18	-7.12	<.0001	Tukey-Kramer	0.0001
AC*MW*Dys	1	3	1	2	2	2	-17.3000	2.0649	18	-8.38	<.0001	Tukey-Kramer	<.0001
AC*MW*Dys	1	3	1	2	3	1	-11.7000	2.0649	18	-5.67	<.0001	Tukey-Kramer	0.0020
AC*MW*Dys	1	3	1	2	3	2	-15.6667	2.0649	18	-7.59	<.0001	Tukey-Kramer	<.0001
AC*MW*Dys	1	3	1	3	1	1	-48.0000	2.0649	18	-23.25	<.0001	Tukey-Kramer	<.0001
AC*MW*Dys	1	3	1	3	1	2	-41.2667	2.0649	18	-19.99	<.0001	Tukey-Kramer	<.0001
AC*MW*Dys	1	3	1	3	2	1	-25.9000	2.0649	18	-12.54	<.0001	Tukey-Kramer	<.0001
AC*MW*Dys	1	3	1	3	2	2	-28.7000	2.0649	18	-13.90	<.0001	Tukey-Kramer	<.0001
AC*MW*Dys	1	3	1	3	3	1	-40.2667	2.0649	18	-19.50	<.0001	Tukey-Kramer	<.0001
AC*MW*Dys	1	3	1	3	3	2	-41.4000	2.0649	18	-20.05	<.0001	Tukey-Kramer	<.0001
AC*MW*Dys	1	3	2	2	1	1	-16.8667	2.0649	18	-8.17	<.0001	Tukey-Kramer	<.0001
AC*MW*Dys	1	3	2	2	1	2	-12.6000	2.0649	18	-6.10	<.0001	Tukey-Kramer	0.0008
AC*MW*Dys	1	3	2	2	2	1	-11.5000	2.0649	18	-5.57	<.0001	Tukey-Kramer	0.0024

AC*MW*Dys	1	3	2	2	2	2	-14.1000	2.0649	18	-6.83	<.0001	Tukey-Kramer	0.0002
AC*MW*Dys	1	3	2	2	3	1	-8.5000	2.0649	18	-4.12	0.0006	Tukey-Kramer	0.0418
AC*MW*Dys	1	3	2	2	3	2	-12.4667	2.0649	18	-6.04	<.0001	Tukey-Kramer	0.0010
AC*MW*Dys	1	3	2	3	1	1	-44.8000	2.0649	18	-21.70	<.0001	Tukey-Kramer	<.0001
AC*MW*Dys	1	3	2	3	1	2	-38.0667	2.0649	18	-18.44	<.0001	Tukey-Kramer	<.0001
AC*MW*Dys	1	3	2	3	2	1	-22.7000	2.0649	18	-10.99	<.0001	Tukey-Kramer	<.0001
AC*MW*Dys	1	3	2	3	2	2	-25.5000	2.0649	18	-12.35	<.0001	Tukey-Kramer	<.0001
AC*MW*Dys	1	3	2	3	3	1	-37.0667	2.0649	18	-17.95	<.0001	Tukey-Kramer	<.0001
AC*MW*Dys	1	3	2	3	3	2	-38.2000	2.0649	18	-18.50	<.0001	Tukey-Kramer	<.0001
AC*MW*Dys	2	1	1	2	1	2	4.2667	1.1932	18	3.58	0.0022	Tukey-Kramer	0.1135
AC*MW*Dys	2	1	1	2	2	1	5.3667	2.0649	18	2.60	0.0181	Tukey-Kramer	0.4972
AC*MW*Dys	2	1	1	2	2	2	2.7667	2.0649	18	1.34	0.1970	Tukey-Kramer	0.9927
AC*MW*Dys	2	1	1	2	3	1	8.3667	2.0649	18	4.05	0.0007	Tukey-Kramer	0.0472
AC*MW*Dys	2	1	1	2	3	2	4.4000	2.0649	18	2.13	0.0471	Tukey-Kramer	0.7707
AC*MW*Dys	2	1	1	3	1	1	-27.9333	2.0649	18	-13.53	<.0001	Tukey-Kramer	<.0001
AC*MW*Dys	2	1	1	3	1	2	-21.2000	2.0649	18	-10.27	<.0001	Tukey-Kramer	<.0001
AC*MW*Dys	2	1	1	3	2	1	-5.8333	2.0649	18	-2.83	0.0112	Tukey-Kramer	0.3738
AC*MW*Dys	2	1	1	3	2	2	-8.6333	2.0649	18	-4.18	0.0006	Tukey-Kramer	0.0369
AC*MW*Dys	2	1	1	3	3	1	-20.2000	2.0649	18	-9.78	<.0001	Tukey-Kramer	<.0001
AC*MW*Dys	2	1	1	3	3	2	-21.3333	2.0649	18	-10.33	<.0001	Tukey-Kramer	<.0001
AC*MW*Dys	2	1	2	2	2	1	1.1000	2.0649	18	0.53	0.6007	Tukey-Kramer	1.0000
AC*MW*Dys	2	1	2	2	2	2	-1.5000	2.0649	18	-0.73	0.4769	Tukey-Kramer	1.0000
AC*MW*Dys	2	1	2	2	3	1	4.1000	2.0649	18	1.99	0.0625	Tukey-Kramer	0.8426
AC*MW*Dys	2	1	2	2	3	2	0.1333	2.0649	18	0.06	0.9492	Tukey-Kramer	1.0000
AC*MW*Dys	2	1	2	3	1	1	-32.2000	2.0649	18	-15.59	<.0001	Tukey-Kramer	<.0001
AC*MW*Dys	2	1	2	3	1	2	-25.4667	2.0649	18	-12.33	<.0001	Tukey-Kramer	<.0001
AC*MW*Dys	2	1	2	3	2	1	-10.1000	2.0649	18	-4.89	0.0001	Tukey-Kramer	0.0091
AC*MW*Dys	2	1	2	3	2	2	-12.9000	2.0649	18	-6.25	<.0001	Tukey-Kramer	0.0006
AC*MW*Dys	2	1	2	3	3	1	-24.4667	2.0649	18	-11.85	<.0001	Tukey-Kramer	<.0001
AC*MW*Dys	2	1	2	3	3	2	-25.6000	2.0649	18	-12.40	<.0001	Tukey-Kramer	<.0001
AC*MW*Dys	2	2	1	2	2	2	-2.6000	1.1932	18	-2.18	0.0429	Tukey-Kramer	0.7445
AC*MW*Dys	2	2	1	2	3	1	3.0000	2.0649	18	1.45	0.1635	Tukey-Kramer	0.9843
AC*MW*Dys	2	2	1	2	3	2	-0.9667	2.0649	18	-0.47	0.6453	Tukey-Kramer	1.0000
AC*MW*Dys	2	2	1	3	1	1	-33.3000	2.0649	18	-16.13	<.0001	Tukey-Kramer	<.0001
AC*MW*Dys	2	2	1	3	1	2	-26.5667	2.0649	18	-12.87	<.0001	Tukey-Kramer	<.0001
AC*MW*Dys	2	2	1	3	2	1	-11.2000	2.0649	18	-5.42	<.0001	Tukey-Kramer	0.0032
AC*MW*Dys	2	2	1	3	2	2	-14.0000	2.0649	18	-6.78	<.0001	Tukey-Kramer	0.0002
AC*MW*Dys	2	2	1	3	3	1	-25.5667	2.0649	18	-12.38	<.0001	Tukey-Kramer	<.0001
AC*MW*Dys	2	2	1	3	3	2	-26.7000	2.0649	18	-12.93	<.0001	Tukey-Kramer	<.0001
AC*MW*Dys	2	2	2	2	3	1	5.6000	2.0649	18	2.71	0.0143	Tukey-Kramer	0.4334
AC*MW*Dys	2	2	2	2	3	2	1.6333	2.0649	18	0.79	0.4392	Tukey-Kramer	1.0000
AC*MW*Dys	2	2	2	3	1	1	-30.7000	2.0649	18	-14.87	<.0001	Tukey-Kramer	<.0001
AC*MW*Dys	2	2	2	3	1	2	-23.9667	2.0649	18	-11.61	<.0001	Tukey-Kramer	<.0001
AC*MW*Dys	2	2	2	3	2	1	-8.6000	2.0649	18	-4.16	0.0006	Tukey-Kramer	0.0380
AC*MW*Dys	2	2	2	3	2	2	-11.4000	2.0649	18	-5.52	<.0001	Tukey-Kramer	0.0026
AC*MW*Dys	2	2	2	3	3	1	-22.9667	2.0649	18	-11.12	<.0001	Tukey-Kramer	<.0001
AC*MW*Dys	2	2	2	3	3	2	-24.1000	2.0649	18	-11.67	<.0001	Tukey-Kramer	<.0001
AC*MW*Dys	2	3	1	2	3	2	-3.9667	1.1932	18	-3.32	0.0038	Tukey-Kramer	0.1749
AC*MW*Dys	2	3	1	3	1	1	-36.3000	2.0649	18	-17.58	<.0001	Tukey-Kramer	<.0001
AC*MW*Dys	2	3	1	3	1	2	-29.5667	2.0649	18	-14.32	<.0001	Tukey-Kramer	<.0001
AC*MW*Dys	2	3	1	3	2	1	-14.2000	2.0649	18	-6.88	<.0001	Tukey-Kramer	0.0002

AC*MW*Dys	2	3	1	3	2	2	-17.0000	2.0649	18	-8.23	<.0001	Tukey-Kramer	<.0001
AC*MW*Dys	2	3	1	3	3	1	-28.5667	2.0649	18	-13.83	<.0001	Tukey-Kramer	<.0001
AC*MW*Dys	2	3	1	3	3	2	-29.7000	2.0649	18	-14.38	<.0001	Tukey-Kramer	<.0001
AC*MW*Dys	2	3	2	3	1	1	-32.3333	2.0649	18	-15.66	<.0001	Tukey-Kramer	<.0001
AC*MW*Dys	2	3	2	3	1	2	-25.6000	2.0649	18	-12.40	<.0001	Tukey-Kramer	<.0001
AC*MW*Dys	2	3	2	3	2	1	-10.2333	2.0649	18	-4.96	0.0001	Tukey-Kramer	0.0080
AC*MW*Dys	2	3	2	3	2	2	-13.0333	2.0649	18	-6.31	<.0001	Tukey-Kramer	0.0006
AC*MW*Dys	2	3	2	3	3	1	-24.6000	2.0649	18	-11.91	<.0001	Tukey-Kramer	<.0001
AC*MW*Dys	2	3	2	3	3	2	-25.7333	2.0649	18	-12.46	<.0001	Tukey-Kramer	<.0001
AC*MW*Dys	3	1	1	3	1	2	6.7333	1.1932	18	5.64	<.0001	Tukey-Kramer	0.0021
AC*MW*Dys	3	1	1	3	2	1	22.1000	2.0649	18	10.70	<.0001	Tukey-Kramer	<.0001
AC*MW*Dys	3	1	1	3	2	2	19.3000	2.0649	18	9.35	<.0001	Tukey-Kramer	<.0001
AC*MW*Dys	3	1	1	3	3	1	7.7333	2.0649	18	3.75	0.0015	Tukey-Kramer	0.0837
AC*MW*Dys	3	1	1	3	3	2	6.6000	2.0649	18	3.20	0.0050	Tukey-Kramer	0.2156
AC*MW*Dys	3	1	2	3	2	1	15.3667	2.0649	18	7.44	<.0001	Tukey-Kramer	<.0001
AC*MW*Dys	3	1	2	3	2	2	12.5667	2.0649	18	6.09	<.0001	Tukey-Kramer	0.0009
AC*MW*Dys	3	1	2	3	3	1	1.0000	2.0649	18	0.48	0.6340	Tukey-Kramer	1.0000
AC*MW*Dys	3	1	2	3	3	2	-0.1333	2.0649	18	-0.06	0.9492	Tukey-Kramer	1.0000
AC*MW*Dys	3	2	1	3	2	2	-2.8000	1.1932	18	-2.35	0.0306	Tukey-Kramer	0.6474
AC*MW*Dys	3	2	1	3	3	1	-14.3667	2.0649	18	-6.96	<.0001	Tukey-Kramer	0.0002
AC*MW*Dys	3	2	1	3	3	2	-15.5000	2.0649	18	-7.51	<.0001	Tukey-Kramer	<.0001
AC*MW*Dys	3	2	2	3	3	1	-11.5667	2.0649	18	-5.60	<.0001	Tukey-Kramer	0.0022
AC*MW*Dys	3	2	2	3	3	2	-12.7000	2.0649	18	-6.15	<.0001	Tukey-Kramer	0.0008
AC*MW*Dys	3	3	1	3	3	2	-1.1333	1.1932	18	-0.95	0.3548	Tukey-Kramer	0.9998

Randomize complete design (one-way anova)
effect of PLGA molecular weight, MOA, and dialysis in Np size
 CRD with proc mixed
post hoc adjustment with macro by Arnold Saxton

Effect=AC ADJUSTMENT=Tukey(P<0.05) bygroup=1

Obs	AC	MW	Dys	Estimate	StdErr	MSGROUP
1	3	_	_	104.69	0.7694	A
2	2	_	_	82.9722	0.7694	B
3	1	_	_	60.3833	0.7694	C

Effect=MW ADJUSTMENT=Tukey(P<0.05) bygroup=2

Obs	AC	MW	Dys	Estimate	StdErr	MSGROUP
4	_	3	_	85.8056	0.7694	A
5	_	2	_	81.1278	0.7694	B
6	_	1	_	81.1111	0.7694	B

Effect=AC*MW ADJUSTMENT=Tukey(P<0.05) bygroup=3

Obs	AC	MW	Dys	Estimate	StdErr	MSGROUP
7	3	1	_	111.73	1.3326	A
8	3	3	_	107.93	1.3326	A
9	3	2	_	94.4000	1.3326	B
10	2	1	_	85.0333	1.3326	C
11	2	2	_	83.1000	1.3326	C
12	2	3	_	80.7833	1.3326	C
13	1	3	_	68.7000	1.3326	D
14	1	2	_	65.8833	1.3326	D
15	1	1	_	46.5667	1.3326	E

Effect=Dys ADJUSTMENT=Tukey-Kramer(P<0.05) bygroup=4

Obs	AC	MW	Dys	Estimate	StdErr	MSGROUP
16	_	_	2	84.0037	0.4867	A
17	_	_	1	81.3593	0.4867	B

Effect=AC*Dys ADJUSTMENT=Tukey-Kramer(P<0.05) bygroup=5

Obs	AC	MW	Dys	Estimate	StdErr	MSGROUP
18	3	_	1	105.16	0.8430	A
19	3	_	2	104.22	0.8430	A
20	2	_	2	83.3556	0.8430	B
21	2	_	1	82.5889	0.8430	B
22	1	_	2	64.4333	0.8430	C
23	1	_	1	56.3333	0.8430	D

Effect=MW*Dys ADJUSTMENT=Tukey-Kramer(P<0.05) bygroup=6

Obs	AC	MW	Dys	Estimate	StdErr	MSGROUP
24	_	3	2	87.1889	0.8430	A
25	_	3	1	84.4222	0.8430	B
26	_	2	2	82.9000	0.8430	BC
27	_	1	2	81.9222	0.8430	BCD

28	_	1	1	80.3000	0.8430	CD
29	_	2	1	79.3556	0.8430	D

Effect=AC*MW*Dys ADJUSTMENT=Tukey-Kramer(P<0.05) bygroup=7

Obs	AC	MW	Dys	Estimate	StdErr	MSGROUP
30	3	1	1	115.10	1.4601	A
31	3	3	2	108.50	1.4601	AB
32	3	1	2	108.37	1.4601	B
33	3	3	1	107.37	1.4601	AB
34	3	2	2	95.8000	1.4601	C
35	3	2	1	93.0000	1.4601	CD
36	2	1	1	87.1667	1.4601	DE
37	2	2	2	84.4000	1.4601	EF
38	2	1	2	82.9000	1.4601	EF
39	2	3	2	82.7667	1.4601	EF
40	2	2	1	81.8000	1.4601	EF
41	2	3	1	78.8000	1.4601	F
42	1	3	2	70.3000	1.4601	GH
43	1	2	2	68.5000	1.4601	G
44	1	3	1	67.1000	1.4601	GH
45	1	2	1	63.2667	1.4601	H
46	1	1	2	54.5000	1.4601	I
47	1	1	1	38.6333	1.4601	J

Randomize complete design (one-way anova)
effect of PLGA molecular weight, MOA, and dialysis in Np size
 CRD with proc mixed
Univariate analysis of residuals

The UNIVARIATE Procedure
Variable: Resid

Moments

N	54	Sum Weights	54
Mean	0	Sum Observations	0
Std Deviation	0.93308206	Variance	0.87064214
Skewness	0.61780823	Kurtosis	1.30643015
Uncorrected SS	46.1440334	Corrected SS	46.1440334
Coeff Variation	.	Std Error Mean	0.12697639

Basic Statistical Measures

Location		Variability	
Mean	0.00000	Std Deviation	0.93308
Median	-0.12025	Variance	0.87064
Mode	.	Range	4.63333
		Interquartile Range	0.89214

Tests for Location: Mu0=0

Test	-Statistic-		-----p Value------	
Student's t	t	0	Pr > |t|	1.0000
Sign	M	-2	Pr >= |M|	0.6835
Signed Rank	S	-54.5	Pr >= |S|	0.6432

Tests for Normality

Test	--Statistic---		-----p Value------	
Shapiro-Wilk	W	0.953407	Pr < W	0.0351
Kolmogorov-Smirnov	D	0.114721	Pr > D	0.0762
Cramer-von Mises	W-Sq	0.156856	Pr > W-Sq	0.0198
Anderson-Darling	A-Sq	0.8974	Pr > A-Sq	0.0215

Quantiles (Definition 5)

Quantile	Estimate
100% Max	2.700799
99%	2.700799
95%	2.040987
90%	1.173660
75% Q3	0.478603
50% Median	-0.120250
25% Q1	-0.413535
10%	-1.092346
5%	-1.641995
1%	-1.932534
0% Min	-1.932534

Extreme Observations

Lowest	Obs	Highest	Obs
-1.93253	20	1.36653	19
-1.82140	15	1.36767	54
-1.64200	26	2.04099	25
-1.50014	46	2.44238	13
-1.20066	48	2.70080	47

```
Stem Leaf                     #  Boxplot
  26 0                        1     0
  24 4                        1     0
  22                          1
  20 4                        1     0
  18                                |
  16                                |
  14                                |
  12 77                       2     |
  10 57                       2     |
   8 8                        1     |
   6 1                        1     |
   4 88267                    5  +-----+
   2 24890                    5  |     |
   0 444838                   6  |  +  |
  -0 96226                    5  *-----*
  -2 62298842                 8  |     |
  -4 76110                    5  +-----+
  -6 12                       2     |
  -8 652                      3     |
 -10 9                        1     |
 -12 0                        1     |
 -14 0                        1     |
 -16 4                        1     |
 -18 32                       2     0
     ----+----+----+----+
 Multiply Stem.Leaf by 10**-1
```

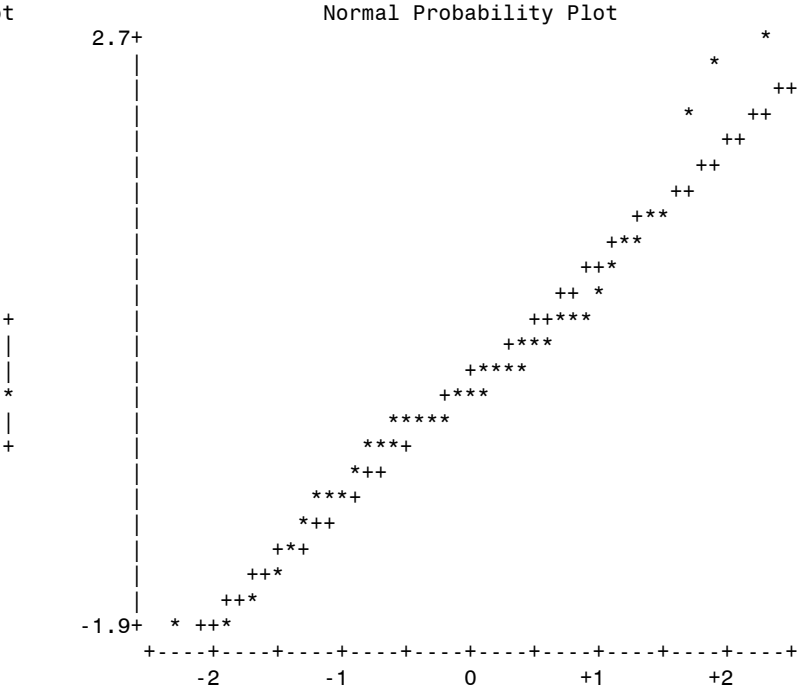

The analysis of sonication amplitude was performed with the same program, but the parameters tested were in molecular weight without addition of MOA and sonication amplitude. The proc mixed procedure ($\alpha = 0.05$) was used.

```
Randomize complete design (one-way anova)
effect of PLGA molecular weight, MOA, and dialysis in Np size
List of Data                                                    SONICATION
EFFECT

Obs    Size    Son    MW    Rep

  1    38.7     1      1     1
  2    38.1     1      1     2
  3    41.4     1      1     3
  4    67.2     1      2     1
  5    68.4     1      2     2
  6    64.9     1      2     3
  7    70.3     1      3     1
  8    70.6     1      3     2
  9    67.1     1      3     3
 10    38.9     2      1     1
 11    38.6     2      1     2
 12    38.4     2      1     3
 13    63.6     2      2     1
 14    63.1     2      2     2
 15    63.1     2      2     3
 16    66.5     2      3     1
 17    67.3     2      3     2
 18    67.5     2      3     3

Randomize complete design (one-way anova)
effect of PLGA molecular weight, MOA, and dialysis in Np size
 CRD with proc mixed
The Mixed Procedure

                 Model Information

Data Set                     WORK.NANOPARTICLES
Dependent Variable           Size
Covariance Structure         Variance Components
Estimation Method            REML
Residual Variance Method     Profile
Fixed Effects SE Method      Model-Based
Degrees of Freedom Method    Containment


             Class Level Information

Class    Levels    Values

Son           2    1 2
MW            3    1 2 3
Rep           3    1 2 3


            Dimensions

Covariance Parameters            2
```

Columns in X	12
Columns in Z	18
Subjects	1
Max Obs Per Subject	18

Number of Observations

Number of Observations Read	18
Number of Observations Used	18
Number of Observations Not Used	0

Iteration History

Iteration	Evaluations	-2 Res Log Like	Criterion
0	1	47.29665069	
1	4	47.29665069	0.00000000

Convergence criteria met.

Covariance Parameter Estimates

Cov Parm	Estimate
Rep(Son*MW)	0
Residual	1.7406

Fit Statistics

-2 Res Log Likelihood	47.3
AIC (smaller is better)	49.3
AICC (smaller is better)	49.7
BIC (smaller is better)	50.2

Type 3 Tests of Fixed Effects

Effect	Num DF	Den DF	F Value	Pr > F
Son	1	12	12.39	0.0042
MW	2	12	885.01	<.0001
Son*MW	2	12	1.69	0.2255

Least Squares Means

Effect	Son	MW	Estimate	Standard Error	DF	t Value	Pr > |t|
Son	1		58.5222	0.4398	12	133.08	<.0001
Son	2		56.3333	0.4398	12	128.10	<.0001
MW		1	39.0167	0.5386	12	72.44	<.0001
MW		2	65.0500	0.5386	12	120.78	<.0001
MW		3	68.2167	0.5386	12	126.65	<.0001
Son*MW	1	1	39.4000	0.7617	12	51.73	<.0001
Son*MW	1	2	66.8333	0.7617	12	87.74	<.0001
Son*MW	1	3	69.3333	0.7617	12	91.02	<.0001
Son*MW	2	1	38.6333	0.7617	12	50.72	<.0001
Son*MW	2	2	63.2667	0.7617	12	83.06	<.0001
Son*MW	2	3	67.1000	0.7617	12	88.09	<.0001

Differences of Least Squares Means

Effect	Son	MW	_Son	_MW	Estimate	Standard Error	DF	t Value	Pr > |t|	Adjustment	Adj P
Son	1		2		2.1889	0.6219	12	3.52	0.0042	Tukey	0.0042
MW		1		2	-26.0333	0.7617	12	-34.18	<.0001	Tukey	<.0001
MW		1		3	-29.2000	0.7617	12	-38.34	<.0001	Tukey	<.0001
MW		2		3	-3.1667	0.7617	12	-4.16	0.0013	Tukey	0.0035
Son*MW	1	1	1	2	-27.4333	1.0772	12	-25.47	<.0001	Tukey	<.0001
Son*MW	1	1	1	3	-29.9333	1.0772	12	-27.79	<.0001	Tukey	<.0001
Son*MW	1	1	2	1	0.7667	1.0772	12	0.71	0.4902	Tukey	0.9768
Son*MW	1	1	2	2	-23.8667	1.0772	12	-22.16	<.0001	Tukey	<.0001
Son*MW	1	1	2	3	-27.7000	1.0772	12	-25.71	<.0001	Tukey	<.0001
Son*MW	1	2	1	3	-2.5000	1.0772	12	-2.32	0.0387	Tukey	0.2577
Son*MW	1	2	2	1	28.2000	1.0772	12	26.18	<.0001	Tukey	<.0001
Son*MW	1	2	2	2	3.5667	1.0772	12	3.31	0.0062	Tukey	0.0542
Son*MW	1	2	2	3	-0.2667	1.0772	12	-0.25	0.8087	Tukey	0.9998
Son*MW	1	3	2	1	30.7000	1.0772	12	28.50	<.0001	Tukey	<.0001
Son*MW	1	3	2	2	6.0667	1.0772	12	5.63	0.0001	Tukey	0.0012
Son*MW	1	3	2	3	2.2333	1.0772	12	2.07	0.0603	Tukey	0.3605
Son*MW	2	1	2	2	-24.6333	1.0772	12	-22.87	<.0001	Tukey	<.0001
Son*MW	2	1	2	3	-28.4667	1.0772	12	-26.43	<.0001	Tukey	<.0001
Son*MW	2	2	2	3	-3.8333	1.0772	12	-3.56	0.0039	Tukey	0.0357

Randomize complete design (one-way anova)
effect of PLGA molecular weight, MOA, and dialysis in Np size
 CRD with proc mixed
post hoc adjustment with macro by Arnold Saxton

Effect=Son ADJUSTMENT=Tukey(P<0.05) bygroup=1

Obs	Son	MW	Estimate	StdErr	MSGROUP
1	1	_	58.5222	0.4398	A
2	2	_	56.3333	0.4398	B

Effect=MW ADJUSTMENT=Tukey(P<0.05) bygroup=2

Obs	Son	MW	Estimate	StdErr	MSGROUP
3	_	3	68.2167	0.5386	A
4	_	2	65.0500	0.5386	B
5	_	1	39.0167	0.5386	C

Effect=Son*MW ADJUSTMENT=Tukey(P<0.05) bygroup=3

Obs	Son	MW	Estimate	StdErr	MSGROUP
6	1	3	69.3333	0.7617	A
7	2	3	67.1000	0.7617	A
8	1	2	66.8333	0.7617	AB
9	2	2	63.2667	0.7617	B
10	1	1	39.4000	0.7617	C
11	2	1	38.6333	0.7617	C

Randomize complete design (one-way anova)
effect of PLGA molecular weight, MOA, and dialysis in Np size
 CRD with proc mixed
Univariate analysis of residuals

The UNIVARIATE Procedure
Variable: Resid

Moments

N	18	Sum Weights	18
Mean	0	Sum Observations	0
Std Deviation	1.10843469	Variance	1.22862745
Skewness	-0.3005744	Kurtosis	0.14206577
Uncorrected SS	20.8866667	Corrected SS	20.8866667
Coeff Variation	.	Std Error Mean	0.26126056

Basic Statistical Measures

Location		Variability	
Mean	0.00000	Std Deviation	1.10843
Median	0.08333	Variance	1.22863
Mode	-0.16667	Range	4.23333
		Interquartile Range	1.00000

Tests for Location: Mu0=0

Test	-Statistic-		-----p Value------	
Student's t	t	0	Pr > |t|	1.0000
Sign	M	0	Pr >= |M|	1.0000
Signed Rank	S	5.5	Pr >= |S|	0.8234

Tests for Normality

Test	--Statistic---		-----p Value------	
Shapiro-Wilk	W	0.968394	Pr < W	0.7670
Kolmogorov-Smirnov	D	0.138858	Pr > D	>0.1500
Cramer-von Mises	W-Sq	0.05184	Pr > W-Sq	>0.2500
Anderson-Darling	A-Sq	0.293812	Pr > A-Sq	>0.2500

Quantiles (Definition 5)

Quantile	Estimate
100% Max	2.0000000
99%	2.0000000
95%	2.0000000
90%	1.5666667
75% Q3	0.4000000
50% Median	0.0833333
25% Q1	-0.6000000
10%	-1.9333333
5%	-2.2333333
1%	-2.2333333
0% Min	-2.2333333

Extreme Observations

------Lowest-----		------Highest-----	
Value	Obs	Value	Obs
-2.23333	9	0.400000	18
-1.93333	6	0.966667	7
-1.30000	2	1.266667	8
-0.70000	1	1.566667	5
-0.60000	16	2.000000	3

```
Stem Leaf                     #  Boxplot                        Normal Probability Plot
   2 0                        1     0        2.25+                                    *++++
   1 6                        1     |           |                                  *++++
   1 03                       2     |           |                                +*++
   0                                |        0.75+                          +++*+
   0 23344                    5  +--+--+        |                       +**+** *
  -0 2220                     4  |     |        |                    **++*
  -0 76                       2  +-----+    -0.75+                 +**++
  -1 3                        1     |           |              ++*+
  -1 9                        1     |           |        +++++*
  -2 2                        1     0       -2.25+   ++++*
     ----+----+----+----+                          +----+----+----+----+----+----+----+----+----+----+
                                                      -2        -1         0        +1        +2
```

The analysis of entrapment efficiency (EE) was performed with the same program, but the parameters tested were in molecular weight (MW), and MOA (AC). The proc mixed procedure ($\alpha = 0.05$) was used with Tukey adjustment.

```
Randomize complete design (one-way anova)
effect of PLGA molecular weight, MOA, and dialysis in Np size
List of Data

Obs      EE     AC    MW    Rep

  1     68.3     2     1     1
  2     49.1     2     1     2
  3     54.7     2     1     3
  4     82.2     2     2     1
  5     72.0     2     2     2
  6     77.8     2     2     3
  7     62.8     2     3     1
  8     93.2     2     3     2
  9     54.6     2     3     3
 10     71.7     3     1     1
 11     64.8     3     1     2
 12     92.3     3     1     3
 13     69.2     3     2     1
 14     84.3     3     2     2
 15     82.7     3     2     3
 16    125.0     3     3     1
 17     58.4     3     3     2
 18     92.2     3     3     3


Randomize complete design (one-way anova)
effect of PLGA molecular weight, MOA, and dialysis in Np size
 CRD with proc mixed

The Mixed Procedure

                  Model Information

Data Set                     WORK.NANOPARTICLES
Dependent Variable           EE
Covariance Structure         Variance Components
Estimation Method            REML
Residual Variance Method     Profile
Fixed Effects SE Method      Model-Based
Degrees of Freedom Method    Containment


             Class Level Information

Class    Levels    Values

AC            2    2 3
MW            3    1 2 3
Rep           3    1 2 3


            Dimensions

Covariance Parameters            2
Columns in X                    12
Columns in Z                    18
Subjects                         1
```

Max Obs Per Subject 18

Number of Observations

Number of Observations Read	18
Number of Observations Used	18
Number of Observations Not Used	0

Iteration History

Iteration	Evaluations	-2 Res Log Like	Criterion
0	1	109.86421701	
1	2	109.86421700	0.00000000

Convergence criteria met.

Covariance Parameter Estimates

Cov Parm	Estimate
Rep(AC*MW)	319.94
Residual	0.007751

Fit Statistics

-2 Res Log Likelihood	109.9
AIC (smaller is better)	113.9
AICC (smaller is better)	115.2
BIC (smaller is better)	115.6

Type 3 Tests of Fixed Effects

Effect	Num DF	Den DF	F Value	Pr > F
AC	1	12	2.75	0.1230
MW	2	12	1.05	0.3790
AC*MW	2	12	0.57	0.5821

Least Squares Means

Effect	AC	MW	Estimate	Standard Error	DF	t Value	Pr > |t|
AC	2		68.3000	5.9624	12	11.46	<.0001
AC	3		82.2889	5.9624	12	13.80	<.0001
MW		1	66.8167	7.3024	12	9.15	<.0001
MW		2	78.0333	7.3024	12	10.69	<.0001
MW		3	81.0333	7.3024	12	11.10	<.0001
AC*MW	2	1	57.3667	10.3272	12	5.55	0.0001
AC*MW	2	2	77.3333	10.3272	12	7.49	<.0001
AC*MW	2	3	70.2000	10.3272	12	6.80	<.0001
AC*MW	3	1	76.2667	10.3272	12	7.39	<.0001
AC*MW	3	2	78.7333	10.3272	12	7.62	<.0001
AC*MW	3	3	91.8667	10.3272	12	8.90	<.0001

Differences of Least Squares Means

Effect	AC	MW	_AC	_MW	Estimate	Standard Error	DF	t Value	Pr > |t|	Adjustment	Adj P
AC	2		3		-13.9889	8.4321	12	-1.66	0.1230	Tukey	0.1230
MW		1		2	-11.2167	10.3272	12	-1.09	0.2988	Tukey	0.5401
MW		1		3	-14.2167	10.3272	12	-1.38	0.1938	Tukey	0.3830
MW		2		3	-3.0000	10.3272	12	-0.29	0.7764	Tukey	0.9547
AC*MW	2	1	2	2	-19.9667	14.6048	12	-1.37	0.1966	Tukey	0.7446
AC*MW	2	1	2	3	-12.8333	14.6048	12	-0.88	0.3968	Tukey	0.9447
AC*MW	2	1	3	1	-18.9000	14.6048	12	-1.29	0.2200	Tukey	0.7829
AC*MW	2	1	3	2	-21.3667	14.6048	12	-1.46	0.1692	Tukey	0.6917
AC*MW	2	1	3	3	-34.5000	14.6048	12	-2.36	0.0359	Tukey	0.2429
AC*MW	2	2	2	3	7.1333	14.6048	12	0.49	0.6341	Tukey	0.9957
AC*MW	2	2	3	1	1.0667	14.6048	12	0.07	0.9430	Tukey	1.0000
AC*MW	2	2	3	2	-1.4000	14.6048	12	-0.10	0.9252	Tukey	1.0000
AC*MW	2	2	3	3	-14.5333	14.6048	12	-1.00	0.3393	Tukey	0.9109
AC*MW	2	3	3	1	-6.0667	14.6048	12	-0.42	0.6852	Tukey	0.9980
AC*MW	2	3	3	2	-8.5333	14.6048	12	-0.58	0.5699	Tukey	0.9902
AC*MW	2	3	3	3	-21.6667	14.6048	12	-1.48	0.1637	Tukey	0.6801
AC*MW	3	1	3	2	-2.4667	14.6048	12	-0.17	0.8687	Tukey	1.0000
AC*MW	3	1	3	3	-15.6000	14.6048	12	-1.07	0.3065	Tukey	0.8848
AC*MW	3	2	3	3	-13.1333	14.6048	12	-0.90	0.3862	Tukey	0.9394

Randomize complete design (one-way anova)
effect of PLGA molecular weight, MOA, and dialysis in Np size
 CRD with proc mixed
post hoc adjustment with macro by Arnold Saxton

Effect=AC ADJUSTMENT=Tukey(P<0.05) bygroup=1

Obs	AC	MW	Estimate	StdErr	MSGROUP
1	3	_	82.2889	5.9624	A
2	2	_	68.3000	5.9624	A

Effect=MW ADJUSTMENT=Tukey(P<0.05) bygroup=2

Obs	AC	MW	Estimate	StdErr	MSGROUP
3	_	3	81.0333	7.3024	A
4	_	2	78.0333	7.3024	A
5	_	1	66.8167	7.3024	A

Effect=AC*MW ADJUSTMENT=Tukey(P<0.05) bygroup=3

Obs	AC	MW	Estimate	StdErr	MSGROUP
6	3	3	91.8667	10.3272	A
7	3	2	78.7333	10.3272	A
8	2	2	77.3333	10.3272	A
9	3	1	76.2667	10.3272	A
10	2	3	70.2000	10.3272	A
11	2	1	57.3667	10.3272	A

Randomize complete design (one-way anova)
effect of PLGA molecular weight, MOA, and dialysis in Np size
 CRD with proc mixed
Univariate analysis of residuals

The UNIVARIATE Procedure
Variable: Resid

Moments

N	18	Sum Weights	18
Mean	-8.29E-15	Sum Observations	-1.492E-13
Std Deviation	0.00036405	Variance	1.32536E-7
Skewness	0.18387008	Kurtosis	1.17850428
Uncorrected SS	2.25311E-6	Corrected SS	2.25311E-6
Coeff Variation	-4.3917E12	Std Error Mean	0.00008581

Basic Statistical Measures

Location		Variability	
Mean	-0.00000	Std Deviation	0.0003641
Median	-0.00003	Variance	1.32536E-7
Mode	.	Range	0.00161
		Interquartile Range	0.0003351

Tests for Location: Mu0=0

Test	-Statistic-		-----p Value------	
Student's t	t	-966E-13	Pr > |t|	1.0000
Sign	M	0	Pr >= |M|	1.0000
Signed Rank	S	-4.5	Pr >= |S|	0.8650

Tests for Normality

Test	--Statistic---		-----p Value------	
Shapiro-Wilk	W	0.969305	Pr < W	0.7845
Kolmogorov-Smirnov	D	0.133315	Pr > D	>0.1500
Cramer-von Mises	W-Sq	0.050249	Pr > W-Sq	>0.2500
Anderson-Darling	A-Sq	0.318331	Pr > A-Sq	>0.2500

Quantiles (Definition 5)

Quantile	Estimate
100% Max	8.02645E-04
99%	8.02645E-04
95%	8.02645E-04
90%	5.57168E-04
75% Q3	1.34851E-04
50% Median	-2.82622E-05
25% Q1	-2.00258E-04
10%	-3.77905E-04
5%	-8.10720E-04
1%	-8.10720E-04
0% Min	-8.10720E-04

Extreme Observations

Lowest		Highest	
Value	Obs	Value	Obs
-0.000810720	17	0.000134851	14
-0.000377905	9	0.000264857	1
-0.000277777	11	0.000388403	12
-0.000230942	13	0.000557168	8
-0.000200258	2	0.000802645	16

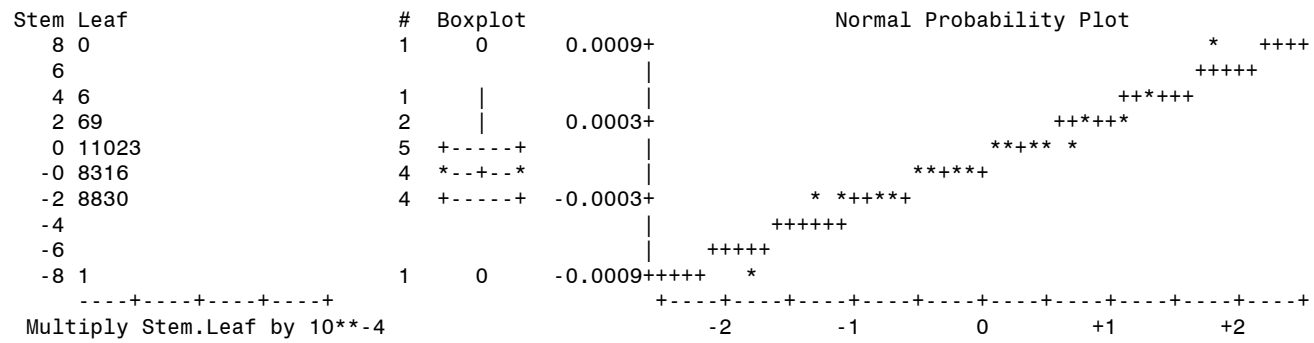

VITA

Carlos Astete graduated from Catholic of Valparaiso University in 1993, Chile. He received his bachelor's degree in Biochemistry Engineering. He was working for three years in Watt's Foods in the position of research engineer and environmental impact. The position was dealing with the impact of industrial contaminations and its management due to new national environmental regulations. The development of new products and improvement of oldest was another important area as well. After, he was working for three years in DAF S.A. A company oriented to project development and informatics. The position was project manager of new accounts. The challenges were related to the development of new interactions with the market by implementation of interactive platforms.

In 2000 he received the degree of Master in Business and Administration from Adolfo Ibanez University, Chile. From 2000 to 2002, he was working in DAF S.A. in the position of product manager. The interaction and relationship with the customer's platform was a key point in the development of internet technical support.

In fall 2003, he was accepted in the department of Biological and Agricultural Engineering for a Master of Science degree, Louisiana State University in Baton Rouge, Louisiana. He was an active member of the Gamma Sigma Delta, Gamma Beta Phi honor societies, and the National Society of Collegiate Scholars. Mr. Carlos Astete will be awarded the degree Master of Science in December 2005, and he is currently following the doctoral studies in the same university.